Phospholipid Flippases in B cells and Platelets

Weidong Jing

July 2019

A thesis submitted for the degree of Doctor of Philosophy of The Australian National University

Statement

The research presented in this thesis is my own original work except where stated otherwise.

Weidong Jing

Acknowledgments

First of all, I would like to express my deepest gratitude to my supervisor, Professor Stefan Bröer, who gave me a lot of beneficial guidance, generous help and support in the process of completing my study. He gave the freedom to explore on my own, and also kept me on the track at every step of my PhD. Then I would like to thank Ms Angelika Bröer, the research officer of our lab, for her careful guidance and selfless help in experimental techniques. I also want to thank all the members of the laboratory, no matter they have left or are still here, they have provided me with the help within their power in the experiment and brought me a lot of joy in life. Thanks also go to our divisional STO Dr. Farid Rahimi for his generous helps during my PhD.

I also would to thank my co-supervisor Associate Professor Anselm Enders from JCSMR, for his help in mice work and his constructive suggestions and ideas on this flippase project. Many thanks go to Dr. Mehmet Yabas, who helped me a lot on flow cytometry and B cell works. Also, many thanks go to Associate Professor Elizabeth Gardiner and Dr. Lucy Coupland from JCSMR, who are experts on platelets biology, they gave me quite a lot of valuable suggestions and generous help on platelet experiments.

Finally, I would like to thank my wife Tina, my daughter Chloe, my parents and my friends, for the selfless care, understanding and help they have given me in life. I would not have been able to carry on and finish my doctoral study without them.

Abbreviations

PS	Phosphatidylserine
PE	Phosphatidylethanolamine
PC	Phosphatidylcholine
SM	Sphingomyelin
TPL	Total phospholipid
ABC	ATP-binding cassette
CDC50	Cell cycle control protein 50
CAMRQ	Cerebellar ataxia, mental retardation and disequilibrium syndrome
TMEM16F	Transmembrane protein 16 F
XKR8	XK-related protein 8
Tim4	T-cell immunoglobulin- and mucin-domain-containing molecule 4
Gas6	Growth arrest-specific protein 6
MFG-E8	Milk fat globule EGF factor 8
MerTK	Tyrosine-protein kinase Mer
BCL2	B-cell lymphoma-2
BH domains	BCL2 homology domains
Fas	First apoptosis signal
FasL	Fas ligand
TNF	Tumor necrosis factor
TNFR1	TNF receptor-1
TRAIL	TNF-related apoptosis-inducing ligand
DISC	Death-inducing signalling complex

FADD	Fas-associated death domain
TGF-β	Transforming growth factor-β
IL	Interleukin
SLE	Systemic lupus erythematosus
TF	Tissue factor
GPVI	Glycoprotein VI
PAR	Protease-activated receptor
SOCE	Store-operated Ca^{2+} entry
ROCE	Receptor-operated Ca^{2+} entry
TRPC	Transient receptor potential C
PKC	Protein kinase C
ER	Endoplasmic reticulum
TGN	Trans-Golgi network
GAP	GTPase-activating protein
EHD1	EH domain containing 1
BAR domains	Bin/amphiphysin/Rvs domains
VEGF	Vascular endothelial growth factor
HSCs	Haematopoietic stem cells
CLPs	Common lymphoid progenitors
RAG	Recombination activating gene proteins
BCR	B cell receptor
SLC proteins	Surrogate light chain proteins
ENU	N-ethyl-N-nitrosourea
YAP	Yes-associated protein
Amb	Ambrosius mouse strain
FCS	Foetal calf serum

PBS	Phosphate-buffered saline
HBSS	Hanks' balanced salt solution
RBC	Red blood cell
ACD	Acid citrate dextrose
EDTA	Ethylenediaminetetraacetic acid
HEPES	4-(2-hydroxyethyl)-1-piperazineethanesulfonic acid
SDS	Sodium dodecyl sulfate
PAGE	Polyacrylamide gel electrophoresis
NBD	Nitrobenzoxadiazole
MFI	Mean fluorescence intensity
BSA	Bovine serum albumin
DAPI	4′,6-diamidino-2-phenylindole
7-AAD	7-Aminoactinomycin D
CFSE	Carboxyfluorescein succinimidyl ester
DMSO	Dimethyl sulfoxide
SEM	Scanning electron microscopy
TEM	Transmission electron microscopy
PEG	Polyethylene glycol
AMR	Ashwell-morell receptor

Abstract

The asymmetric distribution of phospholipids in the plasma membrane is generated and maintained through the action of phospholipid flippases in resting cells, but becomes disrupted in apoptotic cells and activated platelets, resulting in phosphatidylserine (PS) exposure on the cell surface. Exposure of PS is indispensable for the clearance of apoptotic cells and promotion of blood coagulation. Stable PS exposure during apoptosis requires inactivation of flippases to prevent PS from being re-internalised. In addition to the plasma membrane, flippases also function in generating phospholipid asymmetry in intracellular membranes and play critical roles in vesicle-mediated protein trafficking.

In my PhD I investigated the biochemical properties and physiological roles of the flippases ATP11C and ATP8A1. Using ATP11C-deficient mice, I demonstrated that:

1) ATP11C mediated significant flippase activity in murine B cell subsets. Loss of ATP11C resulted in a defective internalization of PS and phosphatidylethanolamine (PE) in comparison to control cells. The diminished flippase activity caused increased PS exposure on viable pro-B cells freshly isolated from the bone marrow of ATP11C-deficient mice, which was corrected upon a 2-hour resting period *in vitro*. These findings identified ATP11C as an aminophospholipid translocase in B cell lineages and suggested that the temporary increased PS accumulation on the surface of pro-B cells caused by impaired

flippase activity contributed to the B cell lymphopenia observed in ATP11C-deficient mice.

2) Loss of ATP11C resulted in reduced life span and increased size of platelets but did not induce thrombocytopenia or affect platelet function. Interestingly, I found that ATP11C did not mediate the flippase activity in platelets as evident by the normal flippase activity in mutant platelets and absence of protein expression of ATP11C in wild type platelets. These results suggested that ATP11C was not a contributing flippase in murine platelets and ATP11C likely regulated cell extrinsic factors that were required for the survival of platelets in the peripheral blood. Together, these findings highlighted a fundamental difference between the action of ATP11C in leukocytes and platelets.

Moreover, I identified that flippase ATP8A1was highly expressed in both murine and human platelets but was not present in the plasma membrane. ATP8A1 was cleaved by the cysteine protease calpain during apoptosis, and the cleavage was prevented indirectly by caspase inhibition, involving blockage of calcium influx into platelets and subsequent calpain activation. In contrast, in platelets activated with thrombin and collagen and exposing PS, ATP8A1 remained intact. These data revealed a novel mechanism of flippase cleavage and suggested that flippase activity in intracellular membranes differed between platelets undergoing apoptosis and activation.

Collectively, these findings extended our understanding on the role of flippases in B cell development and important mechanisms of platelet survival and function.

Table of Contents

CHAPTER 1: Introduction

1.1 Phospholipid asymmetry of the plasma membrane

One of the unique features of the plasma membrane in eukaryotes is the asymmetric distribution of phospholipids between the two leaflets of the bilayer. For example, phosphatidylserine (PS) and phosphatidylethanolamine (PE) are confined predominantly to the cytoplasmic leaflet, and phosphatidylcholine (PC) and sphingomyelin (SM) are concentrated mainly in the outer leaflet (Figure 1.1)[1].

Generally, the asymmetric distribution of phospholipids is generated and maintained by two groups of ATP-dependent transporters; flippases, belonging to the P4-type ATPase family, mediate the transport of PS and PE to the inner plasma leaflet, while floppases, that belong to ATP-binding cassette (ABC) transporters, are responsible for the transport of PC and SM to the exoplasmic leaflet (Figure 1.2)[2, 3]. Under the action of flippases almost all PS is confined to the inner leaflet of the membrane[4, 5]. During certain physiological or pathological processes, the asymmetric distribution of phospholipids in the plasma membrane is disrupted by a third group of transporters, known as scramblases, that function in an ATP-independent manner, resulting in PS exposure on the cell surface (Figure 1.2)[5, 6]. The dynamic regulation of the distribution of phospholipids in the plasma membrane is an important physiological function.

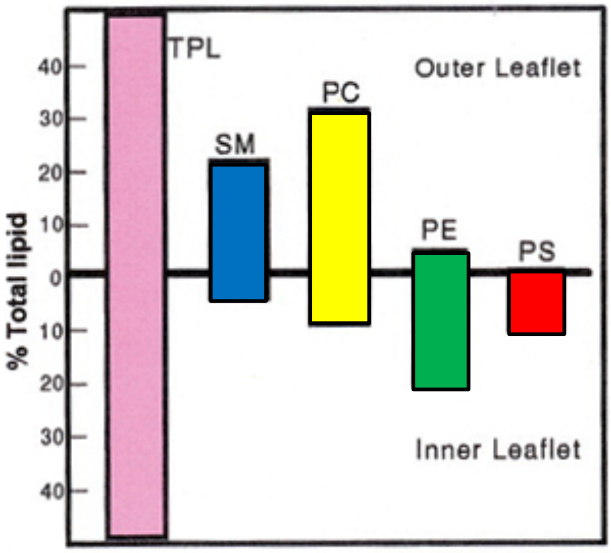

Figure 1.1 Asymmetrical distributions of phospholipids in membranes of human red blood cells

The diagram shows an example of steady state phospholipid asymmetry in the plasma membrane in normal red blood cells (adapted from reference Balasubramanian K. et al, 2003[1]). Expressed as mole percent; TPL, total phospholipid; SM, sphingomyelin; PC, phosphatidylcholine; PE, phosphatidylethanolamine; and PS, phosphatidylserine[1, 4, 7].

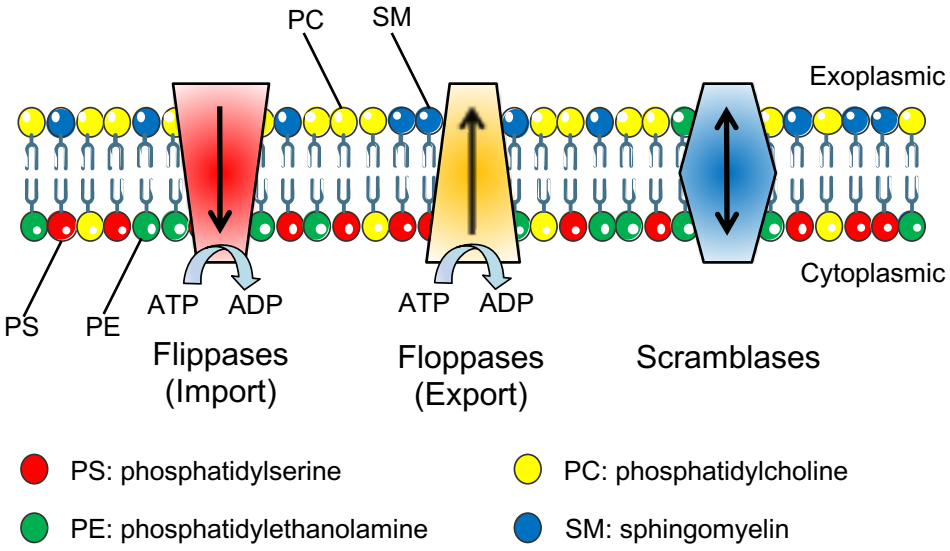

Figure 1.2 Regulation of phospholipid asymmetry in plasma membranes

The distribution of phospholipids in plasma membranes is regulated by three distinct families of membrane transporters: Flippases (P4-ATPases), Floppases (ABC transporters), and scramblases. Flippases catalyze the ATP-dependent transport of the aminophospholipids PS and PE from the extracellular side of the membrane to the cytoplasmic leaflet of the bilayer, while floppases transport PC and SM in the opposite direction. Scramblases are ATP-independent transporters and act to abolish lipid asymmetry by randomizing phospholipid distributions.

1.1.1 P4-type ATPases: aminophospholipid flippases

P4-type ATPase family

P-type ATPases constitute a family of membrane proteins that utilize the energy from ATP hydrolysis to transport ions and lipids across biological membranes[8]. These transporters are found in prokaryotes, archaea and eukaryotes, and are distinguished from other ATP-dependent transporters by the presence of a conserved aspartic acid residue that undergoes transient phosphorylation during the catalytic cycle[3, 9]. On the basis of phylogenetic analysis, P-type ATPases have been organized into five main classes, P1-P5 ATPases[10].

Flippases belong to Type-4 P-type ATPase (P4-ATPase) family, which is only found in eukaryotes and is unique in that they transport or flip phospholipids across membranes. There are 14 members of the P4-type ATPase family in humans (ATP8A1, ATP8A2, ATP8B1, ATP8B2, ATP8B3, ATP8B4, ATP9A, ATP9B, ATP10A, ATP10B, ATP10D, ATP11A, ATP11B and ATP11C) and 15 members in mice (all present in humans plus ATP8B5)[11] (Figure 1.3 A).

Structure of P4-ATPases and ancillary subunit CDC50s

Flippases are made up of ten transmembrane helices and three cytosolic domains involved in the ATPase catalytic cycle[12] (Figure 1.3 B). The three cytosolic domains are a nucleotide-binding (N) domain which binds ATP; a phosphorylation (P) domain which contains the conserved phosphorylation site in the DKTG motif; and an actuator (A) domain which has the DGET motif that

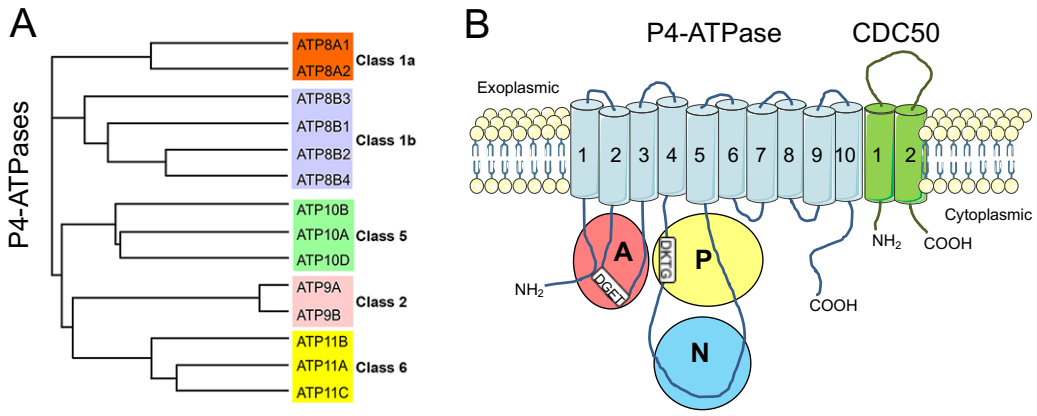

Figure 1.3 Phylogenetic trees of human P4-ATPases and topological model of a P4-ATPase and its subunit CDC50

(A) There are 14 different members of P4-ATPases in humans which are organized into five different subfamilies according to sequence[3].

(B) The ten transmembrane helices of the P4-ATPase are represented by aqua cylinders numbered from 1 to 10. The three cytosolic domains involved in the ATPase catalytic cycle are shown as coloured circles: nucleotide-binding (N) domain which binds ATP; phosphorylation (P) domain which contains the conserved phosphorylation site in the DKTG motif; and actuator (A) domain which has the DGET motif that facilitates the dephosphorylation of the phosphorylated aspartate intermediate[3, 13, 14]. The two transmembrane helices of the β-subunit CDC50 protein are shown as light green cylinders numbered 1 and 2. The diagram is modified from Andersen, J. P. et al, 2016[3] and Van der Mark, V. A. et al, 2013[15].

facilitates the dephosphorylation of the phosphorylated aspartate intermediate[3, 13, 14]. Flippases function in a complex with the ancillary β-subunit, cell cycle control protein 50 (CDC50)[3, 16]. CDC50 proteins possess two putative transmembrane domains separated by a large glycosylated extracellular domain. Despite the existence of 14 the P4-type ATPases in humans (15 in mice), there are only three CDC50 proteins expressed in mammals (CDC50A, CDC50B and CDC50C)[15], indicating that one CDC50 protein can associate with multiple P4-ATPases. It has been shown that most flippases associate specifically with CDC50A to exit the endoplasmic reticulum (ER) and translocate to the plasma membrane[17, 18].

Physiological functions of P4-ATPases

The physiological functions of P4-ATPases are evident from the findings that mutations in many of these transporters are responsible for several human genetic diseases linked to defective phospholipid transport. The two main target flippases studied in this thesis, ATP11C and ATP8A1, will be described in detail in "Section 1.4". Other flippases with known physiological function in mammals are briefly highlighted below.

ATP8B1 was the first member of the P4-type ATPase family to be related to a human disease, known as intrahepatic cholestasis. It is characterised by a defective bile salt extraction from liver into bile[19]. Moreover, mice studies revealed that ATP8B1 functions as a phospholipid flippase to maintain the normal phospholipid asymmetry of the canalicular membrane[20]. Hepatocytes from ATP8B1-deficient animals were shown to be more sensitive to bile salt-induced

membrane damage[21]. Mechanistically it was proposed that loss of ATP8B1 leads to cholestasis by increasing PS in the luminal leaflet of canalicular membranes, which in turn resulted in abnormal lipid packing[22]. This renders the outer leaflet of the canalicular membrane susceptible to bile salt mediated extraction of cholesterol and phospholipids, resulting in reduced activity of the bile salt export protein[19].

Patients with genetic defects in ATP8A2 have a rare neurodegenerative disease known as cerebellar ataxia, mental retardation and disequilibrium syndrome (CAMRQ)[23, 24]. In agreement with human findings, loss of ATP8A2 in mice led to the development of neurodegeneration in the central and peripheral nervous system evidenced by body tremors and ataxia[25]. A recent study illustrated that *Atp8a2*$^{-/-}$ mice also displayed shortened retinal photoreceptor outer segments and decreased photoreceptor viability, indicating a role for ATP8A2 in normal visual function. Moreover, ATP8A2 was required for auditory function as well as the survival of spiral ganglion cells[26]. *In vitro* transfection of cells defective in non-endocytic uptake of PS with ATP8A2 revealed an increase in PS translocation activity, confirming that ATP8A2 is a phospholipid flippase[25]. These studies collectively suggest an essential role for the flippase ATP8A2 in the function and survival of many neuronal cells, as well as in normal vision.

ATP8B3 is expressed in spermatozoa, and is required for asymmetric distribution of PS between the two leaflets of the sperm plasma membrane[27, 28]. Despite normal sperm morphology and motility, sperm from the ATP8B3 deficient animals exhibited compromised *in vitro* fertilization capability, suggesting a

possible role for ATP8B3 in the formation of acrosome and sperm function during fertilization[27].

ATP8B4 has been implicated in Alzheimer's disease based on genome-wide association studies[29].

Dysfunction of ATP10A has been implicated in the development of diet-induced obesity, non-alcoholic fatty liver disease in mice, and is considered as a risk factor for type-2 diabetes in African-Americans[30, 31]. In agreement with this notion, C57BL/6J mice carrying a stop codon in exon 12 of *Atp10d* gene are prone to develop obesity, hyperglycemia and hypertension upon a high-fat diet, suggesting a potential role for flippases in the development of obesity and type-2 diabetes[32].

ATP11A has been suggested to be a predictive marker for prognosis of colorectal cancer[33].

1.1.2 ATP-Binding Cassette (ABC) Transporters: phospholipid floppases

The second group of lipid transporters, known as floppases, belong to ABC-type transporters[2]. ABC transporters comprise a large class of membrane proteins involved in the active transport of a wide variety of compounds across cell membranes including phospholipids[9]. A significant number of ABC proteins are now known to play crucial roles in lipid homeostasis by actively transporting phospholipids from the cytoplasmic to the exoplasmic leaflet of cell membranes or exporting phospholipids to protein acceptors or micelles[2].

Floppase functions of ABC transporters were first identified in erythrocytes using spin- or NBD-labelled lipids[34, 35]. ABC transporters catalyse transport of specific lipids to the exoplasmic leaflet, and the most well characterised members are ABCB1 and ABCB4. ABCB4 has been implicated in the secretion of PC into the bile[36]. Subsequent studies further demonstrated a critical involvement for ABCB4 and ABCB1 in the outward translocation of different lipids including PC, PE, and SM[37, 38]. Other members of the ABC transporter family such as ABCB11, ABCG5 and ABCG8 have also been implicated in intrahepatic cholestasis and biliary excretion of cholesterol[39, 40].

1.1.3 Disruption of phospholipid asymmetry by scramblases

A third group of transporters, named scramblases, function in an ATP-independent manner and disrupt the asymmetric distribution of phospholipids in the plasma membrane, thereby causing PS to be exposed on the cell surface[5, 6]. In contrast to ATP-dependent flippases and floppases, scramblases facilitate bidirectional movement of all types of phospholipids randomly in an ATP-independent manner. Because they disrupt bilayer asymmetry they require activation such as elevation of the intracellular Ca^{2+} levels or the activation of caspases[41, 42]. Transmembrane protein 16F (TMEM16F)[41] has been identified as a calcium-dependent scramblase which initiates PS exposure during platelet activation, while XK-related protein 8 (XKR8)[42] acts as a caspase-activated scramblase to facilitate PS exposure during apoptosis.

TMEM16F

TMEM16F is a member of the TMEM16 family proteins, which are also called anoctamins. Using *in vitro* reconstitution assays, purified TMEM16F orthologues from fungus were first found to have calcium-dependent scramblase activity[43]. A mutation in the TMEM16F gene was found to cause a mild bleeding disorder called Scott syndrome, a haemorrhagic disorder in which Ca^{2+}-induced lipid scrambling was compromised, both in humans[41, 44] and in a canine model[45], further confirming the scramblase activity of TMEM16F, and indicating that TMEM16F was indispensable for the PS exposure in activated platelets and thus required for blood clotting.

XKR8

Different from activated platelets, it was reported that PS exposure occurs in apoptotic platelets even in the absence of functional TMEM16F[46]. Moreover, apoptotic platelets require caspases but not calcium to expose PS[47], suggesting the existence of a different scramblase, which is Ca^{2+}-independent but caspase-dependent. Using an expression cloning strategy, XKR8 was identified, whose overexpression resulted in elevated PS exposure[42]. Moreover, it was reported that XKR8 was cleaved by caspases at a C-terminal cleavage site[48]. Apoptotic cells expressing a caspase-resistant XKR8 could not expose PS, suggesting that caspase cleavage was required to activate scramblase activity of XKR8[48]. In addition, many of the characteristic markers of apoptosis, including caspase activation, cell shrinkage, and DNA degradation, all occurred normally in the

absence of XKR8, suggesting that this protein is not part of the apoptosis inducing machinery, but rather is specific to the process of PS exposure itself[49, 50].

1.2 Phosphatidylserine exposure on the plasma membrane

During certain physiological or pathological processes, the asymmetric distribution of phospholipids in the plasma membranes is disrupted by scramblases, resulting in PS exposure on the cell surface. Exposed PS has important functions in many biological and pathological processes, such as bone mineralization, fertilization, myoblast fusion, erythropoiesis, rod cell shedding, synaptic pruning, and parasite-host interactions[1, 5, 6]. Among them, two physiological applications of PS exposure, apoptotic cell clearance and blood coagulation, are relevant for this thesis. Therefore, they are detailed in this section. During apoptosis PS exposure facilitates the engulfment of apoptotic cells by phagocytes[51, 52] (Figure 1.4 A); During platelet activation by contrast, PS is externalized to support thrombin generation and promote blood coagulation[6, 53] (Figure 1.4 B). In addition, recent evidence showed that, to support stable PS exposure, activation of scramblases alone is insufficient; inactivation of flippases is required as well to prevent PS from being flipped back in apoptotic cells[54, 55].

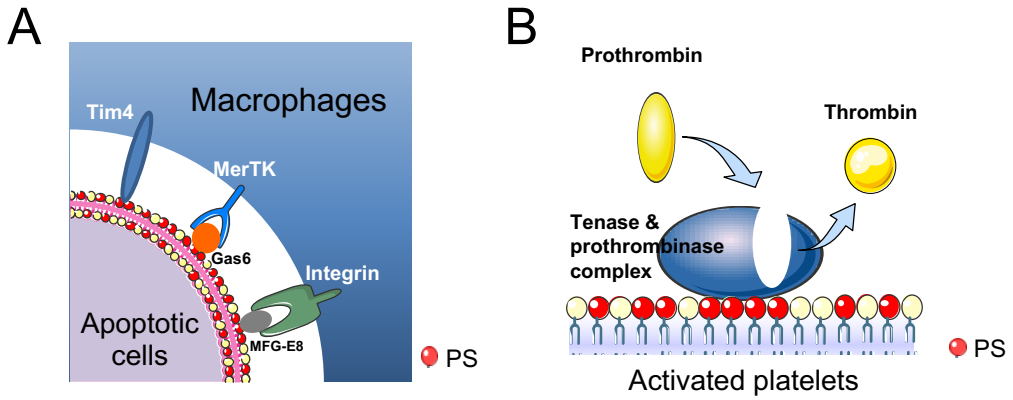

Figure 1.4 Physiological applications of PS exposure in apoptotic cell clearance and blood coagulation

(A) Apoptotic cell clearance: apoptotic cells expose PS as an "eat me" signal to induce phagocytosis by professional and nonprofessional macrophages through PS receptors and PS binding molecules.

(B) Blood coagulation: several reactions of the coagulation cascade, such as the formation of tenase and prothrombinase complex and the generation of active thrombin, are catalysed by the presence of PS-containing lipid surfaces, mainly presented by activated blood platelets. Acronyms: Tim4, T-cell immunoglobulin- and mucin-domain-containing molecule 4; MerTK, tyrosine-protein kinase Mer; Gas6, growth arrest-specific protein 6; MFG-E8, milk fat globule EGF factor 8.

1.2.1 PS exposure and apoptosis

Apoptosis pathways and activation of caspases

Apoptosis is an evolutionarily conserved programmed cell death process that removes unwanted or harmful cells. This process involves chromatin condensation, DNA fragmentation, cell shrinkage, and blebbing of plasma membranes. Usually apoptosis is executed by two distinct but convergent pathways: the intrinsic and extrinsic pathways[51, 56].

The intrinsic pathway is activated during the process of development or by genotoxic stimuli (e.g. antitumor drugs or gamma-rays)[51]. The critical regulators and effectors of this pathway are proteins of the B-cell lymphoma-2 (BCL2) family, which are characterized by the presence of one or more BCL2 homology (BH) domains (named BH1, BH2, BH3 and BH4). In general, pro-survival members of the BCL2 family restrain the activity of pro-death members, such as BCL2-antagonist/killer 1 (BAK1) and BCL2-associated X protein (BAX). Stress signals activate the BH3-only proteins, which triggers BAX/BAK1 oligomerization to cause mitochondrial outer membrane permeabilization[56]. This facilitates diffusion of cytochrome c out of mitochondria, triggering formation of apoptosomes and subsequent activation of caspase-9. This leads to the sequential activation of the downstream effector caspases, caspase-3 and -7[57, 58].

The other apoptotic pathway, the extrinsic, is initiated by death ligands, such as Fas ligand (FasL), tumor necrosis factor (TNF), and TNF-related apoptosis-inducing ligand (TRAIL), binding to cell surface death receptors that belong to

the TNF receptor family, such as the first apoptosis signal receptor (Fas) or TNF receptor-1 (TNFR1)[58]. Once activated, the death-inducing signaling complex (DISC) is assembled, which recruits the adaptor protein FAS-associated death domain (FADD) and caspase-8. Following proteolytic cleavage, the activated form of caspase-8 induces death signalling via activation of downstream effector caspases-3/7[56, 58].

Caspases are a family of cysteine proteases that carry a cysteine residue at the active site and cleave after aspartic acid. Caspases are executioners of both intrinsic and extrinsic apoptosis pathways and are responsible for many of the hallmarks of apoptosis, such as DNA fragmentation, membrane blebbing, and PS exposure[59].

PS exposure and clearance of apoptotic cells

Apoptotic cells are engulfed by macrophages before they rupture, which prevents inflammation or autoimmunity. This differs from necrosis, in which cells swell and plasma membranes are ruptured, spilling out cellular contents[60, 61]. For clean and efficient clearance, apoptotic cells must generate a surface signal that leads to recognition and phagocytic engulfment by professional phagocytes or nonprofessional neighbours. A variety of protein and molecules presented or modified on the surface of apoptotic cells have been proposed as recognition signals, but by far the best characterized “eat me” signal is the exposure of PS in the outer leaflet of the apoptotic cell plasma membrane[62, 63].

Clearance of apoptotic cells is a two-step process, in which phagocytic cells first bind and then engulf the dying cell[51, 58] (Figure 1.4 A). In the binding step, the

PS receptor such as T-cell immunoglobulin- and mucin-domain-containing molecule 4 (Tim4) tightly binds PS on the apoptotic cells and recruits them to the macrophage surface. In the engulfing step, soluble proteins such as growth arrest-specific protein 6 (Gas6) or milk fat globule EGF factor 8 (MFG-E8) bind to PS on apoptotic cells and activate their receptors [Tyrosine-protein kinase Mer (MerTK) or integrin, respectively] on phagocytes, leading to actin polymerization and engulfing of apoptotic cells. Both binding and engulfing steps are essential for the efficient clearance of apoptotic cells by macrophages[59, 60].

Defect of apoptotic cell clearance and autoimmune diseases

The exposure of PS on the surface of apoptotic cells is important not only because it is the basis of an efficient clearance process, but also because it enables this process to be immunologically silent[64]. PS-dependent removal of apoptotic cells results in release of anti-inflammatory mediators [e.g. transforming growth factor-β (TGF-β), IL-10, and prostaglandins] as well as suppression of inflammatory cytokines (e.g. IL-6, IL-8, and TNF)[65]. A defect in PS exposure or reduced phagocytic capacity may cause defective clearance of apoptotic cells, which makes cells undergo necrosis with ensuing loss of plasma membrane integrity. Leaked cellular contents can become autoantigens that challenge immunological tolerance. Generation of immune complexes of autoantigens and autoantibodies can lead to production and release of inflammatory cytokines. Together, these events complete a vicious cycle of chronic inflammation[66]. Indeed, defects in the elimination of apoptotic cells are associated with autoimmune diseases such as systemic lupus erythematosus (SLE) and

rheumatoid arthritis and can be factor in a variety of other conditions, including neurological diseases[65, 67-69].

1.2.2 PS exposure and blood coagulation

Blood coagulation and platelets

Excessive blood loss after vessel wall injury is prevented by blood coagulation. The haemostatic response is initiated when the endothelial cell lining of the circulatory system is breached so that blood cells and proteins contact sub-endothelial structures. According to a widely used model[70] (Figure 1.5), blood coagulation can be divided into three separate phases: 1) an initiation phase, in which low amounts of active coagulant factors are generated; 2) an amplification phase, in which the level of coagulation factors is boosted and the tenase and prothrombinase complexes are formed; and 3) a propagation phase, occurring on surfaces containing PS, in which coagulation factors bind to highly procoagulant membranes of activated platelets and thrombin are generated and fibrin clots are formed.

Platelets are enucleated specialized blood cells essential for haemostasis and thrombosis, and play a dual role in thrombus formation[53]. On the one hand, platelets adhere to the extracellular matrix, in particular collagen, and rapidly aggregate to build a plug that provides the primary arrest of the bleeding; On the other hand, platelets provide a catalytic surface with PS for coagulation factors, promoting the formation of an insoluble meshwork of fibrin polymers that consolidates the thrombus to prevent further blood loss. The formation of this

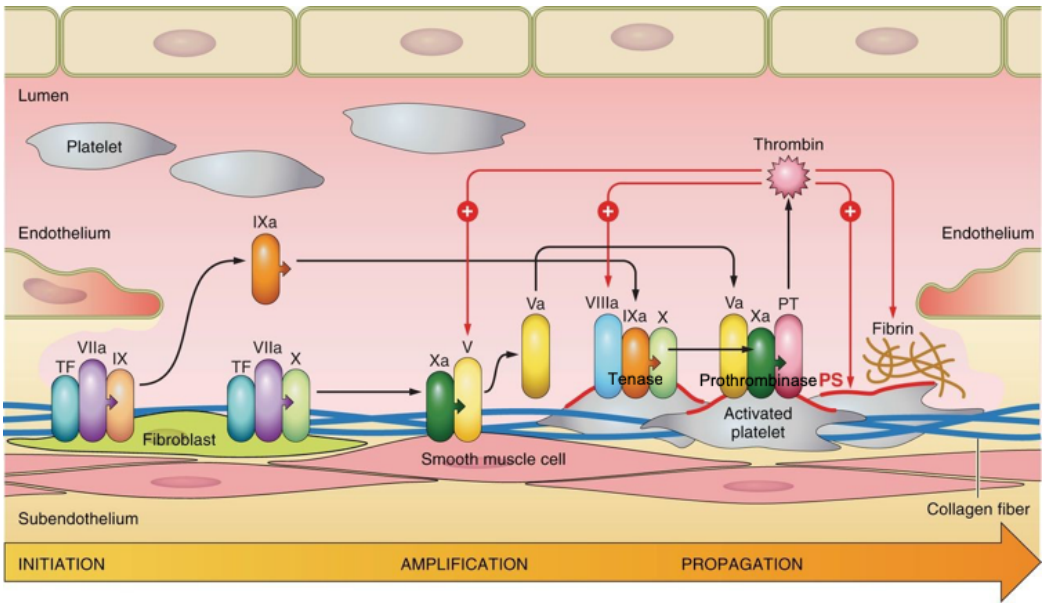

Figure 1.5 Blood coagulation[6]. In the initiation phase, circulating traces of factor VIIa bind to tissue factor (TF) on cells in the subendothelium to form a complex that activates factors IX and X. During the amplification phase, traces of thrombin activate factors VIII and V. Factors IXa and Xa, together with factors VIIIa and Va, form the tenase and prothrombinase complexes, respectively. In the propagation phase, both complexes form on activated platelets that accumulate locally and expose PS in response to collagen and trace amounts of thrombin, to promote the conversion of prothrombin (PT) to thrombin and formation of fibrin. The diagram is modified from Bevers, E.M. and Williamson, P.L. 2016[6].

catalytic surface by exposure of PS is consider as the platelet procoagulant response and is the direct result of the collapse of lipid asymmetry caused by activation of phospholipid scramblase.

Procoagulant function of platelets, PS exposure and Ca^{2+} signal

In activated platelets, PS is exposed on the cell surface. The exposed PS can support the assembly of coagulation complexes, and support the generation of thrombin and formation of fibrin[6, 53] (Figure 1.4B and 1.5). Generally, in the initiation and amplification phase of blood coagulation, circulating traces of coagulation factor VIIa bind to tissue factor (TF) on cells in the sub-endothelium to form a complex that activates factors IX and X[71]. In parallel, slowly accumulating amounts of thrombin activate downstream coagulation factor VIII to form the tenase complex. In the propagation phase, on PS-exposing cell membranes of platelets, the tenase complex catalyzes the conversion of factor X to Xa, after which the prothrombinase complex of factor Xa and Va catalyzes the conversion of prothrombin to thrombin, produces sufficient amounts of thrombin to massively form fibrin fibers[72]. As a final step, the thrombin-activated plasma transglutaminase FXIIIa catalyzes the formation of covalent crosslinks between adjacent fibrin chains to yield an elastic, polymerized fibrin clot[73]. In short, the exposure of PS on platelets provides a scaffold for efficient thrombin generation, promoting blood coagulation[6, 53].

The platelet procoagulant response is provoked by strong agonists that cause a high and persistent elevation of the intracellular Ca^{2+} concentration[74]. The most powerful physiological stimulus is the combination of collagen and thrombin.

Collagen, a major component of the extracellular matrix, interacts with the glycoprotein VI (GPVI) receptor at the platelet membrane. Traces of thrombin, produced locally during the initial stage of coagulation, strongly amplify the effect of collagen on the procoagulant response by cleaving protease-activated receptors PAR1 and PAR4[75]. Co-stimulation by both collagen and thrombin provokes PS exposure in a much larger platelet fraction than either of these two agonists alone. As might be expected, coincident stimulation by both agonists induces a high and sustained Ca^{2+} signal. Either of these two agonists separately causes a transient rise in intracellular Ca^{2+} by "store operated Ca^{2+} entry (SOCE)," a release of Ca^{2+} from internal stores. When applied together, collagen and thrombin activate a store-independent- or receptor-operated Ca^{2+} entry (ROCE) that cannot be induced by either of these two agonists alone[76]. ROCE involves nonselective cation channels of the transient receptor potential cation channel (TRPC) family proteins (e.g. TRPC3 and TRPC6), and a reverse mode of Na^{+}/Ca^{2+} exchange that leads to sustained elevated Ca^{2+}, sufficient to activate the scramblase process[76]. This synergistic action of thrombin and collagen is one illustration of the mutual enforcing interaction between platelets and coagulation during the haemostatic process. In addition, the physiological signal transduction pathways can be bypassed by treatment of cells with a Ca^{2+} ionophore (e.g. compound A23187) in the presence of extracellular Ca^{2+}. With this treatment strong scramblase activation and PS exposure can be directly achieved[77].

Defect of PS exposure in platelets and bleeding disorders

As indicated in "Section 1.1.3", during agonist-mediated activation of platelets, PS exposure is catalysed by a calcium-dependent scramblase TMEM16F[41].

Mutations in the gene encoding TMEM16F result in defective PS exposure and give rise to a rare bleeding disorder known as Scott syndrome[41, 44, 78-80].

Although being a rare disorder, a lot has been learned from Scott syndrome patients[81]. This pathological condition was first described in 1979 by Weiss et al. in a patient with a history of moderate to severe bleeding, and it was called Scott syndrome after the patient, Mrs. M. A. Scott (1939–1996)[82]. This rare disorder appeared to be due to an impaired platelet procoagulant response. In 1985, Rosing et al. reported that the syndrome originated from a defective scramblase activity[83], but it was only in 2010 that mutations in the gene for TMEM16F were shown to be responsible for the defect[41], also confirming that it was an inherited disorder[84]. Recently, TMEM16F knockout or platelet-specific TMEM16F knockout mice showing the Scott phenotype were successfully generated, and data obtained from the limited number human Scott patients could be further confirmed[79, 85, 86].

The most characteristic feature of Scott platelets is a reduced development of tenase and prothrombinase activity caused by reduced PS exposure upon activation. In addition, several morphological changes seen upon adhesion of normal platelets are impaired: Scott platelets do not form balloon-like structures and do not shed microvesicles. However, Scott patients have no prolonged bleeding time after superficial cuts and do not easily bruise, indicating that other platelet functions are normal[87].

1.2.3 PS exposure and inactivation of flippases

Previous evidence, gathered in immune cells and related cell lines, suggested that both activation of scramblases and inactivation of flippases by caspases were required to support stable PS exposure and to prevent PS from being flipped back to the inner leaflet in apoptotic cells[42, 48, 54, 55].

It has been reported that PS flippase ATP11C is inactivated through caspase-mediated cleavage to facilitate apoptotic PS exposure in leukocytes[54]. ATP11C plays a key role in restricting PS to the inner leaflet of the plasma membrane of living cells. ATP11C has three caspase-3 recognition sites at its middle and nucleotide-binding domain, and cleavage of ATP11C at these sites can inactivate its flippase activity. Aspartate to Alanine point mutations in the caspase recognition sites of ATP11C prevent its cleavage by caspase but retain PS transport activity. Cells expressing caspase-resistant ATP11C do not expose PS on the surface of cells during apoptosis and these cells are not ingested by macrophages, indicating that the flippase must be inactivated for apoptotic PS exposure[54].

ATP11C is not the only flippase playing important roles in preventing PS exposure on cell surfaces. In some cells ATP11A, with a similar substrate specificity and plasma membrane localization as ATP11C, can compensate for the loss of ATP11C and prevent the exposure of PS on cell surfaces[55]. Similar to ATP11C, ATP11A has a number of caspase cleavage sites and is inactivated through cleavage during apoptosis[55]. These studies suggest that, besides

activation of the scramblase, inhibition of flippases is required for exposure of PS on cells as a signal for apoptosis.

Additionally, a recent study revealed a mechanism of flippase ATP11C down-regulation via clathrin-mediated endocytosis upon Ca^{2+}-mediated protein kinase C (PKC) activation in non-apoptotic cells[88].

1.3 Flippases in intracellular membranes

In addition to the plasma membrane, flippases also function in generating phospholipid asymmetry in intracellular membranes, including endoplasmic reticulum (ER), trans-Golgi network (TGN), and endosomes[5, 89-91], and play a critical role in vesicle-mediated protein trafficking[92, 93]. As detailed below, studies in *Saccharomyces cerevisiae*, *Arabidopsis thaliana* and *Caenorhabditis elegans*, together with the present findings in mammalian cells, suggest a non-redundant function for the P4-ATPases in secretory vesicle formation and membrane trafficking, and indicate that the function is evolutionally conserved from lower eukaryotes to mammals.

1.3.1 Flippases and intracellular membrane trafficking

Intracellular membrane trafficking is mediated by vesicular and tubular carriers formed at the plasma membrane or organelles. During formation of the vesicular-tubular carriers and fusion of organelles, dynamic membrane shape changes occur. These shape changes are thought to involve modification in the composition and distribution of lipids. Therefore, changes in the transbilayer lipid composition mediated by flippases are thought to be crucial for membrane deformation and resulting vesicle-mediated trafficking within cells[5, 89, 90].

One hypothesis for the mechanism by which flippases function in the generation of intracellular vesicles is that, flippase-mediated unidirectional movement of phospholipids generates an imbalance in the level of lipids between the leaflets of

the bilayer. As a result, the lipid loading in the cytoplasmic leaflet would drive inwardly directed membrane deformation, leading to the membrane curvature, which facilitates membrane budding to form transport vesicles together with budding machinery[16, 94, 95].

Endosomes are multifunctional intracellular vesicular organelles that regulate membrane transport between the plasma membrane and various intracellular compartments[96-98]. After internalised cargoes such as soluble proteins, membrane proteins, and lipids arrive at early endosomes, some are recycled back to the plasma membrane; some are retrograde transported from early endosomes to the Golgi complex, whereas others are transported to late endosomes and lysosomes for degradation[99, 100]. PS is highly enriched in the cytoplasmic leaflet of recycling endosomes and flipping of PS is crucial for endosome-mediated protein trafficking[92, 93]. Therefore, the PS-flipping activity of flippases is thought to be indispensable for endosomal membrane trafficking in eukaryotic cells.

1.3.2 Evidences of flippases in vesicle-mediated protein trafficking

The first evidence for involvement of flippases in vesicular trafficking was demonstrated in the baker's yeast *Saccharomyces cerevisiae*. There are totally five P4-ATPases in yeast (Drs2p, Neo1p, Dnf1p, Dnf2p, and Dnf3p) which are localized to specific cellular compartments. All five flippases in yeast are required for membrane trafficking in the secretory and endocytic pathways at different stages[11, 101]. Studies have shown that Drs2p (a yeast homologue of ATP8A1),

which flips PS and to a lesser extent PE, is essential for membrane traffic between the late Golgi compartment and endosomes. Drs2p predominantly localises to the TGN where clathrin-coated vesicles bud[102, 103]. PS flipping by Drs2p enhances membrane curvature, and increases the negative surface charge which is required for the function of GTPase-activating protein (GAP) Gcs1p. Gcs1p is crucial for protein transport between the TGN and endosomes[104, 105]. In addition, PS flipping at the TGN is required for exocytic protein sorting[106]. Yeast cells depleted of Drs2p accumulated aberrant membrane structures and exhibited impaired formation of clathrin-coated vesicles[106]. Other yeast flippases such as Dnf1 and Dnf2 have also been shown to participate in endocytic vesicle formation[102, 107].

Besides yeast, the involvement of the flippase family in membrane trafficking has also been demonstrated in higher organisms, including *Arabidopsis thaliana* and *Caenorhabditis elegans*[108-110]. In *Arabidopsis thaliana*, a P4-ATPase ALA3 that localizes at the Golgi is essential for the formation of secretory vesicles[108]. In *Caenorhabditis elegans*, loss of the P4-ATPase TAT-1, related to mammalian ATP8A1, leads to the generation of abnormal endo-lysosomal compartments, suggesting that endocytic cargo sorting and recycling are impaired[109, 110].

The functions of P4-ATPases in membrane trafficking are being uncovered in mammalian systems as well.

ATP8A1

ATP8A1 is localized to PS-positive recycling endosomes and is involved in intracellular membrane trafficking. In COS-1 cells, PS flipped by ATP8A1 to the

cytoplasmic leaflet of recycling endosomes is required for recruitment of evectin-2, which plays a role in cholera toxin transport from the endosomes to the Golgi[92]. ATP8A1 catalyzed flipping of PS is also required for the recruitment of the membrane fission protein EH domain containing 1 (EHD1) to recycling endosomes and for endosome-mediated trafficking[111]. Depletion of ATP8A1 impaired the asymmetric transbilayer distribution of PS in recycling endosomes, dissociated EHD1 from recycling endosomes, and generated aberrant endosomal tubules that appear resistant to membrane fission[111]. In HeLa cells, however, it was shown that ATP8A1 localizes to late endosomes, but not early/recycling endosomes[112].

ATP8A2

ATP8A2 is crucial for axon elongation in PC12 cells and hippocampal neurons, suggesting a role of this flippase in vesicle trafficking required for neurite extension[113]. Similarly, ATP8A2 deficient mice show a striking loss in the length of photoreceptor outer segments, suggesting that a decrease in vesicle trafficking between the inner and outer segment of these cells occurs in the absence of ATP8A2[26].

ATP9A

In Hela cells, ATP9A is localized to endosomes and the Golgi complex, and is involved in the formation of transport vesicles or tubules. Depletion of ATP9A delayed the recycling of transferrin from endosomes to the plasma membrane, and caused accumulation of glucose transporter 1 in endosomes, probably by inhibiting their recycling[114].

ATP10A

ATP10A promoted membrane tabulation upon recruitment of Bin/amphiphysin/Rvs (BAR) domains to the plasma membrane[115].

1.3.3 Vesicle-mediated protein trafficking in platelets

Platelets have complete intracellular membrane systems[116], including ER, Golgi complex and endosomes, and possess fundamental membrane trafficking processes such as endocytosis[117]. Endocytosis in platelets is an important process for loading certain granule cargo, such as fibrinogen and vascular endothelial growth factor (VEGF)[117]. Moreover, upon activation platelets undergo dramatic shape change[53] (e.g. swelling of the cell and formation of pseudopodia) and activate exocytosis such as secretion of procoagulant components and release of granules (dense-/α-granule)[118]. These processes require a large number of membrane structures; therefore, it is tempting to speculate that flippase-mediated asymmetric distribution of phospholipids in organelles enable the normal operation of these activities.

1.4 Flippases mainly studied in this thesis

As mentioned in “Section 1.1”, there are 14 members of the P4-ATPase family in human and 15 members in mice[11], and some of these play important roles in physiological and pathological processes. In this section, I will highlight the functions of ATP11C and ATP8A1, which are the two flippases mainly studied in this thesis, as well as diseases caused by their dysfunction. In brief, the loss of ATP11C activity causes B-cell deficiency[119, 120], cholestasis[121] and anemia[122] in mice, and congenital hemolytic anemia in humans[123]. ATP8A1 has been found to promote cell proliferation and migration[124-126], and its dysfunction is associated with delayed hippocampus-dependent learning[127] and autistic-like behaviour in mice[128].

1.4.1 ATP11C and B cell development

Adaptive immune system and B lymphocytes

The immune system provides the body with an effective defence mechanism against potential infections by bacteria, viruses, fungi or parasites. There are two arms of the immune system to help fight off these infectious agents, namely innate and adaptive immune system.

The innate immune system provides the first line defence by a range of different cell types (e.g. macrophages, granulocytes, and dendritic cells) and by physical and chemical barriers that prevent pathogens from entering the body[129].

The adaptive immune system is composed of a population of white blood cells termed lymphocytes. There are two main types of lymphocytes called B cells and T cells that are activated if the innate immune system is unable to rapidly eliminate the pathogen. B cells play a critical role in the generation of humoral immunity through their ability to secrete a large amount of antibodies in response to recognition of a specific antigen[130]. Antibodies can bind to antigens expressed by microbes to make them the main targets for phagocytes. Besides producing antibodies, recent studies suggest that B cells have broader roles in the immune system, which include the ability to act as antigen presenting cells[131] and produce cytokines[132]. Antibodies can only bind to pathogens that are present in the blood and the extracellular spaces. In contrast, T cells can destroy cells infected with intracellular pathogens. The relevant work presented in this thesis will focus primarily on B cells in relation to their development, while T cells are outside the scope of this thesis.

Early B cell development

Like other cells of the immune system, lymphocytes originate from self-renewing haematopoietic stem cells (HSCs) primarily in the foetal liver before birth and in the bone marrow during the postnatal period. The multipotent HSCs-derived B cell progenitors reside and complete their development within the bone marrow. Differentiation of B cells from HSCs is one of the best-defined cell differentiation processes in vertebrates, and different stages (pre/pro-B, pro-B, pre-B, immature B and mature B cells, Figure 1.6) can be characterised by the expression of a variety of specific cell surface molecules[130].

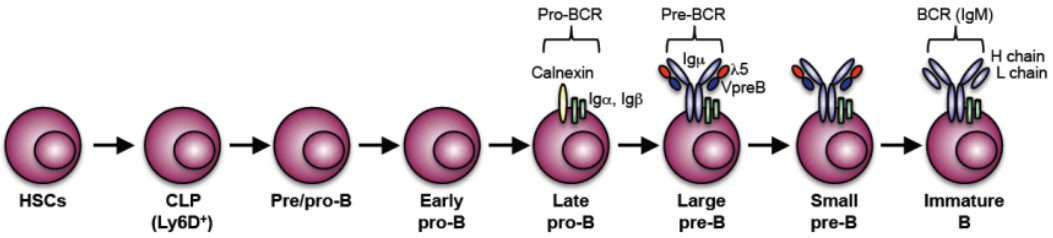

Figure 1.6 Developmental stages of B cells in the bone marrow

The diagram is modified from Yabas M. et al, 2014[133]. HSCs, haematopoietic stem cells; CLP, common lymphoid progenitors; BCR, B-cell receptor.

The earliest B cell progenitor cells, known as pre/pro-B cells are derived from $Ly6D^+$ common lymphoid progenitors (CLPs)[134]. Early studies suggested that pre/pro-B cells express B220 on their surface, but are not yet committed to the B cell lineage and express low levels of recombination activating gene proteins RAG1 and RAG2[135-137].

Pre/pro B cells differentiate into pro-B cells (early and late pro-B cells) that express CD19 on their surface, which is believed to be one of the earliest hallmarks of commitment to the B cell lineage. Pro-B cells express two signalling components known as Igα (CD79a) and Igβ (CD79b). They are, together with the molecular chaperone calnexin, thought to form the pro-B cell receptor (pro-BCR) on the surface of pro-B cells (Figure 1.6)[138].

To generate a diverse repertoire of antigen receptors in B cells, Ig heavy chain D to J rearrangements are initiated at the early pro-B cell stage followed by V to DJ rearrangements in late pro-B cell stage to produce a functional Igμ heavy chain protein in the cytoplasm (Figure 1.6). This VDJ recombination is mediated by the RAG1 and RAG2 proteins, which are highly expressed in pro-B cells[135], and mice deficient for these proteins have a developmental block at the transition from pro-B to pre-B cell stage[139, 140]. Once produced, the functional Igμ associates with the surrogate light chain (SLC) proteins VpreB and λ5, which are highly expressed on pro-B cells[141, 142], as well as the signalling subunits Igα and Igβ, which noncovalently associate with Igμ, to form the precursor (pre)-BCR on their surface (Figure 1.6)[143].

The formation of a functional pre-BCR marks the transition to the pre-B cell stage (large and small pre-B cells), and is an important check-point for the survival, proliferation and differentiation of pre-B cells[144-147]. Animals deficient for any component of the pre-BCR complex exhibit a partial or complete developmental arrest at the pro-B cell stage of B lymphopoiesis in the bone marrow[148-150].

Large pre-B cells eventually exit the cell cycle and become resting small pre-B cells, which begin to undergo Ig light chain V to J rearrangement by reactivating the expression of RAG1 and RAG2 proteins[151]. Successful production of complete and in-frame κ or λ light chain marks the second essential check-point and allows pre-B cells to express IgM on the cell-surface (Figure 1.6)[130]. These cells are now called immature B cells, which leave the bone marrow and migrate to the periphery to undergo the final steps of B cell maturation.

ATP11C deficiency and block of B cell development

As a member of the P4-ATPase family, ATP11C has been shown to play a critical role in regulating phospholipid distribution in the plasma membrane, and its dysfunction is related to many pathological processes. Previous studies showed that loss of ATP11C in mice resulted in a block of B cell development at the pro-B cell stage in the bone marrow, resulting in B cell deficiency[119, 120].

In the study by M. Yabas and colleagues, a previously unknown X-linked B-cell deficiency syndrome in mice was described for the first time, which was caused by *N*-ethyl-*N*-nitrosourea (ENU)-induced mutations of the murine *Atp11c* gene[119]. Functional analysis using fluorescently labelled phospholipid

analogues revealed that cells of the immune system from ATP11C-deficient mice exhibited impaired aminophospholipid flippase activity compared to those from control animals. Loss of ATP11C mediated flippase activity in mice led to a severe B cell deficiency due to a developmental arrest at the pro-B cell stage during early B cell development in the bone marrow. The number of splenic follicular B cells and peritoneal B1 cells was also severely reduced in mutant mice. However, marginal zone B cells as well as other haematopoietic lineages including T, NK and myeloid cells accumulated normally in mutant mice. The requirement for ATP11C in B cells could not be corrected by the enforced expression of the pro-survival protein BCL-2 (which inhibited apoptosis) or by transgenic expression of IL-7 (which significantly increased IL-7 level) or expression of pre-rearranged immunoglobulin transgenes (which bypassed the pre-BCR signalling). These experiments excluded enhanced apoptosis, or attenuated IL-7/pre-BCR signalling as a possibility for the lack of pre-B cells. These results identified an intimate connection between phospholipid transport and B lymphocyte function and suggested that ATP11C mediated internalization of PS was crucial for differentiation of B lymphocytes[119, 120].

1.4.2 ATP11C and erythrocytes

Studies of ATP11C-deficient mice also provided strong evidence for a crucial role of ATP11C in establishing PS asymmetry in developing erythrocytes. The mutant mice exhibited altered erythrocyte shape, reduced erythrocyte life span, and anaemia[122]. More specifically, mice lacking ATP11C were found to display

reduced uptake of fluorescently labelled PS by developing erythrocytes (erythroblasts) but not mature erythrocytes. However, mature circulating erythrocytes from mutant mice had an elevated percentage of PS accumulated on their surface, displayed abnormal shape characteristic of stomatocytosis, and had a shortened lifespan, resulting in anaemia in mice. These studies indicated that ATP11C was critical in generating and maintaining PS asymmetry during erythropoiesis, a process that was important in generating normal mature erythrocytes. The high content of PS and PE on the cytoplasmic leaflet of erythrocytes may be important for the interaction of the spectrin-ankyrin cytoskeletal network with the plasma membrane, which is required for maintaining the normal shape of erythrocytes. Whereas the absence of PS on the exoplasmic leaflet of erythrocytes is important for maintaining the normal lifespan of these cells. Therefore, these findings uncovered an essential role for ATP11C in erythrocyte morphology and survival and provided a new candidate for the rare inherited blood disorder stomatocytosis with uncompensated anaemia.

ATP11C has also been identified as a major flippase in human erythrocytes, and mutations in the gene encoding ATP11C cause haemolytic anaemia in humans[123]. A mutation of the *ATP11C* gene was identified in a male patient with congenital hemolytic anemia that was inherited as an X-linked recessive trait. PS internalization in erythrocytes with the mutant ATP11C was decreased 10-fold compared to that of the control, functionally establishing that ATP11C was a major flippase in human erythrocytes. However, PS was still retained in the inner leaflet of the majority of control and patient mature erythrocytes, suggesting that

PS cannot be externalized as long as scramblase is inactive[123] or the presence of redundant flippase activity.

1.4.3 ATP8A1

ATP8A1 (also known as ATPase II) was the first P4-ATPase discovered in mammals[152]. The gene encoding ATPase II was first cloned and sequenced from bovine chromaffin granules in 1996[152]. ATP8A1 was also the first human member of the P4-ATPase family to be cloned. It was first discovered in the plasma membrane of erythrocytes in 2006[153]. The biochemical characteristics of human ATP8A1 are consistent with the flippase ATPase II from bovine chromaffin granules[154]. Since then ATP8A1 has been shown to be a PS-selective flippase[155, 156] and to be associated specifically with CDC50A to exit the endoplasmic reticulum. ATP8A1 is found in the plasma membrane and intracellular membranes[17, 18].

Functional studies gave insight into the biological roles of ATP8A1. Studies on cell lines revealed role of ATP8A1 in promoting cell proliferation and migration. For example, the complex of ATP8A1 and CDC50A was found to be involved in the formation of membrane ruffles to promote cell migration[124]; MiR-140-3p suppression of cell growth and invasion is thought to be caused by down regulating the expression of ATP8A1 in non-small cell lung cancer[125]. Similarly, the proliferation of yes-associated protein (YAP)-dependent metastatic cancer cells was suppressed by knockdown of ATP8A1[126]. Studies on gene modified mouse models revealed a role of ATP8A1 in neurobiology, for instance

elevated hippocampal ATP8A1 levels are associated with autistic-like behaviour[128] and ATP8A1 deficiency is associated with delayed hippocampus-dependent learning[127]. Furthermore, as described in “Section 1.3.2”, ATP8A1 is localized to the PS-positive recycling endosomes and is involved in intracellular membrane trafficking[92, 111, 112].

Transcriptome[157] and proteome[158-161] studies suggest that ATP8A1 is highly expressed in both human and mouse platelets. However, the physiological roles of ATP8A1 in platelets remain unexplored.

CHAPTER 2: Materials and Methods

2.1 Mice

2.1.1 C57BL/6J (B6)

Inbred mouse strain was originally obtained from Jackson Laboratories, USA. Experiments were conducted on male mice between the ages of 8 and 20 weeks.

2.1.2 ATP11C$^{amb/0}$ (Ambrosius)

The Ambrosius (Amb) mouse strain was generated through N-ethyl-N-nitrosourea (ENU)-induced mutagenesis as described previously[119]. Only one single mutation in the gene *Atp11c* located in X-chromosome was identified in this stain. This mutation was a G to A substitution in the exon 27 splice donor sequence at the +1 position of intron 27, which resulted in skipping of exon 27 and splicing exon 26 to exon 28. The resulting deletion of 104 base pairs introduced a frame shift after the amino acid at position 1010, abolishing the C-terminal residues encoding the last two transmembrane domains and cytoplasmic tail of the ATP11C protein.

This strain was maintained either by breeding heterozygous females with wild-type littermates or with wild-type C57BL/6J males. Mice were genotyped by PCR amplification of DNA isolated from mouse-ear punches. All Amb mice and control littermates used for this study were male mice between 8-16 weeks old, unless otherwise noted.

All experimental mice were housed in specific pathogen free conditions at the Australian Phenomics Facility and all animal procedures were approved by the

Australian National University Animal Ethics and Experimentation Committee (Protocol A2014/62 and A2017/54).

2.2 Human blood

Human blood samples were obtained with consent from healthy donors in accordance with the Declaration of Helsinki under protocols approved by the Australian National University Human Research Ethics Committee (Protocol 2016/317).

2.3 Buffers, solutions and media

Buffers, solutions and media were sourced or prepared as described in Table 2.1.

2.4 Cell preparation

2.4.1 Preparation of leukocytes

Mice were sacrificed by cervical dislocation. Bone marrow and spleen were collected into 3 ml of ice-cold flow cytometry buffer. Bone marrow cells were extracted by pressurised flow of flow cytometry buffer through dissected femurs and tibias. Single cell suspensions from spleen were prepared by passing the tissues through 70 μm Nylon Cell Strainer (Corning). Red blood cells (RBC) in spleen samples were removed by incubating splenocytes with 3 ml of RBC lysis

buffer in 15 ml centrifuge tubes for 1-2 min on ice. Samples were then centrifuged for 5 min at 1500 rpm at 4 ºC, followed by discarding the supernatant. The pellets were washed once in 10 ml of ice-cold flow cytometry buffer followed by centrifugation and resuspension in 3 ml of flow cytometry buffer; and cells were counted using ViCELL cell counter (Beckham Coulter).

Table 2.1 Buffers, solutions and media

Buffers, solutions and media	Source and preparation
Phosphate-buffered saline (PBS) for leukocyte experiments	pH 7.4, Gibco
Flow cytometry buffer	PBS supplemented with 2% bovine serum (Thermo Fisher Scientific) and 0.1% sodium azide (Australian Chemical Reagents)
RBC lysis buffer	150mM NH_4Cl, 10mM $KHCO_3$ and 0.1mM EDTA, pH 7.3
Hanks' balanced salt solution (HBSS)	pH 6.0 or 7.4, containing calcium and magnesium, Gibco
Cell culture medium	RPMI 1640 (Life Technologies) supplemented with 10 mM HEPES (Sigma), 0.1 mM non-essential amino acid solution (Life Technologies), 1 mM sodium pyruvate (Sigma), 55 μM 2-merchapthoethanol (Life Technologies), 2% L-Glutamine 50 U/ml of penicillin-streptomycin (Life Technologies) and 10% heat-inactivated foetal calf serum (FCS) (Life Technologies), pH 7.2-7.5
Annexin-V binding buffer	Biolegend
Acid citrate dextrose (ACD) solution	69 mM citric acid, 85 mM sodium citrate and 20 mg/mL D-glucose, pH 4.6
Modified Tyrode's buffer	138 mM NaCl, 3 mM KCl, 0.5 mM $MgCl_2$, 5.5 mM glucose and 20 mM HEPES, pH 7.4
CGS buffer	123 mM NaCl, 33 mM glucose and 15 mM trisodium citrate, pH 7.0
Hypo-osmotic lysis buffer	15 mM KCl, 2 mM $MgCl_2$, 0.1 mM EDTA and 10 mM HEPES, pH 8.0

RIPA buffer	Sigma
T-PER tissue protein extraction reagent	Thermo Fisher Scientific
PBS for platelet experiments	pH 7.4, Medicago
Pre-lysis buffer for surface biotinylation	PBS supplemented with 1 mM $CaCl_2$ and 0.5 mM $MgCl_2$, pH 8.0
Lysis buffer for surface biotinylation	150 mM NaCl, 1% Triton X-100 and 20 mM Tris-HCl, pH 7.6
4× LDS sample buffer	Thermo Fisher Scientific
10× sample reducing agent	Thermo Fisher Scientific
MOPS-SDS running buffer	Thermo Fisher Scientific
SDS-PAGE transfer buffer	25 mM Tris, 192 mM glycine and 20% v/v methanol
PBS-Tween 20	pH7.4, Medicago
Stripping buffer	62.5 mM Tris-HCl, 2% SDS and 100 mM 2-mercaptoethanol, pH 6.8
Fluo-4 NW dye loading solution	Thermo Fisher Scientific

2.4.2 Preparation of platelets

Mice

For small number of platelets, whole blood (200μL) was collected from mice via retro-orbital bleeding into one-tenth volume of ACD anticoagulant. The sample was diluted into modified Tyrode's buffer (5mL) and centrifuged at 300*g* at room temperature for 10 minutes. The supernatant was collected and centrifuged at 1500*g* at room temperature for 10 minutes; the pelleted platelets were washed once and then resuspended in modified Tyrode's buffer at 5×10^8 cells/mL. For large number of platelets, whole blood (>200μL) was collected by cardiac puncture using a hypodermic needle (23G, Terumo) from mice that had been euthanized by CO_2. Blood was mixed with one-tenth volume of ACD anticoagulant. Washed platelets were prepared as described previously[162]. Briefly, whole blood (2-3 mL) was laid on top of 5 mL OptiPrep™ Density Gradient Medium (Sigma) barrier (1.063 g/mL) and centrifuged at 350 *g* at room temperature for 15 min. The platelet-rich layer was collected and washed twice with modified Tyrode's buffer after centrifugation at 300 *g* at room temperature for 10 min to remove residual red and white blood cells in the pellets. Platelet pellets were obtained through centrifugation at 1500*g* at room temperature for 10 min and then resuspended in modified Tyrode's buffer at 5×10^8 cells/mL.

Human

Human blood was collected into ACD anticoagulant and centrifuged at 110 *g* at room temperature for 20 min. The platelet-rich plasma was then collected and centrifuged at 1270 *g* at room temperature for 15 min. Platelet pellets were

washed three times with CGS buffer after centrifugation at 1270 *g* at room temperature for 15 min and then resuspended in modified Tyrode's buffer at 5×10^8 cells/mL.

2.5 Flippase activity assay

2.5.1 Leukocytes

Flippase activity assays on bone marrow cells and spleen cells were performed as previously described[163], using the following fluorescent lipid analogues: 1-palmitoyl-2-[6-[(7-nitro-2-1,3-benzoxadiazol-4-yl)amino]hexanoyl]-sn-glycero-3-phosphoserine (ammonium salt) (16:0-06:0 NBD-PS), 1-palmitoyl-2-[6-[(7-nitro-2-1,3-benzoxadiazol-4-yl)amino]hexanoyl]-sn-glycero-3-phosphoethanolamine (16:0-06:0 NBD-PE), and 1-palmitoyl-2-[6-[(7-nitro-2-1,3-benzoxadiazol-4-yl)amino]hexanoyl]-sn-glycero-3-phosphocholine (16:0-06:0 NBD-PC) (all from Avanti Polar Lipids). Cells were washed with Hanks' balanced salt solution (HBSS, pH 6.0) containing 1 mM $MgSO_4$ and 1.3 mM $CaCl_2$, and were then incubated with 5 μM NBD-labelled lipids in the same solution for 20 min at 15°C. To stop the assay (flipping of lipid analogues) and to remove unbound analogues from the cell surface, cells were placed on ice and incubated with HBBS (pH 7.4) containing 1 mM $MgSO_4$, 1.3 mM $CaCl_2$ and 1% fatty acid-free bovine serum albumin (BSA) (Sigma) for 5 min. Cells were then sedimented by centrifugation and re-incubated with 1% fatty acid-free BSA followed by centrifugation. Cells were then washed twice in HBBS (pH 7.4) containing 1 mM $MgSO_4$ and 1.3 mM $CaCl_2$ and transferred to a 96-well plate to be stained with fluorescently labelled

antibodies as described below in section "2.6 Flow cytometry and surface antibody staining". The data presented in "CHAPTER 3, Figure 3.1" were calculated based on the following formula: NBD-lipid uptake (%) = (geometric mean fluorescence intensity (MFI) of NBD-PS, -PE or -PC uptake into $CD45.2^+$ subsets / geometric MFI of NBD-PS uptake into $CD45.1^+$ splenic B cells) × 100.

2.5.2 Platelets

Flippase activity of platelets was assessed essentially as described above in section "2.5.1 Leukocytes" with the following modifications. Washed platelets were first stained with Brilliant Violet 421™ anti-mouse CD41 antibody (clone MWReg30, 1:600, Biolegend) and then incubated with 5 μM NBD-PS at room temperature for different periods of time in modified Tyrode's buffer supplemented with 1 mM $CaCl_2$. To extract un-internalised NBD-PS from the exoplasmic leaflet of the plasma membrane, platelets were washed twice with modified Tyrode's buffer containing 1 mM $CaCl_2$ and 4% fatty acid-free BSA followed by centrifugation. Platelets were then resuspended in the same buffer and analysed by a BD™ LSR II flow cytometer (BD Biosciences) to measure fluorescence of NBD-PS translocated into the cytoplasmic leaflet of the plasma membrane.

2.6 Flow cytometry and cell surface antibody staining

2.6.1 Leukocytes

Bone marrow cells or spleen cells were incubated with an optimised antibody cocktail in flow cytometry buffer and incubated for 30 min at 4°C in the dark. Samples were then washed and resuspended in flow cytometry buffer and analyzed on an LSR II or LSR Fortessa flow cytometer (BD Biosciences). Dead cells were excluded by gating on 4′,6-diamidino-2-phenylindole (DAPI) positive cells or 7-Aminoactinomycin D (7-AAD) positive cells. Antibodies and reagents used for cell surface labelling and flow cytometric analysis are listed in Table 2.2.

2.6.2 Platelets

For flow cytometric analysis of platelets, samples were incubated with Brilliant Violet 421™ anti-mouse CD41 antibody (1:600, Biolegend) at room temperature for 20 min and were then diluted in modified Tyrode's buffer with 1 mM $CaCl_2$ and analysed by a BD™ LSR II flow cytometer. Doublets and microparticles were excluded by forward scatter and side scatter gates. Platelets were defined by CD41 positive gates. Antibodies and reagents used are listed in Table 2.2.

2.7 Measurement of PS exposure

PS exposure on the cell surface was assessed by measuring the binding of Annexin-V through flow cytometry in leukocytes and platelets as described in the following.

Table 2.2 List of antibodies and reagents used in the cell surface labelling and flow cytometric analysis

Target	Clone	Conjugation	Company	Dilution
CD45.1	A20	Alexa Fluor 700	Biolegend	1:600
CD45.2	104	BUV 737	BD Biosciences	1:600
CD45.2	104	Pacific Blue	Biolegend	1:600
CD45R/B220	RA3-6B2	APC Cy7	BD Biosciences	1:600
CD24	91	Biotin	Southern Biotech	1:500
CD43	1B11	APC	Biolegend	1:500
IgM	II/41	PE Cy7	eBioscience	1:600
Streptavidin		Brilliant Violet 605	Biolegend	1:500
Streptavidin		Qdot 605	Invitrogen	1:500
Annexin-V		Pacific Blue	Biolegend	1:200
Annexin-V		FITC	Biolegend	1:200
DAPI			Thermo Fisher	1:600
7-AAD			Thermo Fisher	1:600
CD41	MWReg30	Brilliant Violet 421	Biolegend	1:600
CD41	MWReg30	PE	BD Biosciences	1:600
CD62P (P-selectin)	Psel.KO2.3	APC	eBioscience	1:600
CD45	30-F11	Biotin	Biolegend	1:300
TER-119	TER-119	Biotin	Biolegend	1:300

2.7.1 Leukocytes

Single cell suspensions of bone marrow cells were either allowed to rest for 2 hours in tissue culture medium at 37°C and 5% CO_2 (resting cells), or aliquots of freshly isolated bone marrow cells were dispensed into the 96-well round-bottom plates immediately after preparation of single cell suspensions (without resting). Cells were then stained with the appropriate antibodies as detailed above in section "2.5 Flow cytometry and surface antibody staining" and were washed once with flow cytometry buffer and once with Annexin-V binding buffer (Biolegend). Pacific Blue conjugated Annexin-V (1:100, Biolegend) and 7-AAD staining were performed in Annexin-V binding buffer at room temperature for 15 min and washed and resuspended in Annexin-V binding buffer and kept at 4°C until analysis.

2.7.2 Platelets

Washed platelets were incubated at room temperature for 20 min with FITC-labelled Annexin-V (1:200, Biolegend) and Brilliant Violet 421™ anti-mouse CD41 antibody (clone MWReg30, 1:600, Biolegend) in Annexin-V binding buffer (Biolegend). Samples were then diluted in Annexin-V binding buffer and analysed by a BD™ LSR II flow cytometer (BD Biosciences).

2.8 Measurement of P-selectin expression

P-selectin expression on the cell surface of platelets was assessed by measuring the binding of anti-CD62P antibody through flow cytometry. In brief, washed

platelets were incubated at room temperature for 20 min with APC-labelled anti-human/mouse CD62P (P-selectin) antibody (clone Psel.KO2.3, 1:600, eBioscience), and Brilliant Violet 421™ anti-mouse CD41 antibody (clone MWReg30, 1:600, Biolegend) in Annexin-V binding buffer. Samples were then diluted in Annexin-V binding buffer and analysed by flow cytometry.

2.9 Platelet count

An ADVIA 2120 Hematology System (Siemens Healthcare Diagnostics) was used for the analysis of platelet counts in the blood of mice.

2.10 Platelet clearance analysis

In vivo analysis of platelet clearance kinetics using carboxyfluorescein succinimidyl ester (CFSE) in conjunction with mathematical modelling was performed as described previously[164]. In brief, mice were injected via the tail vein with 50 µL of 10 mM CFSE (Thermo Fisher Scientific) in dimethyl sulfoxide (DMSO) mixed with 100 µL phosphate-buffered saline (PBS). Platelet analysis was performed at various time points by taking 5 µL blood from the tail tip and mixing it with 45 µL acid citrate dextrose (ACD) containing 2 µg/mL PE-conjugated anti-CD41 monoclonal antibody (clone MWReg30, BD Biosciences). Blood loss was controlled by cauterization. Lidocaine gel was used on the tail tip to minimize pain. Within 30 minutes of sample collection, 10 µL blood/ACD mixtures was added to 990 µL PBS and the samples were then analyzed by flow

cytometry using a BD FACScan. No platelet activation was observed in tail vein blood samples as evidenced by negative CD62P staining.

Platelets were identified using their characteristic forward and side scatter parameters along with positive CD41-PE staining. To determine the extent of CFSE labeling of platelet populations at each time point, fluorescence was measured on the FITC channel, with the percentage of CFSE-positive platelets being followed over time to determine lifespan. Platelet half-life was obtained by curve fitting as previously described[68].

2.11 Antibody preparation

Rabbit antibodies against mouse ATP11C were custom generated at the Pineda Antikörper-Service. In brief, the peptide CKYVWQSSPYNDEPWYNQ (ATP11C amino acids 310-326) was used to immunize rabbits. The antibodies were affinity-purified from the serum using peptide-coupled Sepharose 6B particles.

2.12 Scanning electron microscopy

Scanning electron microscopy (SEM) analysis of platelets was performed as described previously[165, 166], with minor modifications. Washed platelets were fixed in suspension with 0.125% (w/v) paraformaldehyde (Sigma) in PBS (pH 7.4) at room temperature for 15 minutes, then with 2% paraformaldehyde at room

temperature for an additional 1 hour. Platelet pellets were obtained through centrifugation at 300 *g* at room temperature for 10 minutes and then were washed twice with distilled water. The fixed platelets were layered on poly-L-Lysine (1mg/mL, Sigma) coated 9-mm round coverslips and allowed to settle in a humidified chamber for 12 hours at 4°C. The coverslips were rinsed with distilled water, successively dehydrated by 10 min incubations in a graded series of acetone (v/v, 30%, 50%, 70%, 80%, 90%, and 95%), followed by two 10 min incubations in 100% acetone. The specimens were then critical point dried using a Balzers Critical Point Dryer CPD 030 (BAL-TEC AG), mounted onto stubs using carbon tape and sputter-coated with platinum palladium. Images were taken using a Zeiss UltraPlus analytical field emission scanning electron microscope (accelerating voltage 3.0 kV, working distance 2.9 - 3.2 mm).

2.13 Transmission electron microscopy

Transmission electron microscopy (TEM) was performed as previously described[68]. In brief, washed platelets were first fixed in 2.5% (v/v) glutaraldehyde and 2.0% (v/v) formaldehyde in 0.1 M cacodylate buffer with 2 mM $CaCl_2$ for 1.5 h. Samples were then washed twice with 0.1 M cacodylate buffer, and post-fixed in 1% (w/v) osmium tetroxide in 0.1 M cacodylate buffer for 1 h. After buffer rinsing and dehydration through a graded series of ethanol concentrations, samples were subjected to infiltration with Glauert EMBED resin and cured at 60°C for 2 days. Ultrathin sections were cut and stained with 1% aqueous uranyl acetate and Reynold's lead citrate. Grids were viewed using a

Hitachi H7100FA transmission electron microscope. Digital images were collected using a Gatan Orius SC1000A (4k × 2k) diffraction camera.

2.14 Platelet activation

To induce activation, platelets were treated with A23187 (0.1 μM, 0.2 μM, 0.5 μM, or 1 μM, Sigma), Thrombin (1 U/mL, Sigma), Collagen (50 μg/mL, CHRONO-LOG) or Thrombin and Collagen in the presence of $CaCl_2$ (1-2 mM) at room temperature for 20 minutes or with vehicle (DMSO) in the controls.

2.15 Platelet apoptosis

Washed platelets (5×10^7) remained untreated or were pre-incubated with vehicle (DMSO, Sigma), Calpeptin (50 μg/mL, Sigma) or Q-VD-OPh (25 μM, Sigma) at room temperature for 15 minutes. To induce apoptosis, platelets were treated with ABT737 (1 μM, Selleckchem) at 37℃ in the absence or presence of $CaCl_2$ (1-2 mM) for different periods of time (30 min, 60 min, 90 min, 120 min, 150 min, or 180 min) or with vehicle (DMSO) in the controls.

2.16 Platelet aggregation

Platelet aggregation was measured in a 96-well microplate using washed platelets in modified Tyrode's buffer supplemented with 1 mM $CaCl_2$, as described previously[167, 168]. Aggregation was initiated by addition of thrombin (1 U/mL)

or A23187 (1 μM) to platelet suspensions and monitored for 10 minutes at 37℃ with orbital agitation of the plate (amplitude 1 mm, frequency 582 *rpm*) in a Tecan Infinate M1000 PRO microplate reader (Tecan Group Ltd.) with optical density readings at 620 nm. The extent of platelet aggregation was defined as the percentage change in optical density as measured by the plate reader.

2.17 Reverse transcription (RT)-PCR

Washed platelets were further purified through depletion of residual leukocytes and erythrocytes using biotin labelled anti-mouse CD45 and TER-119 antibodies (clone 30-F11 and clone TER-119, 1:200, Biolegend), followed by separation using Streptavidin MicroBeads, LD Columns and a MidiMACS™ Separator following manufacturer's instructions (Miltenyi Biotec). Total RNA from 1-3×10^9 mouse platelets was isolated by using TRIzol® Reagent (Thermo Fisher Scientific). RNA was quantified with a NanoDrop spectrophotometer (Thermo Fisher Scientific). A 1μg RNA sample was reverse-transcribed into cDNA using SuperScript™ II Reverse Transcriptase (Invitrogen) and Random Hexamers (Sigma). The purity of platelet cDNA was assessed by PCR using primers for CD41 (platelet specific marker, positive control) and CD45 (leukocyte specific marker, negative control). The cDNA of interest was amplified using Taq DNA Polymerase (Qiagen). The PCR products were separated by electrophoresis in a 1% agarose gel and visualized by staining with SYBR® Safe DNA Gel Stain (Invitrogen). The primers used are shown in Table 2.3.

Table 2.3 Primers used for RT-PCR

Target gene	Primer sequences (5'-3')		Product size (bp)
	Sense	Antisense	
ATP8A1	GTGTTTTGCTGTGGCTGAGA	CAAATGACAGCTTTGCAGGA	498
ATP8A2	AAATGGCATGTGGCACACTA	GCATGAGCTTGCTGTCATGT	416
ATP8B1	ATAAGACGGGGACACTCACG	AATGGCAAGGACGTTGTAGG	419
ATP8B2	GCCTGTCAACCTCTTTGAGC	AGCTTGTTGTTGGGTGGTTC	489
ATP8B3	TGGGAAGACAACGTACACCA	CCTGCCAGTCCTACACCAAT	476
ATP8B4	ACATTGCTGACCTCCAGTCC	GTGATGAGCTCTCCGTAGCC	469
ATP8B5	AGCAGATCAACAACCGCTCT	ACCAAACCGTAGCACCAGTC	418
ATP9A	CGTGTACGAGTCCAATGGTG	TGCTCCTCTGTGAGGGACTT	417
ATP9B	ACCCTGTTACGCCAGCATAC	CCCTTGGTGAGGTCCTTGTA	440
ATP10A	CTTTTCTGCATCTGCCATGA	AGATGGAGGGTAGCATGTGG	445
ATP10B	TGCAAACTGCTGGATCAGAC	CTTCCTGCCCAGATATTCCA	445
ATP10D	ATCAAGTTCACCGTCCCTTG	GACCACGACCGACATTCTTT	442
ATP11A	TGCAAGGAACAGCGACTATG	GCACCATCACAGTGAACACC	491
ATP11B	ACCTGGCAAGCTGAAGAAAA	ATGGGCTGAGTTGCTGAGAT	465
ATP11C	GATGGTGCCAATGATGTCAG	AAATGCAGCCAGAAATGTCC	450
CDC50A	CTGCCCACCTTCTTCATCAT	TGGAATAGGCTTGGGATCAG	444
CDC50B	CAACGACTCCTTCTCGCTCT	ACCCATCCAAGAGATGTTGC	424
CDC50C	GTTGTCTGCAAAGAGCACCA	CCACCATGTAAGCCCACTCT	412
CD41	GTCAGCTGCTTCAACATCCA	TCATAGGCTCCCTCACCATC	494
CD45	CCTGCTCCTCAAACTTCGAC	TGCTCATCTCCAGTTCATGC	497

2.18 Calpain cleavage assay

Platelet membrane fractions (10 µg) were incubated with purified human calpain-1 (4 U, Sigma) in the absence or presence of $CaCl_2$ (5 mM) or Calpeptin (50 µg/mL, Sigma) at room temperature for 30 minutes in PBS, pH 7.4 (Medicago). Controls remained untreated. Samples were then denatured for SDS-PAGE and western blot analysis.

2.19 Measurement of intracellular calcium

Intracellular calcium $[Ca^{2+}]_i$ levels were measured using a Fluo-4 NW Calcium Assay Kit (Thermo Fisher Scientific) according to manufacturer's manual. In brief, washed platelets (5×10^7) were preloaded in Fluo-4 NW dye loading solution in the presence of $CaCl_2$ (1.3 mM) and probenecid (5 mM) at 37℃ for 30 minutes, then at room temperature for an additional 30 minutes. Platelets were then treated with ABT737 (1µM, Selleckchem) at 37℃ in the absence or presence of Calpeptin (50 µg/mL, Sigma) or Q-VD-OPh (25 µM, Sigma), or with vehicle (DMSO) in the controls. Calcium ionophore A23187 stimulation was used as a positive control to measure a maximum $[Ca^{2+}]_i$ flux. Fluorescence was measured continuously for a total of 3 hours, using a Tecan Infinate M1000 PRO microplate reader (Tecan Group Ltd.) with wavelength settings: excitation at 494 nm and emission at 516 nm.

2.20 Protein sample preparation

2.20.1 Platelet lysates

Washed platelets were lysed in ice-cold RIPA buffer (Sigma) supplemented with Protease Inhibitor Cocktail (cOmplete™, EDTA-free; Roche). After removing insoluble materials by centrifugation at 16,000 *g* at 4°C for 10 min, total soluble proteins were quantified using Bradford reagent (Sigma).

2.20.2 Liver tissue homogenate preparation

Frozen liver samples were sectioned into ~100 mg blocks and homogenised in 1 mL of ice-cold T-PER^{TM} Tissue Protein Extraction Reagent (Thermo Fisher Scientific) supplemented with Protease Inhibitor Cocktail using a Bio-Gen PRO200 Homogenizer (PRO Scientific). After removing insoluble materials by centrifugation at 16,000 *g* and 4°C for 10 min, total soluble proteins were quantified using Bradford reagent.

2.20.3 Red blood cell membrane preparation

Purified red blood cell (RBC) ghost membranes were prepared by hypotonic haemolysis of erythrocytes with 10 volumes of ice-cold hypo-osmotic buffer (15 mM KCl, 2 mM $MgCl_2$, 0.1 mM EDTA, 10 mM HEPES, pH 8.0) supplemented with Protease Inhibitor Cocktail on ice for 5 min, followed by centrifugation at 26000 *g* and 4 ℃ for 20 minutes, and repeated washings with the same buffer, according to the method described previously[169]. RBC ghost pellets were resuspended in hypo-osmotic buffer and total protein concentration was determined using Bradford reagent.

2.20.4 Platelet whole membrane preparation

Washed platelets (1×10^9) were resuspended in ice-cold hypo-osmotic buffer on ice for 5 min and then homogenized with a hypodermic needle (23G, Terumo). Membranes were isolated by centrifugation at 150,000 *g* and 4°C for 60 min. Pellets were re-suspended in 5 mM glycine and total protein concentration was determined using Bradford reagent.

2.20.5 Plasma membrane extraction and enrichment

The plasma membrane was extracted and enriched using a Plasma Membrane Protein Extraction Kit (Abcam) according to manufacturer's instructions. The kit uses an aqueous polymer two-phase system to separate plasma membranes from organelle membranes. More specifically it uses a two-phase Polyethylene glycol (PEG)/Dextran system in which the plasma membrane tends to concentrate in the upper phase. Whole membrane fractions of platelets were resuspended in 200 µL Upper Phase Solution and mixed well with an equal volume of Lower Phase Solution and incubated on ice for 5 minutes. After centrifugation at 1000 *g* for 5 minutes in a bench top centrifuge, the upper phase was carefully transferred to a new tube and the lower phase was re-extracted once by newly added Upper Phase Solution. The two upper phases were combined and then re-depleted once with newly added Lower Phase Solution. The upper phase was carefully transferred to a new tube, diluted in 5 volumes of water and incubated on ice for 5 minutes. Plasma membranes were collected by centrifugation of the upper phase at top speed (13,000 *rpm*) in a bench top centrifuge for 10 minutes. Pellets were re-

suspended in 5 mM glycine and total protein concentration was determined using Bradford reagent.

2.21 Bradford assay

BSA standards (30 µL) (50, 100, 200, 300, 400, 500 µg/mL milliQ H_2O) were made up to 300 µL samples/well in a 96-well plate by adding 270 µL Bradford's reagent (Sigma). For each protein sample two replicates of at least two dilutions were made in a final volume of 30 µL before Bradford's reagent was added to make a final volume of 300 µL/replicate. Samples and BSA standards were incubated for 2 mins before absorbance at 595 nm was measured using a Tecan Infinate M1000 PRO microplate reader (Tecan Group Ltd.). Standard curves were generated, and total protein sample concentrations were calculated using a Magellan^{TM} program (Tecan Group Ltd.).

2.22 Surface biotinylation

Surface biotinylation of cells was performed as described previously[170] with minor modifications**.** Platelets were washed twice with pre-lysis PBS buffer (PBS supplemented with 1 mM $CaCl_2$, 0.5 mM $MgCl_2$, pH 8.0) followed by biotinylation with 0.5 mg/mL EZ-Link Sulfo-NHS-Biotin (Thermo Fisher Scientific) in pre-lysis PBS buffer for 30 minutes at room temperature on a rotary shaker at low speed. Unbound reagent was quenched by washing twice with pre-lysis PBS buffer supplemented with 100 mM glycine. Cells were then lysed by

addition of 1 mL lysis buffer (150 mM NaCl, 1% Triton X-100, 20 mM Tris-HCl, pH 7.6) and incubation in a 1.5 mL Eppendorf tube on ice for 1 hour with occasional inversions. The cell lysate was centrifuged in a bench top centrifuge at top speed (13,000 *rpm*) for 10 min, and the supernatant was transferred to a new tube and incubated with 40 µL high capacity streptavidin-agarose beads (Thermo Fisher Scientific) at 4°C on a rotating shaker overnight. After washing three times with lysis buffer, the streptavidin beads were mixed with 4× LDS sample buffer and 10× sample reducing agent (Bolt™, Thermo Fisher Scientific), incubated at 95℃ for 10 minutes and applied to SDS-PAGE analysis.

2.23 SDS-PAGE, Western blot analysis and antibodies

Protein samples or platelets were mixed with 4× LDS sample buffer and 10× sample reducing agent (Bolt™, Thermo Fisher Scientific) before incubation at 70 ℃ for 10 minutes. Denatured proteins were separated by a 4-12% Bis-Tris Plus Gel running in MOPS SDS running buffer (Bolt™, Thermo Fisher Scientific). The separated proteins were transferred to Nitrocellulose blotting membranes (GE Healthcare) followed by blocking with 5% skim milk in PBS-Tween 20, pH 7.4 (Medicago). Membranes were probed with primary antibodies in PBS-Tween 20 with 2% membrane blocking reagent (GE Healthcare) at 4 ℃ overnight, followed by incubation with HRP-conjugated secondary antibodies at room temperature for 1 hour. Stained blots were visualized with Luminata^{TM} Forte Western HRP Substrate (Millipore). For re-probing, the same blots were incubated for 30 min at 70 ℃ in stripping buffer (62.5 mM Tris-HCl pH 6.8, 2% SDS and 100 mM 2-

mercaptoethanol). Stripped membranes were washed in PBS-Tween 20 and then blocked in 5% skim milk before re-probing with a new set of antibodies as described above. Antibodies used for western blot analysis are listed in Table 2.4.

2.24 Statistical analysis

Statistical significance between two groups was analysed using an unpaired student's t-test with 2-tailed *p* values. Multiple experimental groups were compared using One-Way Analysis of Variance (ANOVA), followed by pair-wise comparison with a Bonferroni post-test. Differences were taken to be significant when $p < .05$. All statistical analyses were performed using GraphPad Prism software Data are presented as means ± SEM, where n = the number of independent experiments performed. * $p < .05$; ** $p < .01$; *** $p < .001$; # $p < .0001$.

Table 2.4 Antibodies used in western blot analysis

Target	Dilution	Company
ATP11C	1:1000	Pineda Antikörper-Service
ATP8A1	1:1000	Proteintech
caspase-3	1:1000	Cell Signaling
calpain-1 large subunit	1:1000	Cell Signaling
gelsolin	1:1000	Abcam
Na^+/K^+-ATPase	1:5000	Abcam
β-Actin	1:2000	Abcam
HRP-conjugated donkey anti-rabbit IgG	1:2000	GE Healthcare

CHAPTER 3: ATP11C Facilitates Phosphatidylserine Inward Translocation across the Plasma Membrane of B cells

The contents of this chapter are part of the following published study: *Yabas M, Jing W, Shafik S, Bröer S, Enders A (2016) ATP11C Facilitates Phospholipid Translocation across the Plasma Membrane of All Leukocytes. PLoS ONE 11(1): e0146774.* The experiments described in this chapter were conducted under guidance of Dr. Mehmet Yabas.

3.1 Preamble

It was previously reported that ENU-induced mutations in the murine ATP11C gene result in B cell deficiency due to a developmental arrest at the pro-B cell stage of B lymphopoiesis in the bone marrow[119, 120]. It was subsequently shown that ATP11C also plays a critical role in bile secretion[122], as well as erythrocyte longevity and morphology[121]. Moreover, during lymphocyte apoptosis ATP11C undergoes limited proteolysis to facilitate exposure of PS[54]. Despite the importance of ATP11C, its biochemical characterization and physiological function, particularly substrate selectivity of phospholipids, remains mostly unknown.

Considering that loss of flippase ATP11C results in B cell deficiency[119, 120], using ATP11C-deficient mice and fluorescently labelled PS, PE and PC we examined in this study i) the ability of B cell subsets to translocate specific phospholipids between the bilayer of the plasma membrane, ii) whether ATP11C is involved in this lipid translocation activity, and substrate specificity of ATP11C, and iii) the effect of ATP11C dysfunction on PS distribution in the plasma membrane.

3.2 B cells exhibit aminophospholipid translocation activity

We first wanted to test whether B cell subsets in the bone marrow translocate specific aminophospholipids between the two leaflets of the plasma membrane at different ratio. To do so, congenitally-marked CD45.2$^+$ cells from the bone marrow of wild-type animals were mixed with congenitally-marked CD45.1$^+$ wild-type spleen cells and incubated with lipid analogues, NBD-PS, NBD-PE or NBD-PC for 20 minutes, followed by antibody staining and analysis by flow cytometry. To facilitate the comparison between different lipid analogues, the uptake of lipids in different subsets was then normalized to PS incorporation into CD45.1$^+$ splenic B cells.

As shown in Figure 3.1, we observed that all major B cell subsets displayed aminophospholipid flippase activity with PS being the most translocated lipid derivative compared to PE and PC. Moreover, pro-B cells have the highest level of PS internalization compared to other subsets such as pre/pro-B, pre-B, immature B, and mature B cells. By contrast, the uptake of PE and PC did not significantly differ in B cell subpopulations in the bone marrow. Collectively, these results demonstrate that B cell subsets exhibit aminophospholipid translocation activity especially for PS.

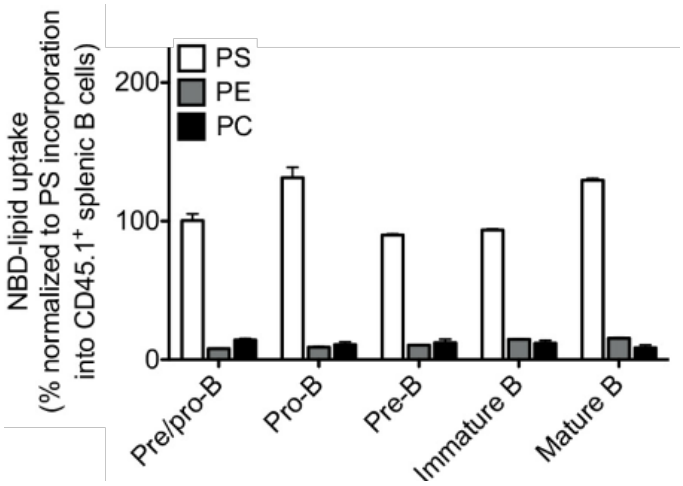

Figure 3.1 B cell subsets exhibit aminophospholipid translocation activity

Graphs represent mean ± S.E.M. of NBD-PS, NBD-PE or NBD-PC uptake into different B cell subsets in the bone marrow of wild-type mice after 20 min of incubation. Data are presented as percentage of NBD-lipid uptake into the indicated subset relative to NBD-PS uptake into CD45.1-marked wild-type splenic $B220^{+}$ cells stained and analysed in the same tube (PS) or for an identical time in a separate tube (PE and PC). Cell populations were identified as follows. In the bone marrow: Pre/pro-B cells ($CD24^{-}CD43^{+}$ in the $B220^{lo}IgM^{-}$ gate), pro-B cells ($CD24^{int}CD43^{+}$ in the $B220^{lo}IgM^{-}$ gate), pre-B cells ($CD24^{hi}CD43^{-}$ in the $B220^{lo}IgM^{-}$ gate), immature B cells ($B220^{lo}IgM^{+}$ gate) and mature B cells ($B220^{hi}IgM^{+}$ gate). $DAPI^{+}$ dead cells were excluded from the analysis. Data are representative of two independent experiments with two to three mice in each. Graphs represent mean values ± SEM from three biological replicates.

3.3 ATP11C acts as a phosphatidylserine flippase in B cell subsets

Given that loss of ATP11C results in a B cell deficiency syndrome caused by a block in early B cell development[119, 120], we decided to test if the observed aminophospholipid translocation activity in B cell subsets derived from bone marrow (Figure 3.1) was ATP11C-dependent. To test this, flippase activity assay was performed in wild-type and ATP11C$^{amb/0}$ bone marrow cells as detailed above in "Section 3.2". For equal staining conditions of wild-type and mutant cells, ATP11C$^{amb/0}$ cells from either CD45.1 or CD45.2 animals were mixed at a 1:1 ratio with cells from wild-type CD45.2 or CD45.1 animals respectively and incubated in one tube with lipid analogues.

As shown in Figure 3.2, all major B cell subsets including pre/pro-B, pro-B and mature B cells from the bone marrow of ATP11C$^{amb/0}$ mice showed a significantly reduced level of PS internalization compared to those from ATP11C$^{+/0}$ mice. P4-ATPases have been suggested to transport mainly PS, but also to a lesser extent PE[3, 15]. Consistent with this notion, all ATP11C$^{amb/0}$ B cell subsets were also deficient in translocating PE to the cytoplasmic leaflet of the plasma membrane. By contrast, the internalization of PC in B cell subsets from ATP11C-deficient mice was largely comparable to their counterparts from control animals. Collectively, these results demonstrate a non-redundant role for ATP11C as a PS flippase in all B cell subsets. It mediates the inward transport of PS and to a lesser extend PE, but not PC, across the plasma membrane.

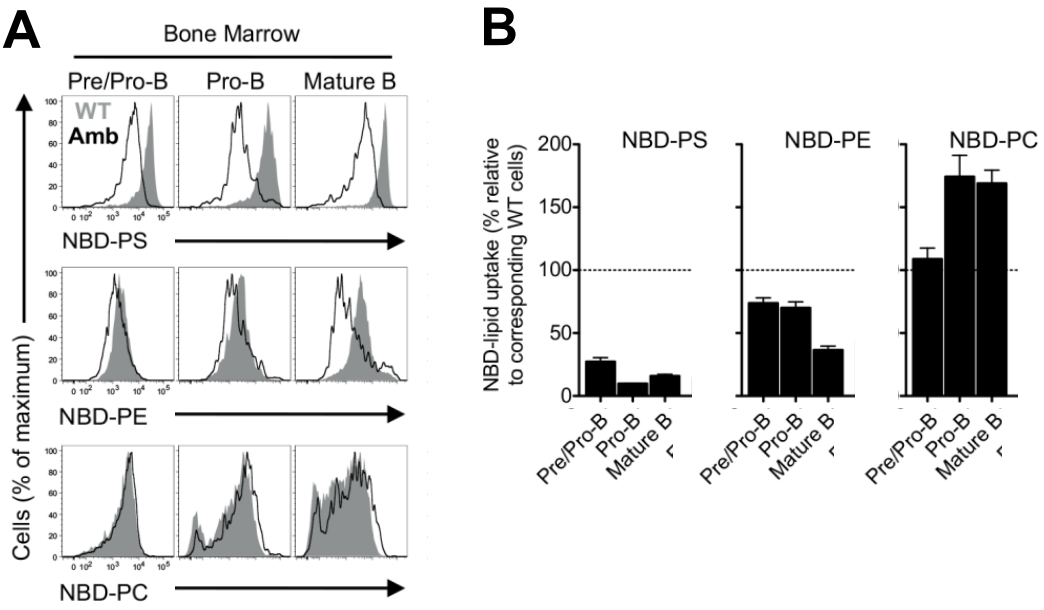

Figure 3.2 B cell subsets from ATP11C-deficient mice display a defective PS and PE flippase activity

(A) Representative overlay histogram of NBD-PS, NBD-PE and NBD-PC fluorescence profiles after 20 min incubation in pre/pro-B, pro-B and mature B cells derived from bone marrow of ATP11C$^{amb/0}$ (Amb, black lines) animals, compared to the corresponding CD45.1- or CD45.2-marked wild-type cells in the same tube (WT, shaded grey).

(B) Graphs represent mean ± SEM of the percentage of NBD-lipid uptake relative to the corresponding wild-type cells in the same tube. Cell types as described in (A). DAPI^{+} dead cells were excluded from the analysis. Data are representative of at least four independent experiments with one to three mice in each.

3.4 Defective flippase activity causes temporary PS exposure on viable pro-B cells from ATP11C-deficient mice

Exposure of PS on the surface of cells is critical for the recognition and clearance of apoptotic cells by macrophages[171]. The impaired flippase activity in B cell subsets from ATP11C-deficient mice raises the possibility that the ATP11C mutation allows an accumulation of PS in the exoplasmic plasma membrane leaflet of cells. To test this hypothesis, freshly isolated bone marrow cells from $ATP11C^{amb/0}$ and $ATP11C^{+/0}$ control animals were analysed using fluorescent Annexin-V, which binds to PS on the cell surface[172], followed by detection with a flow cytometer.

As shown in Figure 3.3, a fraction of viable pro-B cells in the bone marrow from mutant animals had elevated Annexin-V binding. Other B-cell populations remained normal. Surprisingly, when freshly isolated cells were allowed to recover in tissue culture medium for 2 hours before staining, the increased Annexin-V positive population disappeared. This is not a result of that these cells are going to death, as the proportion of dead cell population (Annexin-V^+ 7-AAD^+) is not increasing after recovery[163]. These data suggest that the ATP11C deficiency does not result in a general steady-state increase in PS exposure on the surface of cells, rather than a transient exposure.

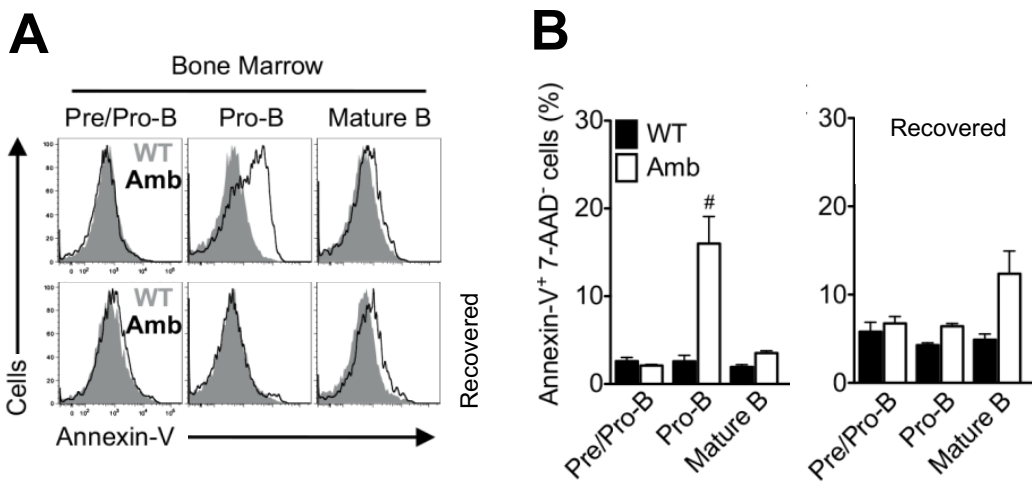

Figure 3.3 Increased PS exposure on viable pro-B cells from ATP11C-deficient mice

(A) Equal numbers of cells from bone marrow of ATP11C$^{+/0}$ and ATP11C$^{amb/0}$ animals were directly tested for Annexin-V binding without being cultured or allowed to recover in tissue culture medium for 2h followed by testing for Annexin-V binding. Representative overlay histogram of Annexin-V staining in pre/pro-B, pro-B and mature B cells in the bone marrow of ATP11C$^{+/0}$ (WT, gray area) and ATP11C$^{amb/0}$ (Amb, black line) animals. Cells were pregated on 7-AAD^{-} cells. Data are representative of three independent experiments with two to three mice per genotype in each.

(B) Graphs represent mean ± SEM of the percentage of Annexin-V^{+} cells in different subsets. Cells were pregated on 7-AAD^{-} cells. Data are pooled from two independent experiments with two to three mice per genotype in each. Statistics were calculated using One-Way ANOVA, followed by pair-wise comparison with a Bonferroni post-test. (# $p < .0001$)

3.5 Discussion

We demonstrated in this chapter that the P4-ATPase ATP11C mediated significant flippase activity in B cell subsets. Loss of ATP11C resulted in a defective internalization of PS and PE in comparison to control cells. The diminished flippase activity caused increased PS exposure on pro-B cells freshly isolated from the bone marrow of ATP11C-deficient mice, which was corrected upon a 2-hour resting period *in vitro*. These findings showed that B cell subsets exhibit flippase activity and ATP11C contributes to aminophospholipid translocation in B cells.

ATP11C-deficient mice have a cell subset-specific defect in early B cell development in the bone marrow[119, 120]. One explanation for the pro-B cell specific defect in development despite the widespread loss of flippase activity in B cell subsets could be that these cells rely more on flippase activity compared to other cells because of an intrinsically increased PS externalization. Consistent with a delicate balance between PS exposure and internalization, viable pro and pre-B cells have been shown to express slightly increased levels of PS on their surface[173, 174]. This is not caused by a loss of flippase activity at the pro-B cell stage because our data show that pro-B cells have the highest PS internalization level of all developing B cell subsets. Instead, this slightly autonomous PS exposure is most likely attributed to pre-BCR or BCR signalling during B cell maturation process. Since the engagement of BCR increases the intracellular Ca^{2+} concentration[175], it is possible that signalling from a pre-BCR or BCR activates B-cell progenitors to expose PS via Ca^{2+}-dependent scramblase.

The increased exposure of PS on freshly isolated cells was particularly pronounced on pro-B cells lacking ATP11C. As discussed above, this could reflect a high reliance of pro-B cells on flippase activity for maintenance of phospholipid asymmetry and may result in an increased vulnerability compared to other B cell subsets during lymphopoiesis in the bone marrow. Since exposure of PS on the surface of cells is critical for the recognition and clearance of apoptotic cells by macrophages[171], an alternative explanation for the stage specific defect in B cell lymphopoiesis could be that the impaired flippase activity causes a temporary increased PS concentration on the cell surface, which in turn results in rapid PS-mediated phagocytosis of pro-B cells in ATP11C-deficient mice.

Our finding of elevated Annexin-V binding on freshly isolated live pro-B cells suggests that during the preparation of cell suspensions, cells may undergo some mechanical stress that leads to increased exposure of PS on the outer leaflet[176], possibly through the activation of scramblases in viable pro-B cells in the bone marrow. However, when cells were rested for 2 hours, they showed no increased Annexin-V staining, presumably because the increased PS exposure is a temporary observation after isolation and it could be corrected through other flippases upon cell recovering in tissue culture medium, and then the normal asymmetric distribution of PS could be re-established. These results are consistent with the recent findings that ATP11C-deficient cells do not generally have increased PS exposure on their surface [54], suggesting the presence of additional flippases in the membrane of immune cells. In agreement with this notion, PS exposure is increased in cells deficient of CDC50A, the essential subunit for a variety of flippases[54].

In conclusion, the results presented in this chapter demonstrated that a mutation in the gene encoding ATP11C resulted in the diminished flippase activity in B cell subsets and suggested that ATP11C was a flippase that selectively transports PS and PE from the outer leaflet of the plasma membrane to the inner leaflet.

CHAPTER 4: Normal Function but Reduced Half-life and Increased Size of Platelets in Mice Deficient in Phospholipid Flippase ATP11C

Left and middle panels of Figure 4.1B appeared in the following published study: *Jing, W., et al., Calpain cleaves phospholipid flippase ATP8A1 during apoptosis in platelets. Blood Adv, 2019. 3(3): p. 219-229.* Dr. Lucy Coupland performed the experiments for the data in Figure 4.2B and Figure 4.3B.

4.1 Preamble

As a member of the P4-type ATPase family, ATP11C has been shown to play a critical role in regulating phospholipid distribution in the plasma membrane, and its dysfunction is related to many pathological processes. As demonstrated in "CHAPTER 3", ATP11C mainly translocated PS from the outer leaflet to the inner leaflet of plasma membranes in B cells, and loss of ATP11C resulted in transient PS exposure in pro-B cell subsets[163]. As a result, loss of ATP11C activity in mice resulted in a block of B cell development at the pro-B cell stage in the bone marrow[119, 120]. Results from our research group demonstrated that ATP11C is a major flippase in different blood cell types. For instance, lack of ATP11C in human and mouse erythrocytes causes anemia and hemolysis[122, 123]. Moreover, it has been shown that ATP11C is cleaved by caspases during apoptosis in leukocytes to facilitate apoptotic PS exposure[54].

Despite the important functions of ATP11C in leukocytes and erythrocytes, it is not yet known whether ATP11C is also involved in the function and/or survival of platelets. In studies demonstrated in this chapter, we investigated platelets from ATP11C-deficient mice, and found that ATP11C was not expressed in murine platelets[177]. However, platelets from ATP11C-deficient mice exhibited reduced life span and increased size. Thus, this study suggests that ATP11C may regulate cell extrinsic factors that control survival of platelets in the peripheral blood.

4.2 ATP11C is not expressed in mouse platelets

ATP11C has been shown both in leukocytes and erythrocytes to function as a flippase which mainly transports PS from the exoplasmic leaflet to the inner leaflet of the plasma membrane[54, 122, 123, 163]. In order to reveal whether ATP11C is also involved in the translocation of PS in platelet membranes we performed a flippase activity assay. Platelets from mutant mice and their control littermates were incubated with NBD labeled PS analogue at room temperature for different periods of time before washing with fatty acid-free BSA to remove unbound analogues. NBD-PS incorporation was analysed by flow cytometry, showing that platelets of ATP11C-deficient mice had normal flippase activity compared to their littermate controls (Figure 4.1A).

Normal flippase activity in platelets from ATP11C-deficient mice could point to the absence of ATP11C in platelets, unlike leukocytes and erythrocytes. Indeed, western blot analysis with an antibody against ATP11C showed lack of ATP11C expression in platelets from control mice (Figure 4.1B, left panel). Although two bands were observed on the western blot, these result from non-specific binding as both of them also appeared in ATP11C-deficient mice (Figure 4.1B, left panel). As ATP11C is highly expressed in liver[54, 55, 119, 120], we also performed the western blot analysis in the liver of mutant and control mice. The presence of a strong band of approximately 120 kDa in liver from wildtype mice was detected, and this band was absent in the liver of ATP11C-deficient mice (Figure 4.1B, middle panel), confirming that the antibody was specific to ATP11C[177]. Moreover, ATP11C protein was also detected in red blood cell ghost membranes,

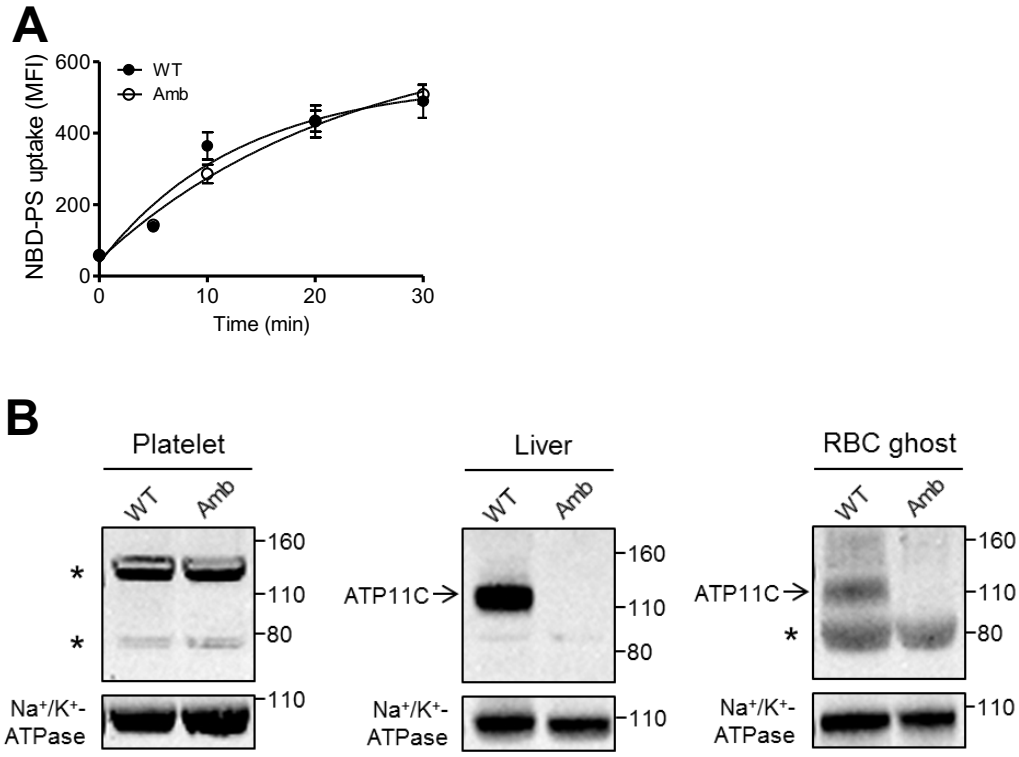

Figure 4.1 ATP11C is not expressed in mouse platelets

(A) The graph shows mean fluorescence intensity (MFI) ± SEM of NBD-PS uptake in platelets from the blood of *Atp11c*$^{+/0}$ (WT, ●) and *Atp11c*$^{amb/0}$ (Amb, ○) mice. Data are representative of three independent experiments, with four mice per genotype in each.

(B) Expression of ATP11C in platelets, liver and red blood cell ghosts from *Atp11c*$^{+/0}$ (WT) and *Atp11c*$^{amb/0}$ (Amb) mice. Mouse platelet whole cell lysates (100 µg), liver tissue homogenates (50 µg), and RBC ghost membranes (100 µg) were denatured for SDS-PAGE and then probed for ATP11C through western blot. An asterisk (*) indicates nonspecific bands. Immunoblots are representative of three independent experiments.

also with a non-specific band underneath (Figure 4.1B, right panel). Collectively, these data show that ATP11C is not a contributing flippase in murine platelets as its loss does not cause a functional defect, which is possibly due to absence of its expression in platelets.

4.3 Normal cell count but reduced half-life and increased size of platelets in ATP11C-deficient mice

Loss of ATP11C in mice resulted in a reduction in the number of B cells and erythrocytes, which are supposed to be caused by both cell intrinsic and extrinsic factors[119, 120, 122, 123, 163]. Therefore, we want to investigate whether ATP11C deficient environment in the host has any effect on platelets despite of lacking intrinsic expression of ATP11C protein. We first investigated if ATP11C-deficient mice have a normal platelet count. To do so, we evaluated the number of platelets in the peripheral blood of ATP11C-deficient mice and their littermate controls at different ages. Although mutant mice at 6 to 8 weeks of age had significantly reduced number of platelets, mature mutant mice had normal number of platelets compared with wild-type littermates in other age groups (Figure 4.2A).

The kinetics of platelet clearance was investigated using dilution of a fluorescent label, carboxyfluorescein succinimidyl ester (CFSE), *in vivo* and mathematical modelling as described previously[164]. Similar to the increased clearance of erythrocytes[122], platelets from ATP11C-deficient mice exhibited increased clearance rate compared with platelets from their control littermates as determined by the percentage of CFSE-labelled platelets in the peripheral blood of mice (Figure 4.2B). Platelet clearance data showed an half-life of 35 hours in mutant animals compared with 44 hours in control littermates (Figure 4.2B).

To determine whether the reduced half-life of platelets observed in ATP11C-deficient mice is due to increased surface exposure of PS, which serves as an

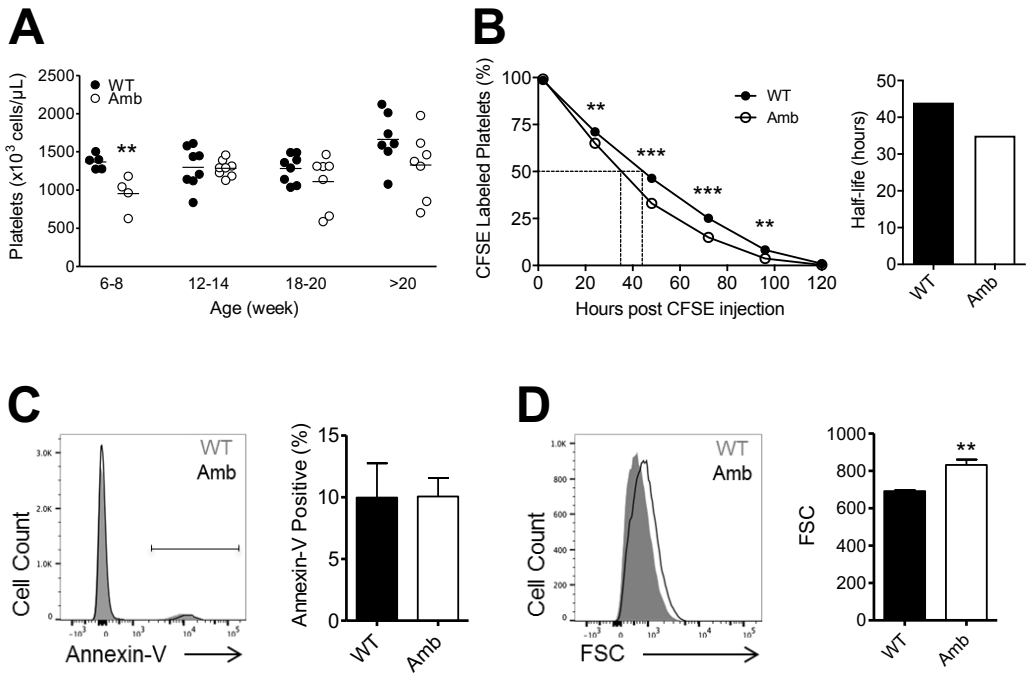

Figure 4.2 Normal cell count but reduced half-life and increased size of platelets in ATP11C-deficient mice

(A) The graph shows the number of platelets in the blood of *Atp11c*$^{+/0}$ (WT, ●) and *Atp11c*$^{amb/0}$ (Amb, ○) mice of the indicated age groups. Each symbol represents an individual mouse.

(B) The graph on the left shows means ± SEM of the percentage of CFSE-labeled platelets in the blood of *Atp11c*$^{+/0}$ (WT, ●) and *Atp11c*$^{amb/0}$ (Amb, ○) mice after *in vivo* labeling. The bar graph on the right represents half-life of platelets determined as in the left panel. Data are representative of two independent experiments, with five mice per genotype in each.

(C) Representative overlay histogram of Annexin-V staining in platelets from the blood of *Atp11c*$^{+/0}$ (WT, grey area) and *Atp11c*$^{amb/0}$ (Amb, black line) mice. The bar graph

represents means ± SEM of the percentage of Annexin-V positive cells in platelets. Data are representative of three independent experiments, with four mice per genotype in each.

(D) Representative overlay histogram of the forward scatter (FSC) profile in platelets from the blood of *Atp11c*$^{+/0}$ (WT, grey area) and *Atp11c*$^{amb/0}$ (Amb, black line) mice. The bar graph represents means ± SEM of the FSC profile in platelets. Data are representative of three independent experiments, with four mice per genotype in each.

Statistical significance was calculated using Student's two-tailed *t* test. (**, $p < 0.01$; ***, $p < 0.001$)

"eat-me" signal to mediate recognition and clearance of platelets by phagocytes[6, 178], platelets from the peripheral blood were stained with the PS-specific probe, Annexin-V[172]. However, no difference in Annexin-V binding was observed on platelets in the blood of ATP11C-deficient and wild-type mice (Figure 4.2C). The percentage of Annexin-V positive platelets in mutant mice was similar to that of control littermates, both being around 10% (Figure 4.2C). These data indicate that the reduced half-life of platelets was not caused by increased PS exposure-mediated clearance in ATP11C-deficient mice.

Interestingly, flow cytometric analysis revealed that platelets in the blood of ATP11C-deficient mice were larger than platelets from control animals as determined by an increase in their forward scatter (FSC) profile (Figure 4.2D), which is similar to observation in erythrocytes[122]. Taken together, ATP11C deficiency in mice did not cause thrombocytopenia but mutant platelets exhibited reduced half-life and increased size.

4.4 Normal morphology and function of platelets in ATP11C-deficient mice

Given that the loss of ATP11C in erythrocytes caused an abnormal shape (stomatocytosis)[122], we determined whether ATP11C had any impact on the normal shape of platelets. Morphological studies of platelets from ATP11C-deficient mice using scanning electron microscopy (SEM) and transmission electron microscopy (TEM) analysis revealed a normal discoid shape (Figure 4.3A) and ultrastructure (Figure 4.3B) compared with platelets from littermate controls.

We next wanted to test whether agonist-induced platelet activation (marked by PS exposure and CD62P surface expression) and aggregation were perturbed in platelets from ATP11C-deficient mice. As shown in Figure 4.3C, exposure of PS was normal in platelets from mutant mice compared to wild-type controls after treatment with thrombin or calcium ionophore A23187. Similarly, agonist induced CD62P expression on the cell surface also remained normal in platelets from mutant mice (Figure 4.3D). Apoptotic PS exposure was normal as well in platelets from mutant mice treated with the pro-apoptotic BH3 mimetic compound ABT737 (Figure 4.3C). ABT737 did not induce CD62P expression in platelets[47] from either genotype (Figure 4.3D).

The dynamics of platelet aggregation was examined by turbidimetric measurements after thrombin stimulation. The experiment showed normal aggregation of platelets from ATP11C-deficient mice compared to wildtype

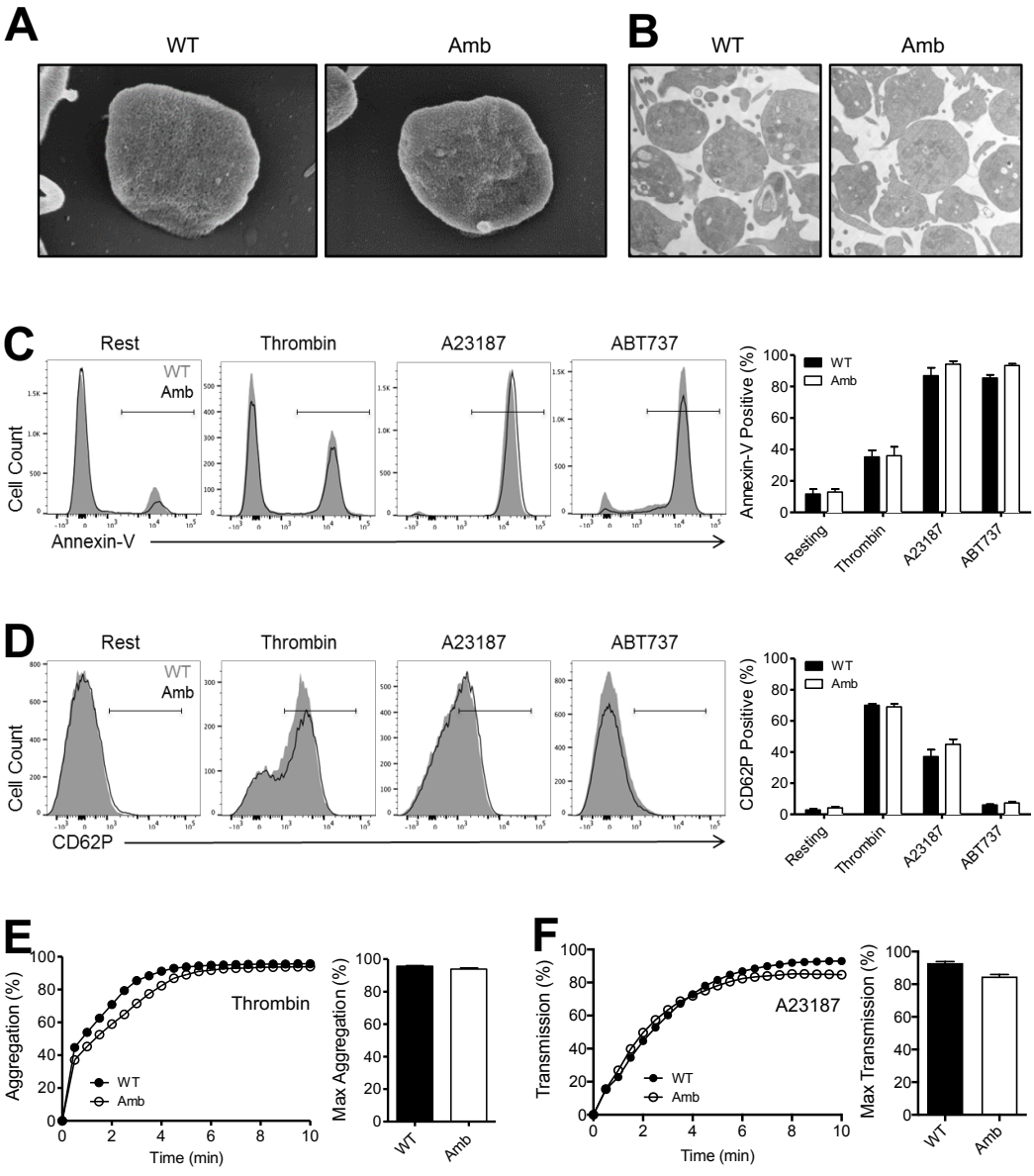

Figure 4.3 Normal morphology and function of platelets in ATP11C-deficient mice

(A) Scanning electron microscopy analysis of platelets from the blood of *Atp11c*$^{+/0}$ (WT) and *Atp11c*$^{amb/0}$ (Amb) mice. Data are representative of two independent experiments, with pooled platelets from four mice per genotype in each.

(B) Transmission electron microscopy analysis of platelets from the blood of *Atp11c*$^{+/0}$ (WT) and *Atp11c*$^{amb/0}$ (Amb) mice. Data are representative of two independent

experiments.

(C and D) Representative overlay histograms of Annexin-V or CD62P staining in platelets from the blood of *Atp11c*$^{+/0}$ (WT, grey area) and *Atp11c*$^{amb/0}$ (Amb, black line) mice treated with Thrombin (1 U/mL, room temperature, 20 min), A23187 (1 μM, room temperature, 20 min) or ABT737 (1 μM, 37 ℃, 90 min) in the presence of $CaCl_2$ (1 mM). Gates represent the percentage of Annexin-V or CD62P positive cells. Data are representative of three independent experiments, with four mice per genotype in each. The bar graphs represent means ± SEM of the percentage of Annexin-V or CD62P positive cells in platelets.

(E and F) Platelet aggregation curves and light transmission changes acquired by stimulating platelets from the blood of *Atp11c*$^{+/0}$ (WT, ●) and *Atp11c*$^{amb/0}$ (Amb, ○) mice by Thrombin (1 U/mL) or A23187 (1 μM) in the presence of $CaCl_2$ (1 mM) at 37 ℃. The bar graphs represent means ± SEM of the percentage of max aggregation or transmission at 10 minutes in platelets. Data are representative of three independent experiments, with four mice per genotype in each.

controls (Figure 4.3E). Calcium ionophore such as A23187 is capable of inducing aggregation-independent light transmission changes in the platelet suspension, which could be detected by turbidimetric measurement as well. This light transmission change is caused by calcium induced shape transformation from discoid platelets to translucent and ballooned structures, leading to clearance of the platelet suspension[79, 179]. Platelets from ATP11C-deficient mice showed normal light transmission changes induced by A23187 compared to wildtype controls (Figure 4.3F).

In summary, platelets from ATP11C-deficient mice showed normal morphology and function.

4.5 Discussion

Despite critical roles for ATP11C in leukocytes and erythrocytes[119, 120, 122, 123, 163], in the present study we show that ATP11C is not present and does not mediate flippase activity in murine platelets, suggesting that ATP11C is not a contributing flippase in platelets. However, our results revealed that platelets in ATP11C-deficient mice showed small differences of half-lifetime and increased size.

Circulating platelet counts reflect a balance between platelet production and clearance. ATP11C-deficient mice demonstrated significantly reduced circulating half-life of platelets compared to controls, suggesting increased clearance of platelets; however, this does not result in significant thrombocytopenia as evidenced by platelet counts which were slightly lower in 6-8-week-old mice with ATP11C deficiency but normal in older mice. It should be noted that data of 6-8 week may be limited by the sample size and should be carefully considered. However, this will not affect the results of other age groups. These results indicate that enhanced platelet generation in adult ATP11C-deficient mice may compensate the increasing of platelet clearance to maintain the steady state of platelet numbers. Our data ruled out increasing exposure of PS on plasma membranes as an underlying mechanism for increased clearance of platelets in ATP11C-deficient mice, however, other mechanisms of platelet clearance may contribute to this process, such as platelet clearance via desialylation or Ashwell-Morell Receptor (AMR) in hepatocytes[180, 181], or autoreactive antibody and Fc receptor mediated clearance in spleen[182, 183].

Increased size of platelets from mutant mice was only observed using flow cytometry, while no distinguishable size change was shown in platelets between wildtype and mutant mice in SEM and TEM analysis. However, without full 3D reconstruction small differences are difficult to detect by standard image analysis.

Given the absence of ATP11C in mouse platelets, the reduced half-life and increased size of platelets observed in ATP11C-deficient mice are most likely caused by cell extrinsic factors. This hypothesis is supported by two previous observations: 1) ATP11C-deficient mice that were irradiated and reconstituted with wild-type bone marrow cells showed apparent defective B cell accumulation in the peripheral blood (9% of total lymphocytes compared to 70% in the control chimeras). Further analysis of B cells subsets in the bone marrow revealed that the percentage of $IgD^{-}IgM^{-}$ bone marrow B cell progenitors and $IgD^{-}IgM^{+}$ immature B cells in the *Atp11c*$^{amb/0}$ mouse transplanted with control bone marrow cells were considerably reduced compared to intact *Atp11c*$^{+/0}$ animal. Also, there was a partial defect at the pro-B cell stage as the percentage of $CD24^{hi}CD43^{-}$ pre-B cells represented 35% of total progenitors compared to 70% in control animal. These results indicate that there is a defect in early B cell development in the bone marrow of the ATP11C-deficient host that received transplants of wildtype haematopoietic cells, suggesting that ATP11C-deficient environment also influences the ability of wild-type hematopoietic stem cells to differentiate into B cell lineage in the bone marrow and/or B cell survival in the periphery[119, 120, 133]. 2) Erythrocytes from ATP11C-deficient mice have normal development and maturation in the bone marrow and spleen, but decreased lifetime and reduced

numbers in circulation, indicating that, in addition to the intrinsic defect, extrinsic factors may also be involved in the regulation of erythrocyte survival[122].

Platelet transfusion experiment could be performed to uncover the intrinsic or extrinsic role of ATP11C on regulating platelet survival. Briefly, CFSE-labelled platelets from donor mice (*Atp11c*$^{+/0}$ or *Atp11c*$^{amb/0}$) can be adoptively transferred into recipients of ATP11C-decifient mice or wildtype littermate control mice [68]. Then the clearance dynamics of the adoptive platelets from the circulation could be analysed as described in this study.

In summary, the present study reports significant changes of half-life and size of platelets from ATP11C-deficient mice and reveal that ATP11C is not the prominent flippase in murine platelets. It is possible that ATP11C deficiency may affect some factors that are indispensable for the homeostasis of platelets in the peripheral blood. These findings also highlight a fundamental difference between the action of ATP11C in leukocytes, erythrocytes and platelets.

CHAPTER 5: Calpain Cleaves Phospholipid Flippase ATP8A1 during Apoptosis in Platelets

The contents of this chapter are part of the following published study: *Jing, W., et al., Calpain cleaves phospholipid flippase ATP8A1 during apoptosis in platelets. Blood Adv, 2019. 3(3): p. 219-229.*

5.1 Preamble

Despite critical roles for ATP11C in leukocytes and erythrocytes[119, 120, 122, 123, 163], it was shown in “CHAPTER 4” that ATP11C was not present and did not mediate flippase activity in murine platelets. These results ruled out ATP11C as a candidate of flippase activity in platelets and suggested the involvement of other flippase(s). In mice there are 15 members of the P4-ATPase family and 14 members in humans[11]. Despite many studies being undertaken on these members, it remains unclear, however, which flippase is active in platelets and how flippase activity is regulated during platelet apoptosis and activation[47].

It is reported in this section that ATP8A1 is the most abundant flippase in mouse and human platelets but is not located at the plasma membrane. During apoptosis it is cleaved by a previously unrecognised pathway involving the calcium-dependent cysteine protease calpain, and not by caspases. Consistently, prevention of calcium influx into platelets through inhibition of caspases indirectly protects ATP8A1 from cleavage due to lack of calpain activation. In contrast to apoptosis, ATP8A1 remains intact during the activation of platelets induced by physiological agonists. Our results provide evidence of a novel pathway of flippase cleavage that happens in apoptotic platelets but not in activated platelets[177].

5.2 ATP8A1 is highly expressed in mouse platelets but not located at the cell surface

Earlier work indicated that expression of flippases is tissue-specific[55, 184]. To determine the major flippase(s) in mouse platelets, we first tested the gene expression profile of 15 flippases and three CDC50 proteins in RNA isolated from mouse platelets[11]. We found that ATP8A1 had the highest expression level compared to other flippases, and CDC50A was the only CDC50 protein expressed in mouse platelets (Figure 5.1A). These data are in agreement with analysis of the murine platelet transcriptome[157] (Figure 5.1B) and proteome[158] (Figure 5.1C).

Further investigations showed that ATP8A1 was not present in the plasma membrane. As shown in Figure 5.1D, ATP8A1 was detected in total membranes of platelets but not in the biotinylated cell surface protein fractions. The absence of ATP8A1 in the plasma membrane was further confirmed by the observation that ATP8A1 was depleted rather than enriched in the plasma membrane fraction extracted from total membranes of platelets. As a marker of plasma membrane protein, Na^+/K^+-ATPase was enriched in both biotinylated and extracted plasma membrane protein fractions. Together, these data indicate that ATP8A1 is predominantly present in intracellular membranes rather than the plasma membrane of platelets.

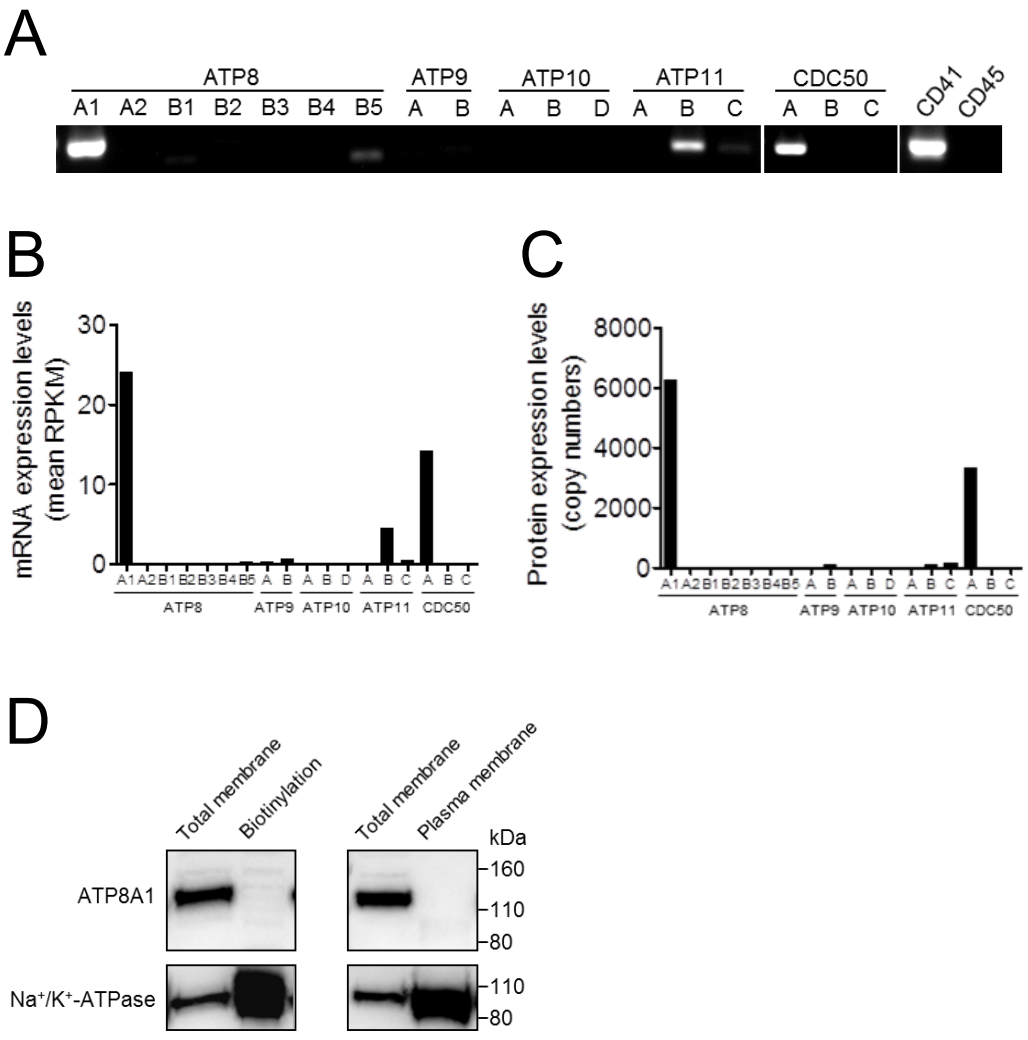

Figure 5.1 ATP8A1 is highly expressed in mouse platelets but not located at the cell surface

(A) Gene expression of P4-type ATPases and CDC50 proteins in mouse platelets. RT-PCR was performed using total RNA isolated from mouse platelets. CD41 and CD45 were used as positive control and negative control, respectively, for the purity of platelet cDNA.

(B) mRNA expression pattern of the P4-type ATPase and CDC50 genes derived from the genome-wide RNA-seq analysis of mouse platelet transcriptome[157]. RPKM: Reads Per

Kilobase of exon model per Million mapped reads. Data was extracted from Supplementary Table S4 of reference Rowley J. W. et al, 2011[157].

(C) Protein expression pattern of the P4-type ATPases and CDC50 proteins derived from the copy number analysis of murine platelet proteome[158]. Data was extracted from Supplementary Table S2 of reference Zeiler M. et al, 2014[158].

(D) Total membrane, biotinylated surface protein, and extracted plasma membrane from mouse platelets were denatured for SDS-PAGE and then probed for ATP8A1 by western blotting. Na^+/K^+-ATPase was used as a marker of plasma membrane protein. Immunoblots are representative of three independent experiments.

5.3 Calpain-mediated cleavage of ATP8A1 depends on caspase activation and calcium influx during platelet apoptosis

It has been reported that PS flippases, ATP11A and ATP11C, are inactivated through caspase-mediated cleavage enabling PS exposure in apoptotic leukocytes[35,40]. To examine whether flippase ATP8A1 is similarly cleaved by caspases during apoptosis in platelets, we assessed levels of cleaved and intact ATP8A1 protein in apoptotic murine platelets. We used the BH3 mimetic compound ABT737 to induce intrinsic apoptosis in murine platelets[68]. After 30 minutes of treatment with ABT737 in the absence of extracellular calcium, we noted cleavage of procaspase-3 from a 32 kDa zymogen into an active form of approximately 17 kDa, which indicated the activation of caspases and onset of platelet apoptosis (Figure 5.2A, left panel). Under these conditions no cleavage of ATP8A1 was observed as shown by immunodetection of the intact protein at 120 kDa (Figure 5.2A, left panel). This suggests that ATP8A1 is not cleaved by caspases during platelet apoptosis.

Intriguingly, ATP8A1 cleavage was observed after 1 hour of treatment with ABT737 in the presence of extracellular calcium, resulting in a lower molecular weight product of around 100 kDa (Figure 5.2A, middle panel). This suggested that ATP8A1 cleavage was most likely mediated by a calcium-dependent protease activated through calcium influx. Calpain is a calcium-dependent cysteine proteinase and functions in apoptosis by cleaving apoptosis-regulating factors and cytoskeleton-associated proteins[185]. Thus, we next investigated whether calpain was involved in ATP8A1 cleavage during apoptosis in platelets.

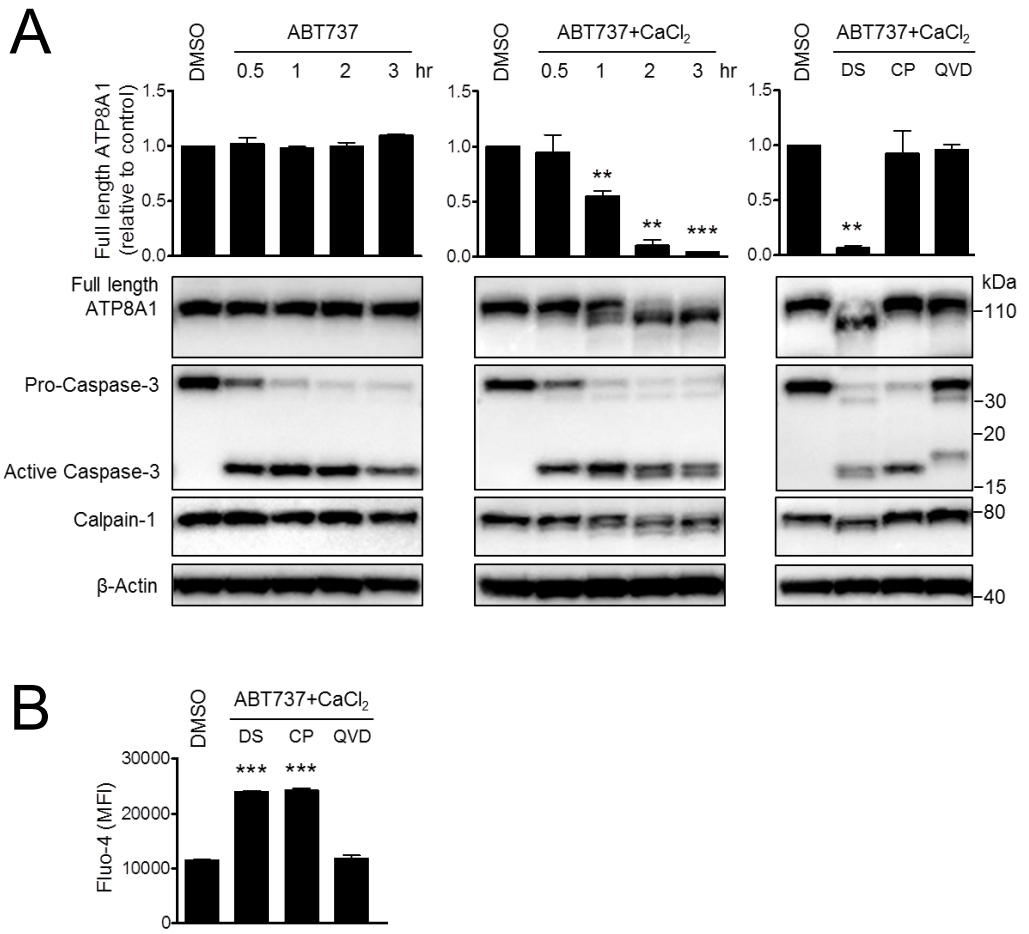

Figure 5.2 Calpain-mediated cleavage of ATP8A1 depends on caspase activation and calcium influx during platelet apoptosis

(A) Washed mouse platelets (5×10^7) were treated with vehicle (DMSO) or ABT737 (1 μM, 37 ℃) in the absence or presence of $CaCl_2$ (2 mM) for the indicated time. In some experiments, platelets were pre-incubated with DMSO (DS), Calpeptin (CP, 50 μg/mL) or Q-VD-OPh (QVD, 25 μM) at room temperature for 15 minutes before treatment with ABT737 (2 hours). Platelets were subsequently lysed for western blot analysis of ATP8A1, Caspase-3, Calpain-1 and β-actin.

(B) Washed mouse platelets (5×10^7) were preloaded with Fluo-4 and treated with vehicle (DMSO) or ABT737 (1 μM) and $CaCl_2$ (1.3 mM) at 37 ℃ for 2 hours in the absence or

presence of Calpeptin (CP, 50 µg/mL) or Q-VD-OPh (QVD, 25 µM). Fluo-4 fluorescence was measured, and data are expressed as mean fluorescence intensity ± SEM (MFI, n=3). Immunoblots are representative of n=3 independent experiments. Bar graphs represent blot quantification of full length ATP8A1 by densitometric analysis (means ± SEM, n=3) of stained bands using Image J, corrected for loading control (β-Actin). Statistical significance was calculated using Student's two-tailed test. (** $p < .01$; *** $p < .001$)

Activation of calpain can be demonstrated by the autolytic cleavage of a peptide from the 80 kDa large catalytic subunit, resulting in the generation of a fully active form at 76 kDa[186]. As shown in the middle and left panels of Figure 5.2A, fully active calpain-1 was only detected in apoptotic platelets treated with ABT737 + $CaCl_2$ but not ABT737 alone. This is consistent with the previous observation that calpain activation is calcium influx-dependent in platelets[187]. Moreover, pre-treatment of platelets with a specific calpain inhibitor, calpeptin (CP) completely inhibited the activation of calpain and cleavage of ATP8A1 in apoptotic platelets despite the presence of active caspase-3 (Figure 5.2A, right panel). Thus, these data indicate that ATP8A1 was cleaved during platelet apoptosis in a calpain-mediated manner.

Interestingly, the addition of the broad-spectrum caspase inhibitor, Q-VD-OPh (QVD), not only inhibited pro-caspase 3 conversion to active caspase-3 but also inhibited the cleavage of ATP8A1 (Figure 5.2A, last lane of right panel). This suggests that although ATP8A1 is not directly cleaved by caspases during platelet apoptosis, it is inactivated by a caspase-dependent mechanism. The lack of ATP8A1 cleavage after QVD treatment most likely resulted from a lack of calpain activation following caspase inhibition, as evident by the observation that auto-proteolysis of calpain-1 was absent (Figure 5.2A, last lane of right panel). To test whether the lack of calpain activation was due to the absence of calcium influx when caspase activity was inhibited, we measured intracellular calcium ($[Ca^{2+}]_i$) levels of platelets using the cytosolic Ca^{2+} probe Fluo-4 (Figure 5.2B). The measurement of Fluo-4 revealed that ABT737-treated apoptotic platelets had elevated $[Ca^{2+}]_i$, as detected by a significant 2-fold increase in mean fluorescence

intensity of Fluo-4, compared with resting platelets (Figure 5.2B). The elevation of $[Ca^{2+}]_i$ in apoptotic platelets was prevented by caspase inhibition. Under this condition $[Ca^{2+}]_i$ remained at the same level as in resting platelets (Figure 5.2B), indicating that influx of extracellular Ca^{2+} across the plasma membrane was blocked. Inhibition of calpain by CP did not affect elevation of $[Ca^{2+}]_i$ (Figure 5.2B) nor caspase activation (Figure 5.2A, right panel) during platelet apoptosis. Also, absence of extracellular calcium did not affect activation of caspases in platelets treated with ABT737 (Figure 5.2A, left panel). Taken together, these data demonstrate that calcium influx and subsequent calpain activation are downstream events of caspase activation; therefore, cleavage of ATP8A1 mediated by calpain is caspase-dependent during platelet apoptosis.

5.4 ATP8A1 is a direct substrate of calpain

To further confirm the molecular interactions leading to ATP8A1 cleavage by calpain, platelet membrane fractions were incubated with purified calpain-1, the isoform that accounts for 80% of the calpain activity in mouse platelets[188], followed by western blotting analysis of ATP8A1. As shown in Figure 5.3A, ATP8A1 was cleaved into the same size protein fragment of approx. 100 kDa, by calpain-1 in a Ca^{2+}-dependent fashion, as observed in apoptotic platelets (Figure 5.2A, middle and right panel). The cleavage was fully inhibited by CP (Figure 5.3A). These data demonstrate that ATP8A1 is a direct substrate of calpain.

As a substrate of calpain, ATP8A1 should be cleaved by calcium-activated endogenous calpain even in the absence of apoptosis and caspase activity. To test this, viable resting platelets were treated with calcium ionophore, A23187, resulting in the activation of endogenous calpain (Figure 5.3B). As shown in Figure 5.3B, the activation of calpain coincided with cleavage of ATP8A1 and both events were completely inhibited by CP. In this model, activation of calpain was directly achieved by A23187-induced calcium flux, bypassing apoptosis and caspase pathways. Caspases remain inactive in this case as shown by the absence of active caspase-3. Accordingly, caspase inhibitor QVD had no effect on calpain activation and ATP8A1 cleavage.

Immunoblots also revealed a lower molecular weight band below pro-caspase-3 (Figure 5.3B) that represents a non-activated cleaved form of pro-caspase-3 generated by active calpain[189] (Figure 5.3C). Gelsolin, a known caspase substrate, was cleaved by the active form of caspase-3 in ABT737 treated

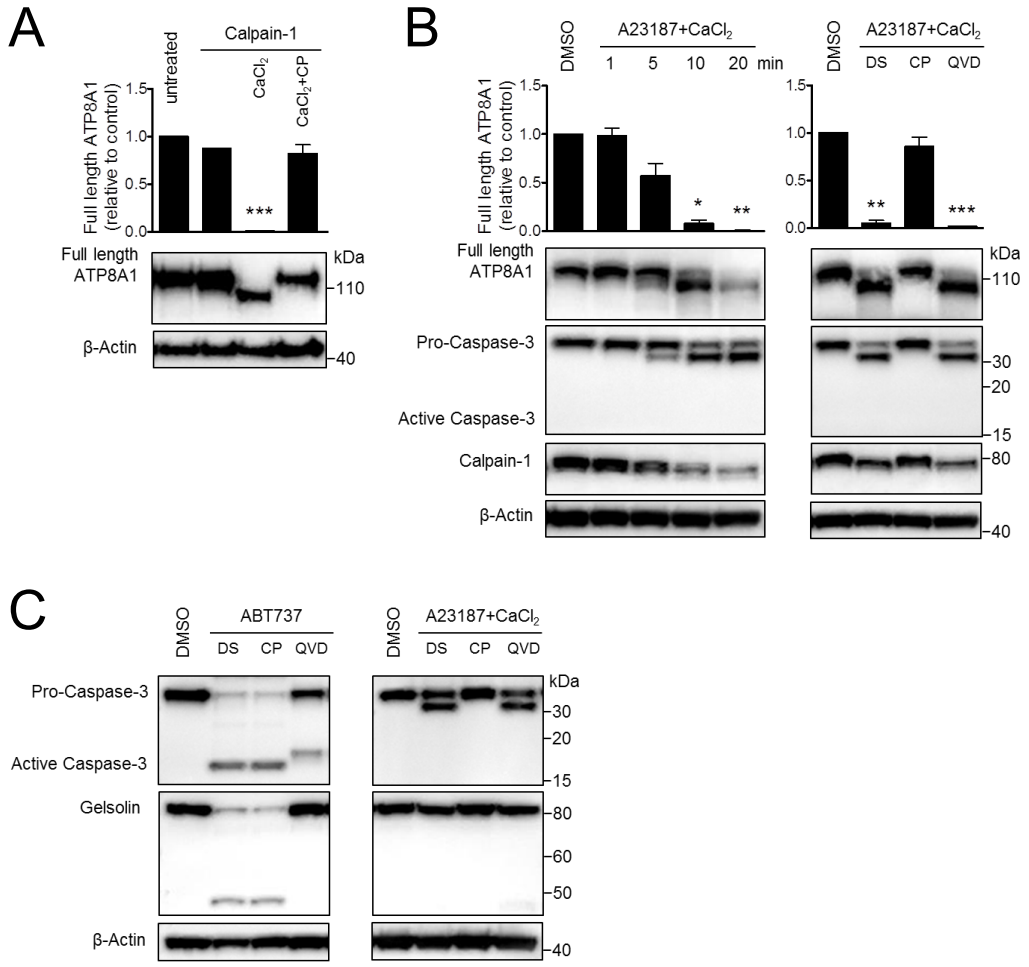

Figure 5.3 ATP8A1 is a direct substrate of calpain

(A) Mouse platelet membrane fractions (10 μg) remained untreated or were incubated with purified human calpain-1 (4 U) in the absence or presence of $CaCl_2$ (5 mM) or Calpeptin (50 μg/mL) at room temperature for 30 minutes. Samples were then denatured for western blot analysis of ATP8A1 and β-actin.

(B and C) Washed mouse platelets (5×10^7) were treated with vehicle (DMSO) or A23187 (1 μM; room temperature) in the presence of $CaCl_2$ (2 mM) for the indicated time. In some experiments, platelets were pre-incubated with DMSO (DS), Calpeptin (CP, 50 μg/mL) or Q-VD-OPh (QVD, 25 μM) at room temperature for 15 minutes before treatment with A23187 (20 minutes) or ABT737 (1 μM, 37 ℃, 2 hours, in the absence of

$CaCl_2$). Platelets were subsequently lysed for western blot analysis of ATP8A1, Caspase-3, Calpain-1, Gelsolin and β-actin. Immunoblots are representative of n=3 independent experiments. Bar graphs represent blot quantification of full length ATP8A1 by densitometric analysis (means ± SEM, n=3) of stained bands using Image J, corrected for loading control (β-Actin).

Statistical significance was calculated using Student's two-tailed test. (* $p < .05$; ** $p < .01$; *** $p < .001$)

apoptotic platelets (Figure 5.3C, left panel) but remained intact in A23187 treated platelets, indicating that the cleaved form of pro-caspase-3 generated by calpain does not activate pro-caspase-3 (Figure 5.3C, right panel).

5.5 Cleavage of human ATP8A1 and predicted calpain cleavage sites in mammalian ATP8A1 orthologues

Similar to murine platelets, ATP8A1 and CDC50A were also found to be highly expressed in human platelets (Figure 5.4A and B) in transcriptomic and proteomic studies[159-161]. Human ATP8A1 protein was also cleaved by endogenous calpain rather than caspases in human platelets treated with ABT737 to induce apoptosis, in a caspase- and calcium influx-dependent manner (Figure 5.4C).

Searches for calpain cleavage sites using the prediction tool GPS-CCD1.0[190] revealed several phylogenetically conserved predicted calpain cleavage sites in mammalian ATP8A1 orthologues. The predicted cleavage site at position R139 in the actuator (A) domain of ATP8A1 generates a fragment of around 100 kDa (Figure 5.4D and E), consistent with the cleaved form observed in the western blot analysis of murine and human platelets. In-depth biochemical and structural characterisation is required to further confirm the molecular interactions leading to ATP8A1 cleavage by calpain.

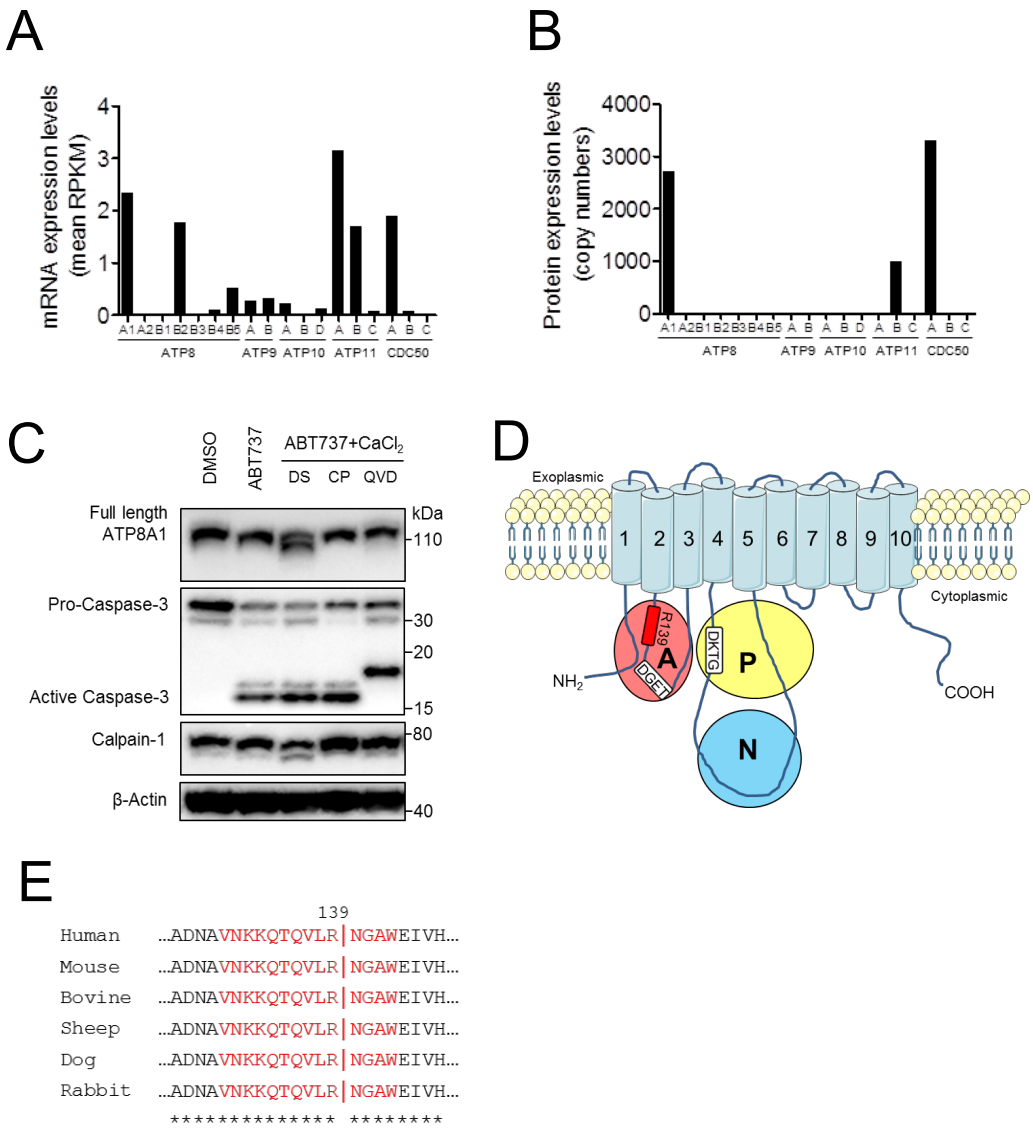

Figure 5.4 Cleavage of human ATP8A1 and predicted calpain cleavage sites in mammalian ATP8A1 orthologues

(A) mRNA expression pattern of the P4-type ATPase and CDC50 genes derived from the genome-wide RNA-seq analysis of human platelet transcriptome[157]. RPKM: Reads Per Kilobase of exon model per Million mapped reads. Data was extracted from Supplementary Table S4 of reference Rowley J. W. et al, 2011[157].

(B) Protein expression pattern of the P4-type ATPases and CDC50 proteins derived from the quantitative analysis of human platelet protein composition[159]. Data was extracted from Supplemental table 3 of reference Burkhart J. M. et al, 2012[159].

(C) Washed human platelets (5×10^7) were pre-incubated with DMSO (DS), Calpeptin (CP, 50 µg/mL) or Q-VD-OPh (QVD, 25 µM) at room temperature for 15 minutes, and then treated with vehicle (DMSO) or ABT737 (1 µM; 37 ℃; 2 hours) in the absence or presence of $CaCl_2$ (2 mM). Platelets were subsequently lysed for western blot analysis. Immunoblots are representative of n=3 independent experiments.

(D) Topology of ATP8A1 and its predicted calpain cleavage site. Transmembrane helices are numbered. Three cytosolic domains involved in the ATPase catalytic cycle are shown as coloured circles: nucleotide-binding (N) domain which binds ATP; phosphorylation (P) domain which contains the conserved phosphorylation site in the DKTG motif; and actuator (A) domain which has the DGET motif that facilitates the dephosphorylation of the phosphorylated aspartate intermediate[3, 13, 14]. Calpain cleavage sites were predicted using GPS-CCD 1.0 (http://ccd.biocuckoo.org)[190]. Although several cleavage sites are predicted, the site at position R139 in the A-domain (indicated by a red box) generates a fragment of around 100 kDa, which is consistent with the western blot fragment size in apoptotic platelets.

(E) Amino acid sequence alignment around the calpain cleavage site in six mammalian ATP8A1 orthologs: human (UniProt, Q9Y2Q0), mouse (P70704), bovine (Q29449), sheep (W5PYS1), dog (F1PHG9), and rabbit (G1TF29). Sequences are aligned, an asterisk (*) indicates fully conserved residues. The calpain recognition sequence is shown in red. A vertical bar (|) indicates the cleavage site.

5.6 ATP8A1 is not cleaved in platelets activated by physiological agonists

We next investigated whether calpain-mediated cleavage of ATP8A1, observed in apoptotic platelets, was also seen in activated platelets. As an artificial agonist, calcium ionophore, A23187, induces strong and sustained calcium flux increasing intracellular Ca^{2+} levels in a dose-dependent manner[191-193]. As shown in the upper panel of Figure 5.5A, 0.5 μM A23187 and 1 μM A23187 induced PS exposure on ~80 % and 100% of platelets, respectively, as detected by the PS-specific probe, Annexin-V[172]. However, calpain activation and the ensuing cleavage of ATP8A1 and pro-caspase-3 were only detected in platelets treated with 1 μM A23187 (Figure 5.5A, lower panel). These data indicate that ATP8A1 is cleaved by calpain only under conditions of high Ca^{2+} concentration in A23187 activated platelets.

To determine the effect of physiological agonists on ATP8A1 cleavage, platelets were treated with thrombin and collagen at concentrations known to induce platelet activation[194, 195]. In contrast to A23187, Figure 5.5B upper panel shows that each agonist alone was a weak trigger of PS exposure, resulting in approximately 20% of Annexin-V positive platelets[194, 195]. Co-stimulation of platelets with thrombin and collagen, however, led to a substantial fraction of platelets (approximately 80%) that exposed PS on their surface[47, 196, 197], similar to that observed on platelets treated with 0.5 μM A23187. Despite this level of PS-exposure, no calpain activation, ATP8A1 cleavage or pro-caspase-3 cleavage was detected (Figure 5.5B, lower panel). Together, these data indicate

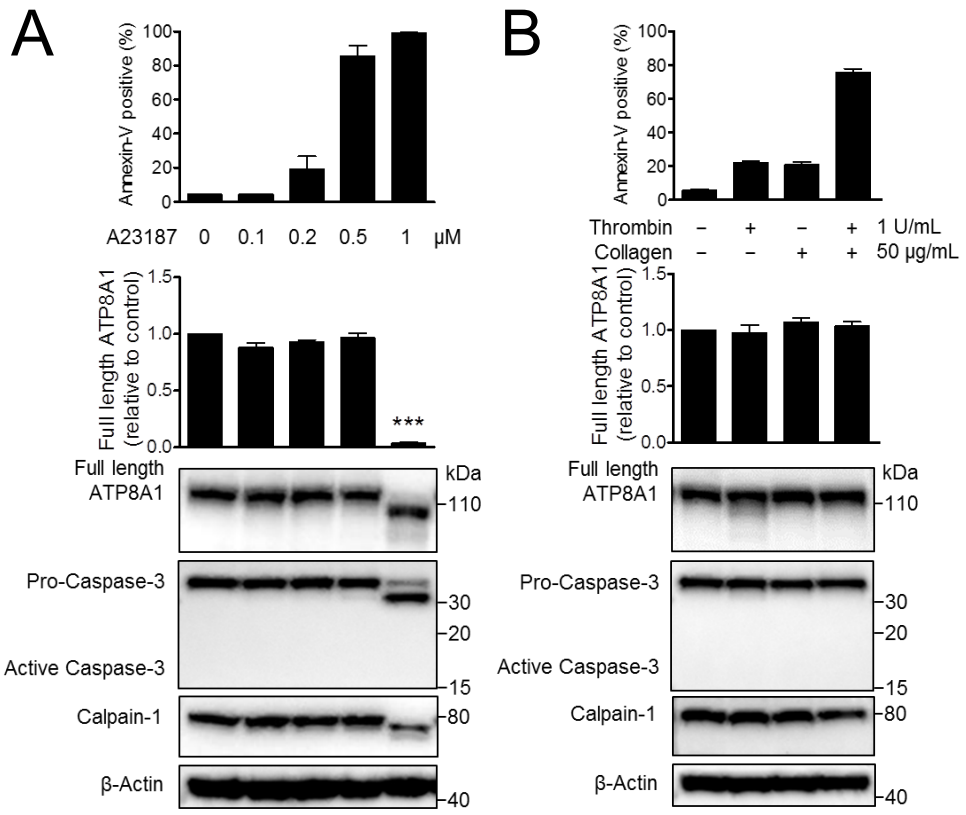

Figure 5.5 ATP8A1 is not cleaved in platelets activated by physiological agonists

(A and B, upper panels) Bar graphs represent means ± SEM (n=3) of the percentage of Annexin-V positive cells in platelets stimulated by A23187, Thrombin, Collagen, or Thrombin and Collagen in the presence of $CaCl_2$ (2 mM) at room temperature for 20 minutes.

(A and B, lower panels) Washed mouse platelets (5×10^7) were treated with vehicle, A23187, Thrombin, Collagen, or Thrombin and Collagen in the presence of $CaCl_2$ (2 mM) at room temperature for 20 minutes. Platelets were subsequently lysed for western blot analysis of ATP8A1, Caspase-3, Calpain-1 and β-actin. Immunoblots are representative of n=3 independent experiments. Bar graphs represent blot quantification of full length ATP8A1 by densitometric analysis (means ± SEM, n=3) of stained bands using Image J, corrected for loading control (β-Actin).

Statistical significance was calculated using Student's two-tailed test. (*** $p < .001$)

that ATP8A1 remains intact in PS-exposed platelets under conditions of physiological activation.

5.7 Discussion

In the present study we show that ATP8A1 is highly expressed in both murine and human platelets but not present in the plasma membrane, and calpain, rather than caspase, catalyses the cleavage of ATP8A1 during platelet apoptosis. To our knowledge, this is the first evidence for calpain-mediated cleavage of flippases. We also ruled out ATP11C as a candidate of flippase in murine platelets as shown in "CHAPTER 4". Interestingly, given the critical role for ATP11C in leukocytes and erythrocytes, and its inactivation by caspases[54, 55, 119, 120, 122, 123, 163], these results suggest that expression and regulation of flippases in platelets is distinct from these other cell types.

Both calpain and caspase play important roles in cell apoptosis. Studies have shown that calpain possesses both pro-survival and pro-apoptotic functions[185, 186], and the biological outcome of calpain activity is dependent on cell types and stimulants[198, 199]. In this study, we provide further evidence for the pro-apoptotic role of calpain in platelets treated with ABT737. In this setting, calpain facilitates apoptosis by cleaving the flippase ATP8A1 (Figure 5.2A). In contrast to calpain, caspase proteinases are centrally involved in pro-apoptotic signalling and execution. Although caspases do not directly cleave ATP8A1 in apoptotic platelets, they contribute to calpain-mediated cleavage in an indirect manner, through their actions on regulating pathways of calcium signalling (Figure 5.2B). In platelets, Ca^{2+} elevation in the cytosol occurs via both the release of stored Ca^{2+} from the dense tubular system and the influx of extracellular Ca^{2+} across the plasma membrane[200-203]. Various components of the Ca^{2+} signaling machinery

have been described to be cleaved by caspases[204]. Additionally, previous reports have shown that calpain activity may play a role downstream of caspases in the degradation phase of apoptosis[205]. The specific signaling mechanisms that link caspase activity, calcium signaling and calpain activation in platelets are beyond the scope of this study.

In addition to the plasma membrane, flippases also function in generating phospholipid asymmetry in intracellular membranes, including endoplasmic reticulum (ER), trans-Golgi network (TGN), and endosomes[5, 89-91], and play a critical role in vesicle-mediated protein trafficking[92, 93]. It is well documented that ATP8A1 associates with CDC50A to exit the ER, but mainly remains in intracellular membranes and to some extent at the plasma membrane[17, 18, 124]·[55]. For example, ATP8A1 was found mainly located in intra-cellular vesicles and partly at the plasma membrane in the presence of CDC50A in W3-Ildm cells[55]. In CHO and Hela cell lines, ATP8A1 exit ER in a CDC50A-dependent manner and mainly localized at the recycling compartments and partially on the plasma membrane[112, 124].

ATP8A1 has also been shown to localize to recycling endosomes and PS flipping by ATP8A1 is required for endosome-mediated protein trafficking[111, 126]. For example, in COS-1 cells, PS flipped by ATP8A1 to the cytoplasmic leaflet of recycling endosomes is required for recruitment of evectin-2[126], which plays a role in cholera toxin transport from the endosomes to the Golgi[92]. ATP8A1 catalyzed flipping of PS is also required for the recruitment of the membrane fission protein EHD1 to recycling endosomes and depletion of ATP8A1 impaired the asymmetric transbilayer distribution of PS in recycling endosomes, dissociated

EHD1 from REs, and generated aberrant endosomal tubules that appear resistant to membrane fission[111].

Given the absence of ATP8A1 in the plasma membrane of platelets (Figure 5.1D), we reason that ATP8A1 is predominantly located in intracellular membranes and is involved in vesicle-mediated trafficking in platelets. Platelets have complete intracellular membrane systems[116], and possess fundamental membrane trafficking processes such as endocytosis[117]. Endocytosis in platelets is an important process for loading certain granule cargo, such as fibrinogen and vascular endothelial growth factor (VEGF)[117]. Moreover, upon activation platelets undergo a dramatic shape change[53] and enhance exocytosis for secretion of procoagulant components and release of granules (dense-/α-granule)[118]. These processes require a large number of membrane structures; therefore, it is tempting to speculate that flippase-mediated asymmetric distribution of phospholipids in organelles enable the normal operation of these activities. As opposed to activation, ATP8A1 was found to be cleaved during platelet apoptosis (Figure 5.2). The cleavage is likely to inactivate flippase activity of ATP8A1, disrupt lipid asymmetry of intracellular membranes and trafficking, which may contribute to the process of apoptosis. In summary, cleavage of ATP8A1 was observed in apoptotic platelets (Figure 5.2) but not in activated platelets (Figure 5.5), indicating that inactivation of flippases is required for apoptosis, however, maintenance of flippase activity is required for normal function of platelets during activation (Figure 5.2 and 5.5).

Experiments using mice models could be performed to uncover the biological function of ATP8A1 *in vivo*. On the one hand, the application of ABT737 in mice

can help us verify the findings of the *in vitro* experiments, especially the cleavage of ATP8A1, and reveal related physiological significance. On the other, generation of mice lacking ATP8A1 could help investigate the biological function of ATP8A1, especially its role in platelet apoptosis and activation *in vivo*.

In conclusion, our findings support a model of calpain-mediated cleavage of phospholipid flippases in apoptotic platelets. In contrast, flippases remain intact in activated platelets despite the presence of PS on the cell surface. Hence, we propose that the modulation of flippase activity in the intracellular membranes of platelets play distinct roles in apoptosis and activation.

CHAPTER 6: Conclusion and Further Discussion

6.1 Conclusion

Studies in ATP11C-deficient mice identified ATP11C as a major flippase in murine B cells, with substrate specificity against PS, and to a less extent PE. Impaired flippase activity caused by ATP11C dysfunction resulted in temporary increased PS exposure on the surface of pro-B cell subsets, which likely contributed to the relevant B cell lymphopenia. However, ATP11C was not a contributing flippase in murine platelets but it was required for the survival of platelets in the peripheral blood. These findings highlight a fundamental difference between the action of ATP11C in leukocytes and platelets. Moreover, it was identified that flippase ATP8A1was highly expressed in both murine and human platelets with localization in intracellular membranes. ATP8A1 was cleaved by calpain in a caspase-dependent manner in apoptotic platelets, whereas remained intact in platelets physiological activated platelets. These data revealed a novel mechanism of flippase cleavage and suggested that flippase activity in intracellular membranes differed between platelets undergoing apoptosis and activation. Collectively, these findings extend our understanding on the role of flippases in B cell development and important mechanisms of platelet survival and function.

6.2 Molecular mechanism underling B cell deficiency caused by ATP11C dysfunction

As mentioned in the introduction section, B cell development in the bone marrow of ATP11C-deficient mice is arrested at the pro-B cell stage[119, 120]. Although a reduction in flippase activity was detected in various B cell subsets in ATP11C-deficient mice[163] (Figure 3.2, CHAPTER 3), the underlying mechanism by which loss of ATP11C caused B cell lymphopenia remained elusive. To find out the answer, many efforts and attempts have been performed by a variety of labs. Since the transition from pro-B cell to pre-B cell stage is dependent on two main signalling pathways, namely IL-7 and pre-BCR signalling[145-147], the focus of the mechanistic studies was mainly on these two signalling pathways.

IL-7 is a cytokine critical for the development of B cells in the bone marrow and it functions through its receptor, IL-7R[206]. However, studies on IL-7 signal pathway suggested that ATP11C most likely had no direct influence on signalling through the IL-7R[133]. Instead, loss of ATP11C may indirectly affect the early B cell factor 1 (EBF1) expression through the IL-7R signalling. Consistently, it was shown that mRNA levels of *Ebf1* in ATP11C$^{amb/0}$ pro-B cells were reduced[133], and EBF1 protein expression was impaired in pre/pro-B cells from ATP11C deficient mice[120].

A synergistic cross talk between the IL-7 and pre-BCR signalling has been suggested to control early B cell development in the bone marrow[146]. The proper expression of pre-BCR is critical for the selection of a population within pro-B cells that can respond to the limiting concentration of IL-7 and that

eventually differentiates into pre-B cells[207]. The developmental arrest at the pro-B cell stage in ATP11C-deficient mice is similar to that observed in mice deficient for pre-BCR signalling[148-150], suggesting that this block of B cell development may be due to a lack of pre-BCR signalling. Indeed, evidence for impaired pre-BCR signalling in ATP11C-deficient pro-B cells was derived from experiments where pre-BCR signalling was mimicked by treating cells with an antibody against Igβ (CD79b), which is a key component of the pre-BCR. It was shown that Igβ-stimulation-induced Ca^{2+} mobilisation was compromised in the mutant pro-B cells[133]. In addition, ATP11C-deficient pro-B cells exhibited reduced mRNA levels of some genes encoding key molecules that are involved in the expression and signalling through the pre-BCR[133].

Besides IL-7 and pre-BCR signalling, a more recent study suggested another possible mechanistic pathway for the B cell deficiency caused by ATP11C defect. Segawa, K. and colleagues[208] found that the bone marrow B-cell progenitors from ATP11C-deficient mice stably exposed PS due to a lack of flippase activity and are engulfed alive by macrophages in a PS-dependent manner.

It was previously reported that a small population of viable B cell progenitors exposed PS autonomously during their maturation process[174]. This is thought to be required for the positive selection of B cells. For example, the number of B-cell progenitors was abruptly reduced at the pre-B-cell stage, at which a large number of precursor B cells normally undergo apoptosis and are engulfed by macrophages in a PS-dependent manner[209]. In addition, since the engagement of BCR during the process of B cell development increases the intracellular Ca^{2+}

concentration[175], it is possible that signaling from a pre-BCR or BCR activates B-cell progenitors to expose PS via Ca^{2+}-dependent scramblase.

Consistently, Segawa, K. and colleagues[208] observed a small proportion of PS exposure (10 to 20%) on freshly isolated progenitor B cells in wild-type mice. They also observed that ATP11C deficiency greatly increased the PS-exposing population in B-cell progenitors in mutant mice, as evidenced by that this proportion was increased to about 30% of the pro-B cells and 50% of the pre-B and immature B cells by the ATP11C deficiency. It is most likely because that in wild-type mice, ATP11C would internalize PS, while, in $ATP11C^{-/0}$ B-cell progenitors, once PS was exposed to the cell surface, it would not be internalized.

Furthermore, they also found that the lymphopenia in the $ATP11C^{-/0}$ bone marrow was rescued by double knockout of the receptor kinases MerTK and Axl in mice, which are known to be essential for the PS-mediated engulfment of apoptotic cells by macrophages. These results indicate that ATP11C in precursor B cells is essential for rapidly internalizing PS from the cell surface and re-establishing the asymmetry of the plasma membrane of B cells, in order to prevent the cells' engulfment by macrophages. In short, the PS-dependent endocytosis of B-cell progenitors could partly explain the B cell lymphopenia caused by ATP11C dysfunction.

Interestingly, our finding shown in "CHAPTER 3" also provided similar clues for the possibility that PS-dependent clearance of pro-B cells contributed to B cell deficiency observed in the ATP11C-decifienct mice. As shown in Figure 3.2 and 3.3, loss of ATP11C resulted in a defective internalization of PS in the mutant B

cell subsets, and the impaired flippase activity caused a temporary increased PS accumulated on the surface of pro-B cells. This is likely in turn result in rapid PS-mediated phagocytosis of pro-B cells in ATP11C-deficient mice.

6.3 Flippases located in the plasma membrane of platelets

By using ATP11C-deficient (Amb) mice and a customized antibody against ATP11C, we demonstrated the absence of protein expression of ATP11C in mouse platelets (Figure 4.4B, CHAPTER 4). Consistently, platelets from ATP11C-decifient mice showed normal flippase activity compared to their littermate controls, indicating that ATP11C was not a flippase contributing to phospholipid asymmetry in the plasma membrane of platelets (Figure 4.4A, CHAPTER 4). Further studies showed in CHAPTER 5 revealed that ATP8A1 was highly expressed in both mouse and human platelets (Figure 5.1A, B and C, CHAPTER 5). However, through cell surface biotinylation and the plasma membrane extraction experiments, we demonstrated that ATP8A1 was not present in the plasma membrane of platelets, indicating its predominant localization in the intracellular membranes (Figure 5.1D, CHAPTER 5). The question arises, therefore, which flippase is the one that generates and maintains phospholipid asymmetry in the plasma membrane of platelets?

RNA and proteomics data showed that platelets had some ATP11B (Figure 5.1A, B and C, CHAPTER 5). Previous studies have shown that ATP11B associates with CDC50A to exit endoplasmic reticulum (ER) and is translocated to the plasma membrane of cells[112, 184, 210]. Without CDC50A, ATP11B remains in the ER[112, 184, 210], indicating that ATP11B is predominantly localized in the plasma membrane. Therefore, it is likely that ATP11B exists in the plasma membrane of platelets. However, due to lack of high-quality antibodies against ATP11B, we were unable to test for ATP11B protein expression and localization

by western blot. Development of antibodies against flippases and generation of gene knockout mice of specific flippases will be helpful for answering these questions.

6.4 Flippases' association with CDC50s and their subcellular localization

As shown in Figure 5.1 of CHAPTER 5, ATP8A1 was not localized in the plasma membrane of platelets, despite high expression of its β-subunit CDC50A. This is consistent with studies in cell lines that ATP8A1 associates with CDC50A to exit the endoplasmic reticulum (ER), but mainly remains in intracellular membranes[17, 18, 55, 124].

Normally, most P4-ATPases require their β-subunit CDC50 proteins to exit the ER and complete final subcellular localization; however, some exceptions were reported. The yeast P4-ATPases Drs2p, Dnf1p/Dnf2p, and Dnf3p associate with CDC50 proteins Cdc50p, Lem3p, and Crf1p, respectively[211, 212]; whereas the P4-ATPase Neo1p does not associate with either Cdc50p or Lem3p[211]. In mammalians, class 1 (ATP8A1, ATP8A2, ATP8B1, ATP8B2, ATP8B3, and ATP8B4), class 5 (ATP10A, ATP10B, and ATP10D) and class 6 (ATP11A, ATP11B, and ATP11C) P4-ATPases require CDC50 proteins, primarily CDC50A, for their exit from the ER and final subcellular localization[3, 18, 55, 111, 112, 124, 213-216]. However, similar to yeast, class 2 P4-ATPases ATP9A and ATP9B (an orthologue of yeast Neo1p) require neither CDC50A nor CDC50B for exiting the ER or localizing to the trans-Golgi network[215, 216]. Consistently, overexpression of CDC50A did not change their localization[55, 112].

The subcellular localization of flippases is diverse, some localize in the plasma membrane, and some are confined in the intracellular membrane systems. Some studies reported conflicting subcellular localization of flippases. For instance, the

P4-ATPases ATP8A1, ATP8A2, ATP10B, and ATP11B were reported to be confined largely to the Golgi complex and recycling endosomal system when overexpressed in cultured cells[55, 111, 112, 124, 215]. However, in other studies several of these P4-ATPases (e.g. ATP8A2, ATP11A) were reported to located in the plasma membrane and that this depended on CDC50A[55, 112]. Also, ATP8A1 was found to be localised in the membrane of erythrocytes[153].

Although most flippases require CDC50s to exit the ER, their ultimate cellular localization seems to depend on the flippases themselves but not on the CDC50 proteins. For example, although ATP9A and ATP9B show a high overall sequence similarity, ATP9A localizes to endosomes and the trans-Golgi network (TGN), whereas ATP9B localizes exclusively to the TGN. A chimeric ATP9 protein in which the N-terminal cytoplasmic region of ATP9A was replaced with the corresponding region of ATP9B localized exclusively to the TGN indicating that a segment within the N-terminal cytoplasmic region of ATP9 proteins is responsible for subcellular localization[112].

Taken together, it is believed that P4-ATPases can localize both in the plasma membrane and intracellular membranes such as the ER, TGN and endosomal recycling system, but preferentially localize to either of which depending on the specific P4-ATPase or cell type.

6.5 Flippase activity of ATP8A1 after cleavage

As demonstrated in "CHPTER 5" in this thesis, in both human and mouse platelets flippase ATP8A1 (120 kDa) was cleaved by calpain during apoptosis in the presence of extracellular calcium, resulting in a lower molecular weight product of around 100 kDa (Figure 5.2A and Figure 5.4C, CHPTER 5). Furthermore, in an *in vitro* cleavage assay, ATP8A1 was cleaved into the same size protein fragment of approx. 100 kDa, by calpain-1 in a Ca^{2+}-dependent fashion, as observed in apoptotic platelets (Figure 5.3A, CHPTER 5). Moreover, direct activation of calpain by calcium ionophore resulted in the same fragment (Figure 5.3B, CHPTER 5).

Searches using GPS-CCD1.0[190] revealed a predicted calpain cleavage site at position R139 in the actuator (A) domain of ATP8A1. Cleavage at this site generates a fragment of around 100 kDa (Figure 5.4D, CHAPTER 5), consistent with the cleaved form observed in the western blot analysis of murine and human platelets. The actuator domain has a conserved DGET motif that facilitates the dephosphorylation of the phospho-ATP8A1 intermediate during the catalytic cycle[3, 13, 14]. It is proposed that cleavage in the A domain of ATP8A1 most likely destablizes its structure thereby disrupting DGET motif-mediated dephosphorylation, which in turn abolishes the function of ATP8A1.

According to the classic Post-Albers or E1E2 model[217, 218], P-type ATPases cycle through four main separate conformations when transporting ligands. Take Na^+/K^+-ATPase for an instance, in the E1 state the enzyme has high affinity for intracellular ligands which is Na^+; Binding of ATP to the N-domain and

subsequent phosphorylation of the P-domain results in the E1-P state. While converting from E1-P to E2-P, intracellular ligands (3 Na^+) are released into the exoplasmic milieu and the A-domain rotates. This allows binding of extracellular ligands (2 K^+). Dephosphorylation changes the enzyme from the E2-P to the E2 state. Movement of the A-domain away from the P-domain reverts the ATPase back to the E1 state thereby translocating the extracellular ligands to the cytoplasmic side[2, 13, 15].

It has been suggested that the reaction cycle of P4-ATPases is analogous to those of established P-type ATPases[3, 219]. Indeed, P4-ATPases are phosphorylated by ATP at the conserved P-domain aspartate in the E1-P state[14, 17, 154]. Translocation of specific phospholipid substrates (such as PS and PE) from the exoplasmic to the cytoplasmic leaflet of the lipid bilayer facilitate the dephosphorylation of DGET motif of A-domain in the E2-P state. Notably, crystal structures of the P2-ATPase ion pumps Na^+/K^+-ATPase and Ca^{2+}-ATPase have shown how the conserved glutamate of the A-domain TGES motif (in P4-ATPases DGET) is brought into the correct position for catalyzing the hydrolysis of the aspartyl phosphoryl bond in the P-domain. This unique event consists of a 90° rotation of the A-domain in relation to the E1P-E2P transition followed by an additional, smaller change of conformation elicited by the binding of the ion to be transported from the exoplasm toward the cytoplasm[8]. Similar structural changes are expected to result in dephosphorylation of P4-ATPases. Accordingly, it was demonstrated for ATP8A2 that the E198Q mutation replacing the glutamate in the conserved DGET motif of the A domain with glutamine blocked PS-induced dephosphorylation[14].

To directly confirm that calpain-mediated cleavage inactivates flippase activity of ATP8A1, functional analysis of ATP8A1 before and after cleavage is needed. Activity of flippases could be determined in two different ways, namely by flippase assay and ATPase assay. The rationale of flippase assay was described in our previous studies[119, 122, 163]. In brief, when incubating with cells, fluorescent labelled lipid analogues such as NBD-PS are incorporate into the outer leaflet of the plasma membrane and are translocated by flippases to the inner leaflet. After washing with fatty acid-free BSA, which binds lipid analogues left in the outer leaflet and extracts them out of the membrane, the intensity of fluorescence left inside cells reflect the activity of flippases.

However, the flippase assay is unsuitable to determine activity of ATP8A1 after cleavage in the current study, as this assay works only in living cells but not in apoptotic cells. In apoptotic cells, scramblases (e.g. XKR8)[42, 51, 63] are activated by caspases, disrupting the asymmetric distribution of phospholipids in the plasma membrane. Given the non-specific and bi-directional properties of scramblases, added lipid analogues could also be inwardly translocated by active scramblases in apoptotic cells. As a result, the fluorescence left in cells reflects the action of not only flippases but also of activated scramblases, disturbing the measurement of flippase activity. As shown in the current study, the cleavage of ATP8A1 happened in apoptotic platelets, therefore, excluding a flippase assay in this condition.

As a member of P4-ATPase family, the activity of ATP8A1 could also be determined by ATPase assay, which detects free phosphate generated by ATPase-catalyzed hydrolysis of ATP[55, 184, 220]. However, purified bioactive protein is

required for ATPase assay. I tried to purify ATP8A1 by immunoprecipitation (IP); however, the antibody against ATP8A1 was not avid enough for IP, probably because the antibody can only recognize the linear peptide sequence of denatured ATP8A1 in western-blot but not the innate tertiary structure of the native protein.

6.6 Procoagulant responses of platelets – PS exposure in activation, apoptosis and necrosis

Platelets play a dual role during the haemostasis process: (1) They aggregate to form a plug that seals the gap in the damaged blood vessel; (2) They provide a catalytic surface for coagulation factors and promote the generation of thrombin and the formation of fibrin that consolidates thrombus (1.2.2 PS exposure and blood coagulation)[53]. This latter mentioned catalytic reaction is considered as the platelet procoagulant function which is mediated by exposed PS on the cell surface[6]. PS exposure happens not only in activated platelets during processes of thrombosis and haemostasis, but this phenomenon has also been demonstrated in platelets undergoing other biological procedures such as cell death including apoptosis and necrosis[77, 197, 221]. The potential procoagulant responses of platelets at different states, such as activation, apoptosis and necrosis, are discussed below.

Calcium-dependent PS exposure during platelet activation

Integrin activation and platelet aggregation are easily achieved by stimulation of platelets by most agonists, which occur at low cytosolic Ca^{2+} levels. By contrast, induction of PS exposure and platelet procoagulant response requires a high and persistent elevation of the intracellular Ca^{2+} concentration which is normally mediated by stimulation of platelet receptors by strong agonists, such as the combination of collagen and thrombin (Figure 5.5B)[74].

Studies on procoagulant platelets result in several descriptions on their properties, emphasising on their morphological changes and dependency on Ca^{2+} signalling.

For example, (1) Balloon-shaped procoagulant platelets: a hallmark feature of procoagulant platelets that readily distinguishes them from other forms of activated platelets[222]. (2) COllagen And Thrombin-activated platelets (COAT/COATED platelets): representing a subset of platelets with their surface coating by adhesive proteins and coagulation factors after potent platelet stimulation with thrombin and collagen[223]. (3) Sustained Calcium-Induced Platelets (SCIPs): reflecting the central role of high levels of sustained cytosolic Ca^{2+} in stimulating platelet procoagulant function[224].

Further studies have converged the reason why platelets depend on Ca^{2+} for their PS exposure and procoagulant function to a calcium-dependent phospholipid scramblase namely TMEM16F. When activated by elevated cytosolic Ca^{2+} during platelet activation, TMEM16F directly disrupts lipid asymmetry of the plasma membrane, resulting in PS exposure on the cell surface (1.2.2 PS exposure and blood coagulation)[6, 41].

Caspase-dependent PS exposure during platelet apoptosis

PS exposure during apoptosis serves as a signal for phagocyte-mediated clearance of dead cells (1.2.1 PS exposure and apoptosis)[51]. Theoretically, all natural membranes may function as a procoagulant phospholipid surface if sufficient PS is present in the out leaflet. Therefore, apoptotic platelets with PS on the cell surface may possess procoagulant responses. Indeed, studies found that although lacking ability of integrin activation and platelet aggregation, apoptotic platelets retain procoagulant function[46, 47]. This is supported by the observation of enhanced thrombin generation by apoptotic platelets in *in vitro* experiments.

However, PS exposure and procoagulant function of apoptotic platelets are independent of both TMEM16F and Ca^{2+}[46, 47]. First, platelets lacking TMEM16F from Scott syndrome patients are deficient in calcium- and agonist-induced PS exposure but expose PS normally during apoptosis induced by ABT737. Second, chelation of intracellular Ca^{2+} fully blocked calcium- and agonist-induced PS exposure during platelet activation whilst only partially blocked apoptotic PS exposure induced by ABT737. These observations suggest there is a calcium-independent PS exposure pathway during platelet apoptosis.

Strikingly, AB737-induced apoptotic PS exposure in platelets was completely abrogated by inhibition of caspase activity, implying the exist of caspase-dependent phospholipid scramblases[46, 47]. Notably, it was reported that a possible scramblase namely Xkr8 contributed to PS exposure in a caspase-activated manner during apoptosis in leukocytes[42]. However, whether Xkr8 functions in platelets or other caspase-dependent scramblases exist in platelets are yet to be illustrated. Further studies are also needed to investigate the physiological role of potential procoagulant responses of apoptotic platelets *in vivo*.

Platelet procoagulant responses and necrosis

Apoptosis and necrosis reflect distinct cell death processes. Apoptosis is characterized by the silent destruction and removal of cells in the absence of inflammation. In contrast, necrosis can lead to cell lysis and release of cellular contents into the extracellular environment, resulting in inflammatory responses[225].

Platelets undergoing necrosis like cell death have previously been identified at sites of vascular injury *in vivo*, which may play important roles in inducing inflammatory and repair processes[197]. Notably, many evidences suggest that the morphological, biochemical and functional changes underlying agonist-induced platelet procoagulant function are broadly consistent with cell necrosis, such as high and sustained levels of cytosolic Ca^{2+}, rapid loss of plasma membrane integrity and PS exposure, release of cellular contents and dysfunction of mitochondrial[221, 226]. These observations raise the possibility that necrosis may also regulate platelet procoagulant function.

Collectively, there are still debates that whether procoagulant platelets are undergoing a form of cell death, or cell death pathways may also regulate platelet function. Also, whether other programmed cell death pathways, such as autophagy, can contribute to platelet procoagulant function remains to be established. Further studies in understanding the molecular events underlining platelet activation and cell death are required to uncover the similarities and differences of these two reactions and to reveal their physiological roles in regulating thrombosis and haemostasis *in vivo*."

References

1. Balasubramanian, K. and A.J. Schroit, *Aminophospholipid asymmetry: A matter of life and death.* Annu Rev Physiol, 2003. **65**: p. 701-34.
2. Coleman, J.A., F. Quazi, and R.S. Molday, *Mammalian P4-ATPases and ABC transporters and their role in phospholipid transport.* Biochim Biophys Acta, 2013. **1831**(3): p. 555-74.
3. Andersen, J.P., et al., *P4-ATPases as Phospholipid Flippases-Structure, Function, and Enigmas.* Front Physiol, 2016. **7**: p. 275.
4. Rothman, J.E. and J. Lenard, *Membrane Asymmetry.* Science, 1977. **195**(4280): p. 743-753.
5. Leventis, P.A. and S. Grinstein, *The distribution and function of phosphatidylserine in cellular membranes.* Annu Rev Biophys, 2010. **39**: p. 407-27.
6. Bevers, E.M. and P.L. Williamson, *Getting to the Outer Leaflet: Physiology of Phosphatidylserine Exposure at the Plasma Membrane.* Physiol Rev, 2016. **96**(2): p. 605-45.
7. Verkleij AJ, Z.R., Roelofsen B, Comfurius P, Kastelijn D, van Deenen LL., *The asymmetric distribution of phospholipids in the human red cell membrane. A combined study using phospholipases and freeze-etch electron microscopy.* Biochim Biophys Acta, 1973. **Oct 11**(323(2)): p. 178-93.
8. Palmgren, M.G. and P. Nissen, *P-type ATPases.* Annu Rev Biophys, 2011. **40**: p. 243-66.
9. Lopez-Marques, R.L., et al., *Structure and mechanism of ATP-dependent phospholipid transporters.* Biochim Biophys Acta, 2015. **1850**(3): p. 461-75.
10. Palmgren, M.G. and K.B. Axelsen, *Evolution of P-type ATPases.* Biochim Biophys Acta, 1998. **1365**(1-2): p. 37-45.
11. Sebastian, T.T., et al., *Phospholipid flippases: building asymmetric membranes and transport vesicles.* Biochim Biophys Acta, 2012. **1821**(8): p. 1068-77.
12. Montigny, C., et al., *On the molecular mechanism of flippase- and scramblase-mediated phospholipid transport.* Biochim Biophys Acta, 2016. **1861**(8 Pt B): p. 767-83.
13. Lenoir, G., et al., *Cdc50p plays a vital role in the ATPase reaction cycle of the putative aminophospholipid transporter Drs2p.* J Biol Chem, 2009. **284**(27): p. 17956-67.
14. Coleman, J.A., et al., *Critical role of a transmembrane lysine in aminophospholipid transport by mammalian photoreceptor P4-ATPase ATP8A2.* Proc Natl Acad Sci U S A, 2012. **109**(5): p. 1449-54.
15. van der Mark, V.A., R.P. Elferink, and C.C. Paulusma, *P4 ATPases: flippases in health and disease.* Int J Mol Sci, 2013. **14**(4): p. 7897-922.
16. Panatala, R., H. Hennrich, and J.C. Holthuis, *Inner workings and biological impact of phospholipid flippases.* J Cell Sci, 2015. **128**(11): p. 2021-32.
17. Bryde, S., et al., *CDC50 proteins are critical components of the human class-1 P4-ATPase transport machinery.* J Biol Chem, 2010. **285**(52): p. 40562-72.
18. van der Velden, L.M., et al., *Heteromeric interactions required for abundance and subcellular localization of human CDC50 proteins and class 1 P4-ATPases.* J Biol Chem, 2010. **285**(51): p. 40088-96.

19. Bull, L.N., et al., *A gene encoding a P-type ATPase mutated in two forms of hereditary cholestasis.* Nat Genet, 1998. **18**(3): p. 219-24.
20. Cai, S.Y., et al., *ATP8B1 deficiency disrupts the bile canalicular membrane bilayer structure in hepatocytes, but FXR expression and activity are maintained.* Gastroenterology, 2009. **136**(3): p. 1060-9.
21. Paulusma, C.C., et al., *Atp8b1 deficiency in mice reduces resistance of the canalicular membrane to hydrophobic bile salts and impairs bile salt transport.* Hepatology, 2006. **44**(1): p. 195-204.
22. Folmer, D.E., R.P. Elferink, and C.C. Paulusma, *P4 ATPases - lipid flippases and their role in disease.* Biochim Biophys Acta, 2009. **1791**(7): p. 628-35.
23. Cacciagli, P., et al., *Disruption of the ATP8A2 gene in a patient with a t(10;13) de novo balanced translocation and a severe neurological phenotype.* Eur J Hum Genet, 2010. **18**(12): p. 1360-3.
24. Onat, O.E., et al., *Missense mutation in the ATPase, aminophospholipid transporter protein ATP8A2 is associated with cerebellar atrophy and quadrupedal locomotion.* Eur J Hum Genet, 2013. **21**(3): p. 281-5.
25. Zhu, X., et al., *Mutations in a P-type ATPase gene cause axonal degeneration.* PLoS Genet, 2012. **8**(8): p. e1002853.
26. Coleman, J.A., et al., *Phospholipid flippase ATP8A2 is required for normal visual and auditory function and photoreceptor and spiral ganglion cell survival.* J Cell Sci, 2014. **127**(Pt 5): p. 1138-49.
27. Wang, L., C. Beserra, and D.L. Garbers, *A novel aminophospholipid transporter exclusively expressed in spermatozoa is required for membrane lipid asymmetry and normal fertilization.* Dev Biol, 2004. **267**(1): p. 203-15.
28. Gong, E.Y., et al., *Expression of Atp8b3 in murine testis and its characterization as a testis specific P-type ATPase.* Reproduction, 2009. **137**(2): p. 345-51.
29. Li, H., et al., *Candidate single-nucleotide polymorphisms from a genomewide association study of Alzheimer disease.* Archives of Neurology, 2008. **65**(1): p. 45-53.
30. Dhar, M.S., et al., *Mice heterozygous for Atp10c, a putative amphipath, represent a novel model of obesity and type 2 diabetes.* J Nutr, 2004. **134**(4): p. 799-805.
31. Dhar, M.S., et al., *A type IV P-type ATPase affects insulin-mediated glucose uptake in adipose tissue and skeletal muscle in mice.* J Nutr Biochem, 2006. **17**(12): p. 811-20.
32. Flamant, S., et al., *Characterization of a putative type IV aminophospholipid transporter P-type ATPase.* Mamm Genome, 2003. **14**(1): p. 21-30.
33. Mori, *ATP11A is a novel predictive marker for metachronous metastasis of colorectal cancer.* Oncology Reports, 2009. **23**(2).
34. Bitbol, M. and P.F. Devaux, *Measurement of outward translocation of phospholipids across human erythrocyte membrane.* Proc Natl Acad Sci U S A, 1988. **85**(18): p. 6783-7.
35. Connor, J., et al., *Bidirectional transbilayer movement of phospholipid analogs in human red blood cells. Evidence for an ATP-dependent and protein-mediated process.* J Biol Chem, 1992. **267**(27): p. 19412-7.
36. Smit, J.J., et al., *Homozygous disruption of the murine mdr2 P-glycoprotein gene leads to a complete absence of phospholipid from bile and to liver disease.* Cell, 1993. **75**(3): p. 451-62.

37. vanHelvoort, A., et al., *MDR1 P-glycoprotein is a lipid translocase of broad specificity, while MDR3 P-glycoprotein specifically translocates phosphatidylcholine.* Cell, 1996. **87**(3): p. 507-517.
38. Morita, S.Y., et al., *Bile salt-dependent efflux of cellular phospholipids mediated by ATP binding cassette protein B4.* Hepatology, 2007. **46**(1): p. 188-99.
39. Wang, R., et al., *Targeted inactivation of sister of P-glycoprotein gene (spgp) in mice results in nonprogressive but persistent intrahepatic cholestasis.* Proc Natl Acad Sci U S A, 2001. **98**(4): p. 2011-6.
40. Berge, K.E., et al., *Accumulation of dietary cholesterol in sitosterolemia caused by mutations in adjacent ABC transporters.* Science, 2000. **290**(5497): p. 1771-5.
41. Suzuki, J., et al., *Calcium-dependent phospholipid scrambling by TMEM16F.* Nature, 2010. **468**(7325): p. 834-8.
42. Suzuki, J., et al., *Xk-related protein 8 and CED-8 promote phosphatidylserine exposure in apoptotic cells.* Science, 2013. **341**(6144): p. 403-6.
43. Bratton, D.L., et al., *Appearance of phosphatidylserine on apoptotic cells requires calcium-mediated nonspecific flip-flop and is enhanced by loss of the aminophospholipid translocase.* Journal of Biological Chemistry, 1997. **272**(42): p. 26159-26165.
44. Castoldi, E., et al., *Compound heterozygosity for 2 novel TMEM16F mutations in a patient with Scott syndrome.* Blood, 2011. **117**(16): p. 4399-400.
45. Brooks, M.B., et al., *A TMEM16F point mutation causes an absence of canine platelet TMEM16F and ineffective activation and death-induced phospholipid scrambling.* J Thromb Haemost, 2015. **13**(12): p. 2240-52.
46. van Kruchten, R., et al., *Both TMEM16F-dependent and TMEM16F-independent pathways contribute to phosphatidylserine exposure in platelet apoptosis and platelet activation.* Blood, 2013. **121**(10): p. 1850-1857.
47. Schoenwaelder, S.M., et al., *Two distinct pathways regulate platelet phosphatidylserine exposure and procoagulant function.* Blood, 2009. **114**(3): p. 663-6.
48. Suzuki, J., E. Imanishi, and S. Nagata, *Exposure of phosphatidylserine by Xk-related protein family members during apoptosis.* J Biol Chem, 2014. **289**(44): p. 30257-67.
49. Suzuki, J., E. Imanishi, and S. Nagata, *Xkr8 phospholipid scrambling complex in apoptotic phosphatidylserine exposure.* Proc Natl Acad Sci U S A, 2016. **113**(34): p. 9509-14.
50. Kim, G.W., et al., *Xk-related protein 8 regulates myoblast differentiation and survival.* FEBS J, 2017. **284**(21): p. 3575-3588.
51. Segawa, K. and S. Nagata, *An Apoptotic 'Eat Me' Signal: Phosphatidylserine Exposure.* Trends Cell Biol, 2015. **25**(11): p. 639-50.
52. Nagata, S., R. Hanayama, and K. Kawane, *Autoimmunity and the clearance of dead cells.* Cell, 2010. **140**(5): p. 619-30.
53. Versteeg, H.H., et al., *New fundamentals in hemostasis.* Physiol Rev, 2013. **93**(1): p. 327-58.
54. Segawa, K., et al., *Caspase-mediated cleavage of phospholipid flippase for apoptotic phosphatidylserine exposure.* Science, 2014. **344**(6188): p. 1164-8.
55. Segawa, K., S. Kurata, and S. Nagata, *Human Type IV P-type ATPases That Work as Plasma Membrane Phospholipid Flippases and Their Regulation by Caspase and Calcium.* J Biol Chem, 2016. **291**(2): p. 762-72.
56. Kile, B.T., *The role of apoptosis in megakaryocytes and platelets.* Br J Haematol, 2014. **165**(2): p. 217-26.

57. Ow, Y.P., et al., *Cytochrome c: functions beyond respiration.* Nat Rev Mol Cell Biol, 2008. **9**(7): p. 532-42.
58. Nagata, S., *Apoptosis and Clearance of Apoptotic Cells.* Annu Rev Immunol, 2018. **36**: p. 489-517.
59. Poon, I.K., et al., *Apoptotic cell clearance: basic biology and therapeutic potential.* Nat Rev Immunol, 2014. **14**(3): p. 166-80.
60. Toda, S., et al., *Clearance of Apoptotic Cells and Pyrenocytes.* Curr Top Dev Biol, 2015. **114**: p. 267-95.
61. Nagata, S. and M. Tanaka, *Programmed cell death and the immune system.* Nature Reviews Immunology, 2017. **17**(5): p. 333-340.
62. Erwig, L.P. and P.M. Henson, *Clearance of apoptotic cells by phagocytes.* Cell Death Differ, 2008. **15**(2): p. 243-50.
63. Nagata, S., et al., *Exposure of phosphatidylserine on the cell surface.* Cell Death Differ, 2016. **23**(6): p. 952-61.
64. Galluzzi, L., et al., *Cell death modalities: classification and pathophysiological implications.* Cell Death Differ, 2007. **14**(7): p. 1237-43.
65. Elliott, M.R. and K.S. Ravichandran, *Clearance of apoptotic cells: implications in health and disease.* J Cell Biol, 2010. **189**(7): p. 1059-70.
66. Biermann, M.H., et al., *The role of dead cell clearance in the etiology and pathogenesis of systemic lupus erythematosus: dendritic cells as potential targets.* Expert Rev Clin Immunol, 2014. **10**(9): p. 1151-64.
67. Kawano, M. and S. Nagata, *Lupus-like autoimmune disease caused by a lack of Xkr8, a caspase-dependent phospholipid scramblase.* Proceedings of the National Academy of Sciences of the United States of America, 2018. **115**(9): p. 2132-2137.
68. Mason, K.D., et al., *Programmed anuclear cell death delimits platelet life span.* Cell, 2007. **128**(6): p. 1173-86.
69. Zhang, H., et al., *Bcl-2 family proteins are essential for platelet survival.* Cell Death Differ, 2007. **14**(5): p. 943-51.
70. Monroe, D.M. and M. Hoffman, *What does it take to make the perfect clot?* Arterioscler Thromb Vasc Biol, 2006. **26**(1): p. 41-8.
71. Inoue, O., K. Suzuki-Inoue, and Y. Ozaki, *Redundant mechanism of platelet adhesion to laminin and collagen under flow: involvement of von Willebrand factor and glycoprotein Ib-IX-V.* J Biol Chem, 2008. **283**(24): p. 16279-82.
72. Lentz, B.R., *Exposure of platelet membrane phosphatidylserine regulates blood coagulation.* Progress in Lipid Research, 2003. **42**(5): p. 423-438.
73. Ariens, R.A., et al., *Role of factor XIII in fibrin clot formation and effects of genetic polymorphisms.* Blood, 2002. **100**(3): p. 743-54.
74. Obydennyy, S.I., et al., *Dynamics of calcium spiking, mitochondrial collapse and phosphatidylserine exposure in platelet subpopulations during activation.* J Thromb Haemost, 2016. **14**(9): p. 1867-81.
75. Keuren, J.F., et al., *Synergistic effect of thrombin on collagen-induced platelet procoagulant activity is mediated through protease-activated receptor-1.* Arterioscler Thromb Vasc Biol, 2005. **25**(7): p. 1499-505.
76. Harper, M.T., et al., *Transient receptor potential channels function as a coincidence signal detector mediating phosphatidylserine exposure.* Sci Signal, 2013. **6**(281): p. ra50.
77. Agbani, E.O. and A.W. Poole, *Procoagulant platelets: generation, function, and therapeutic targeting in thrombosis.* Blood, 2017. **130**(20): p. 2171-2179.

78. Yang, H., et al., *TMEM16F forms a Ca2+-activated cation channel required for lipid scrambling in platelets during blood coagulation.* Cell, 2012. **151**(1): p. 111-22.
79. Mattheij, N.J., et al., *Survival protein anoctamin-6 controls multiple platelet responses including phospholipid scrambling, swelling, and protein cleavage.* FASEB J, 2016. **30**(2): p. 727-37.
80. Boisseau, P., et al., *A new mutation of ANO6 in two familial cases of Scott syndrome.* Br J Haematol, 2016.
81. Zwaal, R.F., P. Comfurius, and E.M. Bevers, *Scott syndrome, a bleeding disorder caused by defective scrambling of membrane phospholipids.* Biochim Biophys Acta, 2004. **1636**(2-3): p. 119-28.
82. Weiss, H.J., et al., *Isolated deficiency of platelet procoagulant activity.* Am J Med, 1979. **67**(2): p. 206-13.
83. Rosing, J., et al., *Impaired factor X and prothrombin activation associated with decreased phospholipid exposure in platelets from a patient with a bleeding disorder.* Blood, 1985. **65**(6): p. 1557-61.
84. Toti, F., et al., *Scott syndrome, characterized by impaired transmembrane migration of procoagulant phosphatidylserine and hemorrhagic complications, is an inherited disorder.* Blood, 1996. **87**(4): p. 1409-1415.
85. Fujii, T., et al., *TMEM16F is required for phosphatidylserine exposure and microparticle release in activated mouse platelets.* Proc Natl Acad Sci U S A, 2015. **112**(41): p. 12800-5.
86. Baig, A., et al., *TMEM16F-Mediated Platelet Membrane Phospholipid Scrambling Is Critical for Hemostasis and Thrombosis but not Thromboinflammation in Mice-Brief Report.* Arteriosclerosis, Thrombosis, and Vascular Biology, 2016. **36**(11): p. 2152-2157.
87. van Geffen, J.P., F. Swieringa, and J.W. Heemskerk, *Platelets and coagulation in thrombus formation: aberrations in the Scott syndrome.* Thromb Res, 2016. **141 Suppl 2**: p. S12-6.
88. Takatsu, H., et al., *Phospholipid flippase ATP11C is endocytosed and downregulated following Ca(2+)-mediated protein kinase C activation.* Nat Commun, 2017. **8**(1): p. 1423.
89. Yang, Y., M. Lee, and G.D. Fairn, *Phospholipid subcellular localization and dynamics.* J Biol Chem, 2018. **293**(17): p. 6230-6240.
90. Drin, G., *Topological regulation of lipid balance in cells.* Annu Rev Biochem, 2014. **83**: p. 51-77.
91. Graham, T.R., *Flippases and vesicle-mediated protein transport.* Trends Cell Biol, 2004. **14**(12): p. 670-7.
92. Uchida, Y., et al., *Intracellular phosphatidylserine is essential for retrograde membrane traffic through endosomes.* Proceedings of the National Academy of Sciences of the United States of America, 2011. **108**(38): p. 15846-15851.
93. Fairn, G.D., et al., *High-resolution mapping reveals topologically distinct cellular pools of phosphatidylserine.* J Cell Biol, 2011. **194**(2): p. 257-75.
94. Hankins, H.M., et al., *Role of flippases, scramblases and transfer proteins in phosphatidylserine subcellular distribution.* Traffic, 2015. **16**(1): p. 35-47.
95. Takeda, M., K. Yamagami, and K. Tanaka, *Role of phosphatidylserine in phospholipid flippase-mediated vesicle transport in Saccharomyces cerevisiae.* Eukaryot Cell, 2014. **13**(3): p. 363-75.
96. Grant, B.D. and J.G. Donaldson, *Pathways and mechanisms of endocytic recycling.* Nat Rev Mol Cell Biol, 2009. **10**(9): p. 597-608.

97. Chia, P.Z. and P.A. Gleeson, *The regulation of endosome-to-Golgi retrograde transport by tethers and scaffolds.* Traffic, 2011. **12**(8): p. 939-47.
98. Johannes, L. and C. Wunder, *Retrograde transport: two (or more) roads diverged in an endosomal tree?* Traffic, 2011. **12**(8): p. 956-62.
99. Mellman, I., *Endocytosis and molecular sorting.* Annu Rev Cell Dev Biol, 1996. **12**: p. 575-625.
100. Maxfield, F.R. and T.E. McGraw, *Endocytic recycling.* Nat Rev Mol Cell Biol, 2004. **5**(2): p. 121-32.
101. Muthusamy, B.P., et al., *Linking phospholipid flippases to vesicle-mediated protein transport.* Biochim Biophys Acta, 2009. **1791**(7): p. 612-9.
102. Hua, Z., P. Fatheddin, and T.R. Graham, *An essential subfamily of Drs2p-related P-type ATPases is required for protein trafficking between Golgi complex and endosomal/vacuolar system.* Mol Biol Cell, 2002. **13**(9): p. 3162-77.
103. Natarajan, P., et al., *Drs2p-coupled aminophospholipid translocase activity in yeast Golgi membranes and relationship to in vivo function.* Proc Natl Acad Sci U S A, 2004. **101**(29): p. 10614-9.
104. Xu, P., et al., *Phosphatidylserine flipping enhances membrane curvature and negative charge required for vesicular transport.* J Cell Biol, 2013. **202**(6): p. 875-86.
105. Hankins, H.M., et al., *Phosphatidylserine translocation at the yeast trans-Golgi network regulates protein sorting into exocytic vesicles.* Mol Biol Cell, 2015. **26**(25): p. 4674-85.
106. Chen, C.-Y., et al., *Role for Drs2p, a P-Type Atpase and Potential Aminophospholipid Translocase, in Yeast Late Golgi Function.* The Journal of Cell Biology, 1999. **147**(6): p. 1223-1236.
107. Pomorski, T., et al., *Drs2p-related P-type ATPases Dnf1p and Dnf2p are required for phospholipid translocation across the yeast plasma membrane and serve a role in endocytosis.* Mol Biol Cell, 2003. **14**(3): p. 1240-54.
108. Poulsen, L.R., et al., *The Arabidopsis P4-ATPase ALA3 localizes to the golgi and requires a beta-subunit to function in lipid translocation and secretory vesicle formation.* Plant Cell, 2008. **20**(3): p. 658-76.
109. Ruaud, A.F., et al., *The C. elegans P4-ATPase TAT-1 regulates lysosome biogenesis and endocytosis.* Traffic, 2009. **10**(1): p. 88-100.
110. Chen, B., et al., *Endocytic sorting and recycling require membrane phosphatidylserine asymmetry maintained by TAT-1/CHAT-1.* PLoS Genet, 2010. **6**(12): p. e1001235.
111. Lee, S., et al., *Transport through recycling endosomes requires EHD1 recruitment by a phosphatidylserine translocase.* EMBO J, 2015. **34**(5): p. 669-88.
112. Takatsu, H., et al., *ATP9B, a P4-ATPase (a putative aminophospholipid translocase), localizes to the trans-Golgi network in a CDC50 protein-independent manner.* J Biol Chem, 2011. **286**(44): p. 38159-67.
113. Xu, Q., et al., *P4-ATPase ATP8A2 acts in synergy with CDC50A to enhance neurite outgrowth.* FEBS Lett, 2012. **586**(13): p. 1803-12.
114. Tanaka, Y., et al., *The phospholipid flippase ATP9A is required for the recycling pathway from the endosomes to the plasma membrane.* Mol Biol Cell, 2016. **27**(24): p. 3883-3893.
115. Takada, N., et al., *Phospholipid-flipping activity of P4-ATPase drives membrane curvature.* EMBO J, 2018. **37**(9).
116. Walsh, T.G., et al., *Small GTPases in platelet membrane trafficking.* Platelets, 2018: p. 1-10.

117. Manne, B.K., S.C. Xiang, and M.T. Rondina, *Platelet secretion in inflammatory and infectious diseases.* Platelets, 2017. **28**(2): p. 155-164.
118. Sharda, A. and R. Flaumenhaft, *The life cycle of platelet granules.* F1000Res, 2018. **7**: p. 236.
119. Yabas, M., et al., *ATP11C is critical for the internalization of phosphatidylserine and differentiation of B lymphocytes.* Nat Immunol, 2011. **12**(5): p. 441-9.
120. Siggs, O.M., et al., *The P4-type ATPase ATP11C is essential for B lymphopoiesis in adult bone marrow.* Nat Immunol, 2011. **12**(5): p. 434-40.
121. Siggs, O.M., et al., *X-linked cholestasis in mouse due to mutations of the P4-ATPase ATP11C.* Proceedings of the National Academy of Sciences of the United States of America, 2011. **108**(19): p. 7890-7895.
122. Yabas, M., et al., *Mice deficient in the putative phospholipid flippase ATP11C exhibit altered erythrocyte shape, anemia, and reduced erythrocyte life span.* J Biol Chem, 2014. **289**(28): p. 19531-7.
123. Arashiki, N., et al., *ATP11C is a major flippase in human erythrocytes and its defect causes congenital hemolytic anemia.* Haematologica, 2016. **101**(5): p. 559-65.
124. Kato, U., et al., *Role for phospholipid flippase complex of ATP8A1 and CDC50A proteins in cell migration.* J Biol Chem, 2013. **288**(7): p. 4922-34.
125. Dong, W., et al., *MiR-140-3p suppressed cell growth and invasion by downregulating the expression of ATP8A1 in non-small cell lung cancer.* Tumour Biol, 2016. **37**(3): p. 2973-85.
126. Matsudaira, T., et al., *Endosomal phosphatidylserine is critical for the YAP signalling pathway in proliferating cells.* Nat Commun, 2017. **8**(1): p. 1246.
127. Levano, K., et al., *Atp8a1 deficiency is associated with phosphatidylserine externalization in hippocampus and delayed hippocampus-dependent learning.* J Neurochem, 2012. **120**(2): p. 302-13.
128. Kerr, D.J., et al., *Aberrant hippocampal Atp8a1 levels are associated with altered synaptic strength, electrical activity, and autistic-like behavior.* Biochim Biophys Acta, 2016. **1862**(9): p. 1755-65.
129. Brubaker, S.W., et al., *Innate immune pattern recognition: a cell biological perspective.* Annu Rev Immunol, 2015. **33**: p. 257-90.
130. Hardy, R.R. and K. Hayakawa, *B cell development pathways.* Annu Rev Immunol, 2001. **19**: p. 595-621.
131. Rodriguez-Pinto, D., *B cells as antigen presenting cells.* Cell Immunol, 2005. **238**(2): p. 67-75.
132. Lund, F.E., *Cytokine-producing B lymphocytes-key regulators of immunity.* Curr Opin Immunol, 2008. **20**(3): p. 332-8.
133. Yabas, M., *B cell deficiency and anaemia caused by mutations in the murine atp11c gene.* Thesis (Ph.D.) - Australian National University, 2014: p. 285. p. 193-201.
134. Inlay, M.A., et al., *Ly6d marks the earliest stage of B-cell specification and identifies the branchpoint between B-cell and T-cell development.* Genes Dev, 2009. **23**(20): p. 2376-81.
135. Li, Y.S., *The regulated expression of B lineage associated genes during B cell differentiation in bone marrow and fetal liver.* Journal of Experimental Medicine, 1993. **178**(3): p. 951-960.
136. Li, Y.S., et al., *Identification of the earliest B lineage stage in mouse bone marrow.* Immunity, 1996. **5**(6): p. 527-35.

137. Hardy, R.R., *Resolution and characterization of pro-B and pre-pro-B cell stages in normal mouse bone marrow.* Journal of Experimental Medicine, 1991. **173**(5): p. 1213-1225.
138. Nagata K1, N.T., Kitamura F, Kuramochi S, Taki S, Campbell KS, Karasuyama H., *The Ig alpha/Igbeta heterodimer on mu-negative proB cells is competent for transducing signals to induce early B cell differentiation.* Immunity, 1997. **7**(4): p. 559-70.
139. Shinkai, Y., et al., *RAG-2-deficient mice lack mature lymphocytes owing to inability to initiate V(D)J rearrangement.* Cell, 1992. **68**(5): p. 855-67.
140. Mombaerts, P., et al., *Rag-1-Deficient Mice Have No Mature Lymphocytes-B and Lymphocytes-T.* Cell, 1992. **68**(5): p. 869-877.
141. Sakaguchi, N. and F. Melchers, *Lambda 5, a new light-chain-related locus selectively expressed in pre-B lymphocytes.* Nature, 1986. **324**(6097): p. 579-82.
142. Kudo A1, M.F., *A second gene, VpreB in the lambda 5 locus of the mouse, which appears to be selectively expressed in pre-B lymphocytes.* EMBO J, 1987 **6**(8): p. 2267-72.
143. Nishimoto, N., et al., *Normal pre-B cells express a receptor complex of mu heavy chains and surrogate light-chain proteins.* Proc Natl Acad Sci U S A, 1991. **88**(14): p. 6284-8.
144. Hendriks, R.W. and S. Middendorp, *The pre-BCR checkpoint as a cell-autonomous proliferation switch.* Trends Immunol, 2004. **25**(5): p. 249-56.
145. Herzog, S., M. Reth, and H. Jumaa, *Regulation of B-cell proliferation and differentiation by pre-B-cell receptor signalling.* Nat Rev Immunol, 2009. **9**(3): p. 195-205.
146. Clark, M.R., et al., *Orchestrating B cell lymphopoiesis through interplay of IL-7 receptor and pre-B cell receptor signalling.* Nat Rev Immunol, 2014. **14**(2): p. 69-80.
147. Reth, M. and P. Nielsen, *Signaling circuits in early B-cell development.* Adv Immunol, 2014. **122**: p. 129-75.
148. Gong, S. and M.C. Nussenzweig, *Regulation of an early developmental checkpoint in the B cell pathway by Ig beta.* Science, 1996. **272**(5260): p. 411-4.
149. Mundt, C., et al., *Loss of Precursor B Cell Expansion but Not Allelic Exclusion inVpreB1/VpreB2Double-Deficient Mice.* The Journal of Experimental Medicine, 2001. **193**(4): p. 435-446.
150. Pelanda, R., et al., *B Cell Progenitors Are Arrested in Maturation but Have Intact VDJ Recombination in the Absence of Ig- and Ig-* The Journal of Immunology, 2002. **169**(2): p. 865-872.
151. Grawunder, U., et al., *Down-regulation of RAG1 and RAG2 gene expression in preB cells after functional immunoglobulin heavy chain rearrangement.* Immunity, 1995. **3**(5): p. 601-8.
152. Tang, X., et al., *A subfamily of P-type ATPases with aminophospholipid transporting activity.* Science, 1996. **272**(5267): p. 1495-7.
153. Soupene, E. and F.A. Kuypers, *Identification of an erythroid ATP-dependent aminophospholipid transporter.* Br J Haematol, 2006. **133**(4): p. 436-8.
154. Ding, J., et al., *Identification and functional expression of four isoforms of ATPase II, the putative aminophospholipid translocase. Effect of isoform variation on the ATPase activity and phospholipid specificity.* J Biol Chem, 2000. **275**(30): p. 23378-86.
155. Paterson, J.K., et al., *Lipid specific activation of the murine P4-ATPase Atp8a1 (ATPase II).* Biochemistry, 2006. **45**(16): p. 5367-76.

156. Soupene, E., D.U. Kemaladewi, and F.A. Kuypers, *ATP8A1 activity and phosphatidylserine transbilayer movement.* J Receptor Ligand Channel Res, 2008. **1**: p. 1-10.
157. Rowley, J.W., et al., *Genome-wide RNA-seq analysis of human and mouse platelet transcriptomes.* Blood, 2011. **118**(14): p. e101-11.
158. Zeiler, M., M. Moser, and M. Mann, *Copy number analysis of the murine platelet proteome spanning the complete abundance range.* Mol Cell Proteomics, 2014. **13**(12): p. 3435-45.
159. Burkhart, J.M., et al., *The first comprehensive and quantitative analysis of human platelet protein composition allows the comparative analysis of structural and functional pathways.* Blood, 2012. **120**(15): p. e73-82.
160. Solari, F.A., et al., *Combined Quantification of the Global Proteome, Phosphoproteome, and Proteolytic Cleavage to Characterize Altered Platelet Functions in the Human Scott Syndrome.* Mol Cell Proteomics, 2016. **15**(10): p. 3154-3169.
161. Krishnan, S., et al., *OFFgel-based multidimensional LC-MS/MS approach to the cataloguing of the human platelet proteome for an interactomic profile.* Electrophoresis, 2011. **32**(6-7): p. 686-95.
162. Trichler, S.A., et al., *Ultra-pure platelet isolation from canine whole blood.* BMC Vet Res, 2013. **9**: p. 144.
163. Yabas, M., et al., *ATP11C Facilitates Phospholipid Translocation across the Plasma Membrane of All Leukocytes.* PLoS One, 2016. **11**(1): p. e0146774.
164. Coupland, L.A., et al., *A novel fluorescent-based assay reveals that thrombopoietin signaling and Bcl-X(L) influence, respectively, platelet and erythrocyte lifespans.* Exp Hematol, 2010. **38**(6): p. 453-461 e1.
165. Peter Zilla, M.D., Roland Fasol, M.D., A. Hammerle, M.D., S. Yildiz, M.S., M. Kadletz, M.D., Gunther Laufer, M.D., Gregor Wollenek, M.D., R. Seitelberger, M.D., and M. Deutsch, M.D., *Scanning Electron Microscopy of Circulating Platelets Reveals New Aspects of Platelet Alteration*

During Cardiopulmonary Bypass Operations. Texas Heart Institute Journal, 1987. **14**(1).
166. White, J.G., *Electron microscopy methods for studying platelet structure and function.* Methods Mol Biol, 2004. **272**: p. 47-63.
167. Salmoz, D.M., *Optimisation of platelet aggregometry utilizing micotitreplate technology and integrated software.* Thrombosis Research, 1996. **84**(3): p. 213-216.
168. Jarvis, G.E., *Platelet aggregation: turbidimetric measurements.* Methods Mol Biol, 2004. **272**: p. 65-76.
169. Dodge J T, M.C., Hanahan D J, *The preparation and chemical characteristics of hemoglobin–free ghosts of human erythrocytes.* Arch. Biochem. Biophys., 1963. **100**: p. 119–130.
170. Broer, A., F. Rahimi, and S. Broer, *Deletion of Amino Acid Transporter ASCT2 (SLC1A5) Reveals an Essential Role for Transporters SNAT1 (SLC38A1) and SNAT2 (SLC38A2) to Sustain Glutaminolysis in Cancer Cells.* J Biol Chem, 2016. **291**(25): p. 13194-205.
171. V A Fadok, D.R.V., P A Campbell, J J Cohen, D L Bratton and P M Henson, *Exposure of phosphatidylserine on the surface of apoptotic lymphocytes triggers specific recognition and removal by macrophages.* J Immunol, 1992. **148**(7): p. 2207-2216.

172. Koopman, G., et al., *Annexin V for flow cytometric detection of phosphatidylserine expression on B cells undergoing apoptosis.* Blood, 1994. **84**(5): p. 1415-20.
173. Dillon, S.R., et al., *Annexin V Binds to Viable B Cells and Colocalizes with a Marker of Lipid Rafts upon B Cell Receptor Activation.* The Journal of Immunology, 2000. **164**(3): p. 1322-1332.
174. Dillon, S.R., A. Constantinescu, and M.S. Schlissel, *Annexin V Binds to Positively Selected B Cells.* The Journal of Immunology, 2001. **166**(1): p. 58-71.
175. Baba Y, K.T., *Role of Calcium Signaling in B Cell Activation and Biology.* Curr Top Microbiol Immunol, 2016. **393**: p. 143-174.
176. Pozarowski, P., J. Grabarek, and Z. Darzynkiewicz, *Flow cytometry of apoptosis.* Curr Protoc Cytom, 2003. **Chapter 7**: p. Unit 7 19.
177. Jing, W., et al., *Calpain cleaves phospholipid flippase ATP8A1 during apoptosis in platelets.* Blood Adv, 2019. **3**(3): p. 219-229.
178. Alonzo, M.T., et al., *Platelet apoptosis and apoptotic platelet clearance by macrophages in secondary dengue virus infections.* J Infect Dis, 2012. **205**(8): p. 1321-9.
179. Mattheij, N.J., et al., *Dual mechanism of integrin alphaIIbbeta3 closure in procoagulant platelets.* J Biol Chem, 2013. **288**(19): p. 13325-36.
180. Li, J., et al., *Desialylation is a mechanism of Fc-independent platelet clearance and a therapeutic target in immune thrombocytopenia.* Nat Commun, 2015. **6**: p. 7737.
181. Hoffmeister, K.M. and H. Falet, *Platelet clearance by the hepatic Ashwell-Morrell receptor: mechanisms and biological significance.* Thrombosis Research, 2016. **141**: p. S68-S72.
182. Renata Grozovsky, S.G., Herv´e Falet, and Karin M. Hoffmeister, *Regulating billions of blood platelets: glycans and beyond.* Blood, 2015. **126**(16): p. 1877-1884.
183. Li, R., K.M. Hoffmeister, and H. Falet, *Glycans and the platelet life cycle.* Platelets, 2016. **27**(6): p. 505-11.
184. Wang, J., et al., *Proteomic Analysis and Functional Characterization of P4-ATPase Phospholipid Flippases from Murine Tissues.* Sci Rep, 2018. **8**(1): p. 10795.
185. Storr, S.J., et al., *The calpain system and cancer.* Nat Rev Cancer, 2011. **11**(5): p. 364-74.
186. Goll, D.E., et al., *The calpain system.* Physiol Rev, 2003. **83**(3): p. 731-801.
187. Pasquet, J.M., J. DacharyPrigent, and A.T. Nurden, *Calcium influx is a determining factor of calpain activation and microparticle formation in platelets.* European Journal of Biochemistry, 1996. **239**(3): p. 647-654.
188. Kuchay, S.M. and A.H. Chishti, *Calpain-mediated regulation of platelet signaling pathways.* Curr Opin Hematol, 2007. **14**(3): p. 249-54.
189. Wolf, B.B., et al., *Calpain functions in a caspase-independent manner to promote apoptosis-like events during platelet activation.* Blood, 1999. **94**(5): p. 1683-92.
190. Liu, Z., et al., *GPS-CCD: a novel computational program for the prediction of calpain cleavage sites.* PLoS One, 2011. **6**(4): p. e19001.
191. Babcock DF, F.N., Lardy HA., *Action of ionophore A23187 at the cellular level. Separation of effects at the plasma and mitochondrial membranes.* J Biol Chem, 1976. **251(13)**(Jul 10): p. 3881-3886.
192. Qiu ZH1, G.M., de Carvalho MS, Spencer DM, Leslie CC, *The Role of Calcium and Phosphorylation of Cytosolic Phospholipase A2 in Regulating Arachidonic Acid Release in Macrophages.* J Biol Chem, 1998. **273(14)**(Apr 3): p. 8203-11.

193. Schoenwaelder, S.M., et al., *14-3-3zeta regulates the mitochondrial respiratory reserve linked to platelet phosphatidylserine exposure and procoagulant function.* Nat Commun, 2016. **7**: p. 12862.
194. De Candia, E., *Mechanisms of platelet activation by thrombin: a short history.* Thromb Res, 2012. **129**(3): p. 250-6.
195. Coughlin, S.R., *Thrombin signalling and protease-activated receptors.* Nature, 2000. **407**(6801): p. 258-264.
196. Kulkarni, S., et al., *Conversion of platelets from a proaggregatory to a proinflammatory adhesive phenotype: role of PAF in spatially regulating neutrophil adhesion and spreading.* Blood, 2007. **110**(6): p. 1879-86.
197. Jackson, S.P. and S.M. Schoenwaelder, *Procoagulant platelets: are they necrotic?* Blood, 2010. **116**(12): p. 2011-2018.
198. Kidd, V.J., J.M. Lahti, and T. Teitz, *Proteolytic regulation of apoptosis.* Semin Cell Dev Biol, 2000. **11**(3): p. 191-201.
199. Tan, Y., et al., *Ubiquitous calpains promote both apoptosis and survival signals in response to different cell death stimuli.* J Biol Chem, 2006. **281**(26): p. 17689-98.
200. Ohlmann, P., et al., *Measurement and manipulation of [Ca2+]i in suspensions of platelets and cell cultures.* Methods Mol Biol, 2004. **273**: p. 229-50.
201. Rink, T.J. and S.O. Sage, *Calcium Signaling in Human Platelets.* Annual Review of Physiology, 1990. **52**(52): p. 431-449.
202. Heemskerk, J.W. and S.O. Sage, *Calcium signalling in platelets and other cells.* Platelets, 1994. **5**(6): p. 295-316.
203. Varga-Szabo, D., A. Braun, and B. Nieswandt, *Calcium signaling in platelets.* J Thromb Haemost, 2009. **7**(7): p. 1057-66.
204. Pinton, P., et al., *Calcium and apoptosis: ER-mitochondria Ca2+ transfer in the control of apoptosis.* Oncogene, 2008. **27**(50): p. 6407-18.
205. Wood, D.E. and E.W. Newcomb, *Caspase-dependent activation of calpain during drug-induced apoptosis.* Journal of Biological Chemistry, 1999. **274**(12): p. 8309-8315.
206. Corfe, S.A. and C.J. Paige, *The many roles of IL-7 in B cell development; mediator of survival, proliferation and differentiation.* Semin Immunol, 2012. **24**(3): p. 198-208.
207. Fleming, H.E. and C.J. Paige, *Cooperation between IL-7 and the pre-B cell receptor: a key to B cell selection.* Seminars in Immunology, 2002. **14**(6): p. 423-430.
208. Segawa, K., et al., *Phospholipid flippases enable precursor B cells to flee engulfment by macrophages.* Proc Natl Acad Sci U S A, 2018. **115**(48): p. 12212-12217.
209. Melchers, F., *Checkpoints that control B cell development.* J Clin Invest, 2015. **125**(6): p. 2203-10.
210. Moreno-Smith, M., et al., *ATP11B mediates platinum resistance in ovarian cancer.* Journal of Clinical Investigation, 2013. **123**(5): p. 2119-2130.
211. Saito, K., et al., *Cdc50p, a protein required for polarized growth, associates with the Drs2p P-type ATPase implicated in phospholipid translocation in Saccharomyces cerevisiae.* Mol Biol Cell, 2004. **15**(7): p. 3418-32.
212. Furuta, N., et al., *Endocytic recycling in yeast is regulated by putative phospholipid translocases and the Ypt31p/32p-Rcy1p pathway.* Mol Biol Cell, 2007. **18**(1): p. 295-312.

213. Takatsu, H., et al., *Phospholipid flippase activities and substrate specificities of human type IV P-type ATPases localized to the plasma membrane.* J Biol Chem, 2014. **289**(48): p. 33543-56.
214. Naito, T., et al., *Phospholipid Flippase ATP10A Translocates Phosphatidylcholine and Is Involved in Plasma Membrane Dynamics.* J Biol Chem, 2015. **290**(24): p. 15004-17.
215. Coleman, J.A. and R.S. Molday, *Critical role of the beta-subunit CDC50A in the stable expression, assembly, subcellular localization, and lipid transport activity of the P4-ATPase ATP8A2.* J Biol Chem, 2011. **286**(19): p. 17205-16.
216. Paulusma, C.C., et al., *ATP8B1 requires an accessory protein for endoplasmic reticulum exit and plasma membrane lipid flippase activity.* Hepatology, 2008. **47**(1): p. 268-78.
217. Albers, R.W., *Biochemical Aspects of Active Transport.* Annual Review of Biochemistry, 1967. **36**(1): p. 727-756.
218. Post, R.L., C. Hegyvary, and S. Kume, *Activation by adenosine triphosphate in the phosphorylation kinetics of sodium and potassium ion transport adenosine triphosphatase.* J Biol Chem, 1972. **247**(20): p. 6530-40.
219. Bublitz, M., J.P. Morth, and P. Nissen, *P-type ATPases at a glance.* J Cell Sci, 2011. **124**(Pt 15): p. 2515-9.
220. Coleman, J.A., M.C. Kwok, and R.S. Molday, *Localization, purification, and functional reconstitution of the P4-ATPase Atp8a2, a phosphatidylserine flippase in photoreceptor disc membranes.* J Biol Chem, 2009. **284**(47): p. 32670-9.
221. Hua, V.M., et al., *Necrotic platelets provide a procoagulant surface during thrombosis.* Blood, 2015. **126**(26): p. 2852-62.
222. Heemskerk, J.W., Vuist, W. M., Feijge, M. A., Reutelingsperger, C. P., & Lindhout, T. , *Collagen but not fibrinogen surfaces induce bleb formation, exposure of phosphatidylserine, and procoagulant activity of adherent platelets: evidence for regulation by protein tyrosine kinase-dependent Ca2+ responses. .* Blood, 1997. **90**(7): p. 2615–2625.
223. Dale, G.L., et al., *Stimulated platelets use serotonin to enhance their retention of procoagulant proteins on the cell surface.* Nature, 2002. **415**(6868): p. 175-179.
224. Kulkarni, S. and S.P. Jackson, *Platelet factor XIII and calpain negatively regulate integrin alphaIIbbeta3 adhesive function and thrombus growth.* J Biol Chem, 2004. **279**(29): p. 30697-706.
225. Zong, W.X. and C.B. Thompson, *Necrotic death as a cell fate.* Genes & Development, 2006. **20**(1): p. 1-15.
226. Jobe, S.M., et al., *Critical role for the mitochondrial permeability transition pore and cyclophilin D in platelet activation and thrombosis.* Blood, 2008. **111**(3): p. 1257-65.